Chain-Limiting Operation of Fischer-Tropsch Reactor

Final Report

Work Performed Under
Contract No.: **DE-FG26-99FT40680**

Prepared by

Apostolos A. Nikolopoulos
Santosh K. Gangwal
Center for Energy Technology
RTI
P.O. Box 12194
Research Triangle Park, NC 27709-2194

Submitted to

US Department of Energy
National Energy Technology Laboratory
P.O. Box 10940
Pittsburgh, PA 15236-0940
USA

June 2003

RTI
INTERNATIONAL

Chain-Limiting Operation of Fischer-Tropsch Reactor

Final Report

Apostolos A. Nikolopoulos and Santosh K. Gangwal

RTI
3040 Cornwallis Road
P.O. Box 12194
Research Triangle Park, NC 27709-2194
USA

DISCLAIMER

ABSTRACT

The use of pulsing in Fischer-Tropsch (FT) synthesis to limit the hydrocarbon chain growth and maximize the yield of diesel-range (C_{10}-C_{20}) products was examined on high-chain-growth-probability ($\alpha \geq 0.9$) FT catalysts. Pulsing experiments were conducted using a stainless-steel fixed-bed micro-reactor, equipped with both on-line (for the permanent gases and light hydrocarbons, C_1-C_{15}) and off-line (for the heavier hydrocarbons, C_{10}-C_{65}) gas chromatography analysis. Additional experiments were performed using a highly active attrition-resistant iron-based FT synthesis catalyst in a 1-liter continuous stirred-tank rector (CSTR).

On both a Co-ZrO_2/SiO_2 and a Co/Al_2O_3 FT synthesis catalyst application of H_2 pulsing causes significant increase in CO conversion, and only an instantaneous increase in undesirable selectivity to CH_4. Increasing the frequency of H_2 pulsing enhances the selectivity to C_{10}-C_{20} compounds but the chain-growth probability α remains essentially unaffected. Increasing the duration of H_2 pulsing results in enhancing the maximum obtained CO conversion and an instantaneous selectivity to CH_4. An optimum set of H_2 pulse parameters (pulse frequency, pulse duration) is required for maximizing the yield of desirable diesel-range C_{10}-C_{20} products.

Application of a suitable H_2 pulse in the presence of added steam in the feed is a simple method to overcome the loss in activity and the shift in paraffin vs. olefin selectivity (increase in the olefin/paraffin ratio) caused by the excess steam. A decrease in syngas concentration has a strong suppressing effect on the olefin/paraffin ratio of the light hydrocarbon products. Higher syngas concentration can increase the chain growth probability α and thus allow for better evaluation of the effect of pulsing on FT synthesis.

On a high-α Fe/K/Cu/SiO_2 FT synthesis catalyst H_2 pulsing enhances the yield of C_{10}-C_{20} but at the same time decreases the catalyst activity (CO conversion) and increases the selectivity to CH_4. On the other hand, pulsing with CO also increases the yield of C_{10}-C_{20} but has no impact on the selectivity to CH_4 or CO_2 and decreases catalytic activity only moderately.

FT reaction experiments using the Fe/K/Cu/SiO_2 FT synthesis catalyst in a 1-liter CSTR indicate that both the catalyst activity and yield of all products (both favorable and unfavorable) are enhanced by increasing reaction pressure and H_2:CO feed ratio, as well as with decreasing reaction temperature. The selectivity to the desirable C_{5+} product fraction is favored by lower reaction temperatures and H_2:CO feed ratios.

Based on the results of this study, the following recommendations should be considered: Pulsing experiments on FT synthesis catalysts (either cobalt-based or iron-based) should be performed under conditions that maximize the yield of the heavy hydrocarbon products (high chain-growth probability α), such as high synthesis gas partial pressure and low space velocity. More aggressive pulsing conditions (higher pulse frequency) should be examined, so as to establish the long-term impact of pulsing on product formation beyond experimental uncertainty. Also, more emphasis should be given to pulsing experiments in the CSTR which, due to its superior control of the catalyst temperature, would allow the evaluation of a more extensive range of pulsing parameters (pulse frequency and duration).

TABLE OF CONTENTS

LIST OF FIGURES

LIST OF FIGURES (continued)

LIST OF FIGURES (continued)

LIST OF TABLES

ABBREVIATIONS AND ACRONYMS

%	percent
°C	degree Celcius
°F	degree Farenheit
Al, Al_2O_3	Aluminum, Alumina
Ar	Argon
atm	atmosphere (14.7 psi)
BET	Brunauer-Emmett-Teller
C	Carbon
ca.	about
cat	catalyst
cc, cm^3	cubic centimeter
CH_4	Methane
C_i	Hydrocarbon with carbon number = i
CO	Carbon Monoxide
Co	Cobalt
CO_2	Carbon Dioxide
CSTR	Continuous Stirred Tank Reactor
Cu	Copper
CYL	Cylinder
DOE	Department of Energy
FBR	Fixed-Bed Reactor
Fe	Iron
FID	flame ionization detector
FT, FTS	Fischer-Tropsch, Fischer-Tropsch Synthesis
g	gram
GC	gas chromatograph
h, h^{-1}	hour, inverse hour
H_2	Hydrogen
H_2O	water, steam
Hg	Mercury
HP5890, HP6890	Hewlett-Packard gas chromatograph
HPR	Hampton-Pittsburgh-RTI
i.d.	inside diameter
K	Potassium, thermocouple type
L	liter
mg	milligram (10^{-3} grams)
mL	milliliter, 10^{-3} liters
N_2	Nitrogen
NC	North Carolina
NETL	National Energy Technology Laboratory
O, O_2	Oxygen
o.d.	outside diameter
P	pressure
P.O.	Post Office

ABBREVIATIONS AND ACRONYMS (continued)

psia, psig	pounds per square inch (absolute, gage)
RPM	revolutions per minute
RTI	Research Triangle Institute
Ru	Ruthenium
scc	standard cubic centimeter
sccm	standard cubic centimeter per minute
SFA	Schultz-Flory-Anderson
Si, SiO_2	Silicon, Silica
SV	space velocity (h^{-1})
Syngas	synthesis gas
T	temperature
TC, TE	thermocouple
TCD	thermal conductivity detector
U.S.	United States
X	Conversion (mol%)
Y	Yield (cc / cc cat / h, or mg C / g cat / h)
Z	Productivity (cc CO / cc cat / h)
Zr, ZrO_2	Zirconium, Zirconia
α	Chain-growth probability (alpha)
μL	microliter, 10^{-6} liters
μm	micrometer, 10^{-6} meters

ACKNOWLEDGEMENTS

EXECUTIVE SUMMARY

Objective

The objective of this research project was to limit the chain growth of Fiscer-Tropsch (FT) products by removing the growing hydrocarbons from the catalyst surface. The work focused on investigating the effect of pulsing on the activity and product distribution of high-α FT synthesis catalysts, in an attempt to limit chain growth to C_{20} hydrocarbons, thus maximizing the desirable diesel-range C_{10}-C_{20} yield.

Experimental

This investigation involved periodic substitution of the reactant (H_2+CO) flow by an equal flow of a selected "pulse" gas (typically H_2) and monitoring the resulting changes in productivity and product distribution of a particular FT synthesis catalyst. The evaluation of various FT catalysts was based on maximizing the C_{10}-C_{20} product yield. Optimization of the pulse sequence characteristics (frequency, duration, gas type, and gas concentration) was also within the scope of this research. Catalysts based on cobalt, iron, and ruthenium were used. Experiments were conducted primarily using a fixed-bed reactor system with pulsing capability. A continuous stirred-tank reactor was also used to test a high-α iron-based catalyst.

Summary of Results

Five materials were examined for evaluating the chain-limiting concept on FT synthesis in terms of activity and product selectivity. These were:

- a high-purity, low-surface-area (0.2-m^2/g) α-alumina (SA 5397, Norton), which was an "inert" material and was also used for diluting the other examined FT catalysts,

- a high-α (~0.9) 25pbw Co-18pbw Zr-100pbw SiO_2 catalyst, synthesized at RTI,

- a high-α (~0.9) 20wt% $CoOx$/Al_2O_3 catalyst, provided by Energy International,

- a very-high-α (~0.95) Fe/K/Cu/SiO_2 catalyst, synthesized by the Hampton University, RTI, University of Pittsburgh team under a previous DOE contract (DE-FG22-96PC96217), and

- a very-high-α (0.95 or more) 0.5wt% Ru/alumina catalyst (synthesized at North Carolina State University, in sub-contract to RTI).

Preliminary FT synthesis runs were performed on the α-alumina catalyst at 208 and 270°C, so as to establish a "blank" activity in the absence of a metal-supported FT catalyst. This α-alumina catalyst exhibited no measurable activity for FT synthesis at 208°C and 270°C; thus, its presence did not contribute to the activity measurements for the other examined catalysts.

The chain-limiting concept was examined on the two cobalt-supported FT synthesis catalysts using a series of pulse runs of varying pulse gas, pulse frequency, and pulse duration.

"Blank" pulse runs (i.e., involving a switch between two feed streams of the same composition) had no effect on the progress of FT synthesis in terms of activity and product distribution. Pulsing with an inert gas (N_2) gave only minimal variations in catalyst activity (as measured by CO conversion) and product yield for FT reaction.

Pulsing with reactant H_2 resulted in a significant increase in CO conversion, along with an enhanced reaction exotherm, while only instantaneously increasing the selectivity to CH_4. The activity decreased gradually until the next pulse, indicating a tendency to return to its steady-state value, whereas the selectivity to CH_4 is quickly restored to its steady-state value.

The extent of CH_4 formation appears to be correlated to the increase in H_2 concentration as caused by pulsing. The FT reaction, however, appears to have a different dependence on H_2 concentration, since it progressed within a different time frame.

The effect of H_2 pulsing on light hydrocarbon formation is like a *rippling* phenomenon. The formation of paraffinic (and apparently olefinic also) hydrocarbons exhibits a local maximum with respect to the time after the pulse, whereas this maximum shifts to longer times with increasing carbon number. Furthermore, the magnitude of the observed increase in formation is greater for paraffins than for the corresponding olefins, and appears to decline with increasing carbon number.

Addition of 10% steam in the feed causes a decrease in catalytic activity and suppresses the formation of CH_4 while enhancing the formation of CO_2 by enhancing the extent of the water gas shift reaction. It increases the olefin/paraffin ratio of the light hydrocarbons. Application of a H_2 pulse in the presence of added steam decreases this olefin/paraffin ratio.

A decrease in syngas concentration has a strong suppressing effect in the olefin/paraffin ratio of the light (C_2-C_9) hydrocarbons. Higher syngas concentration (and lower space velocity, to a lesser extent) can increase the chain growth probability α and thus serve as a more favorable reaction condition for investigating the effect of pulsing.

Hydrogen pulsing has only minimal effect on the activity and product distribution of the Ru/alumina FT synthesis catalyst, which exhibited enhanced activity towards methanation and water-gas-shift reaction. This could be due to a lower reaction pressure (ca. 28 atm) and higher reaction temperature compared to those commonly used for supported-Ru FT catalysts (typically 100-1000 atm, 160-170°C). Application of a second reduction procedure produced a better-activated catalyst, exhibiting the same activity at lower temperatures, along with lower selectivity to undesirable compounds CH_4 and CO_2. Still there is only minimal impact of H_2 pulsing on the catalyst performance even after the second reduction.

Hydrogen pulsing has a positive effect on the C_{10}-C_{20} yield of the high-α Fe/K/Cu/SiO$_2$ FT catalyst. However, it also causes a significant decrease in catalyst activity (CO conversion) and an undesirable increase in the selectivity to CH_4. Pulsing with CO also has a positive effect on the C_{10}-C_{20} yield and no measurable effect on the selectivity to CH_4 and CO_2, and causes only a moderate decrease in CO conversion. Pulsing with a 24%CO_2/N_2 gas mixture has essentially no effect on catalytic activity or product distribution (α-value, C_{10}-C_{20} yield).

An increase in reaction pressure enhances the activity of the HPR-43 (Fe/K/Cu/SiO$_2$) FT catalyst studied in a CSTR. The yield of all the products of the reaction (CO$_2$, CH$_4$, C$_2$-C$_4$ light gases, and desirable C$_{5+}$ hydrocarbons) increases with increasing reaction pressure. However, due to enhanced activity of the catalyst towards CO$_2$ at the high temperature of the experiment, the C$_{5+}$ product as fraction of the total converted carbon decreased with increasing pressure. An increase in reaction pressure also decreases the olefin/paraffin ratio of the C$_2$-C$_8$ product range. The increase in reaction pressure appears to promote the secondary adsorption of the formed olefins, possibly leading to longer-chain products, and resulting in a lower outlet concentration of olefins.

A decrease in reaction temperature decreases the activity as well as the yield of all reaction products of HPR-43. However, due mainly to a lower selectivity towards CO$_2$, the C$_{5+}$ product as fraction of the total converted carbon increases with decreasing temperature.

An increase in the feed H$_2$:CO ratio increases the activity as well as the yield of all reaction products of HPR-43. However, it decreases the C$_{5+}$ product as fraction of the total converted carbon. An increase in the feed H$_2$:CO ratio also decreases the olefin/paraffin ratio of the C$_2$-C$_8$ product range. Higher concentrations of inlet H$_2$ tend to enhance the rate of hydrogenation of olefins, suppressing their outlet concentration while enhancing the outlet paraffin concentration, thus decreasing the measured olefin/paraffin ratio.

Main Conclusions

H$_2$ pulsing increases the catalytic activity of cobalt-based FT synthesis catalysts while only briefly increasing the undesirable formation of CH$_4$. An increase in the H$_2$ pulse frequency enhances the selectivity to C$_{10}$-C$_{20}$ compounds (while maintaining or slightly decreasing the selectivity to CH$_4$), but the chain-growth probability α remains essentially unaffected. An increase in the H$_2$ pulse duration increases the maximum obtained CO conversion as well as the instantaneous selectivity to CH$_4$.

Higher syngas concentration (and lower space velocity, to a lesser extent) can increase the chain growth probability α and thus serve as a more favorable reaction condition for investigating the effect of pulsing. Also, H$_2$ pulsing is a simple method to overcome the loss of activity and shift in paraffin vs. olefin selectivity caused by the presence of excess steam. An optimum set of pulse parameters (pulse frequency, pulse duration) is required for maximizing the yield of desirable (diesel-range) C$_{10}$-C$_{20}$ products.

Hydrogen pulsing has a positive effect on the C$_{10}$-C$_{20}$ yield of a high-α Fe/K/Cu/SiO$_2$ FT catalyst. However, it also causes a significant decrease in catalyst activity (CO conversion) and an undesirable increase in the selectivity to CH$_4$. Pulsing with CO also has a positive effect on the C$_{10}$-C$_{20}$ yield and no measurable effect on the selectivity to CH$_4$ and CO$_2$, and causes only a moderate decrease in CO conversion.

FT synthesis experiments using an iron-based catalyst in a CSTR indicate that lower reaction temperatures appear to favor the C$_{5+}$ selectivity, whereas high H$_2$:CO ratios appear to be less favorable towards the selectivity to the desirable C$_{5+}$ product fraction.

Recommendations

Pulsing experiments on FT synthesis catalysts (either cobalt-based or iron-based) should be performed under conditions that maximize the yield of the heavy hydrocarbon products (high chain-growth probability α). These conditions are: high synthesis gas partial pressure (high total reaction pressure, minimal or no presence of inerts), and low space velocity. High temperatures favor the formation of excess light gases, so moderate temperatures are more preferable for pulse-type runs.

More aggressive pulsing conditions (specifically, higher pulse frequency) need to be examined, in order to establish the long-term impact of pulsing on product formation beyond experimental uncertainty. Also, more emphasis should be given to pulsing experiments using the CSTR. The superior control of the catalyst temperature in the CSTR compared to the FBR would allow the evaluation of a more extensive range of pulsing parameters (pulse frequency and duration) and their true intrinsic impact on the performance of the catalyst for FT synthesis.

Publications

"Effect of Periodic Pulsed Operation on Product Selectivity in Fischer-Tropsch Synthesis on Co-ZrO$_2$/SiO$_2$", A.A. Nikolopoulos, S.K. Gangwal, and J.J. Spivey, in *Studies in Surface Science and Catalysis* **136**: *Natural Gas Conversion VI* (E. Iglesia, J.J. Spivey, and T.H. Fleisch, eds., Elsevier Science) (2001) 351.

Presentations

1. "Fischer-Tropsch Synthesis on a Co-ZrO$_2$/SiO$_2$ Catalyst: Effect of H$_2$ Pulsing", 17th North American Catalysis Society Meeting, Toronto, Canada, June 3-8, 2001.

2. "Effect of Periodic Pulsed Operation on Product Selectivity in Fischer-Tropsch Synthesis on Co-ZrO$_2$/SiO$_2$", 6th Natural Gas Conversion Symposium, Girdwood, Alaska, June 17-21, 2001.

Keywords

Chain-limiting
Cobalt
Diesel
Fischer-Tropsch synthesis
Iron
Pulsing
Ruthenium

1. INTRODUCTION

The Fischer-Tropsch synthesis (FTS) can convert solid fuel- or natural gas-derived syngas ($CO+H_2$) to liquid fuels and high-value products. The extensively reviewed Fischer-Tropsch (FT) reaction [1-3] produces a non-selective distribution of hydrocarbons (C_1-C_{100+}) from syngas. FT catalysts are typically based on Group-VIII metals (Fe, Co, Ni, and Ru), with Fe and Co most frequently used. The product distribution over these catalysts is generally governed by the Schultz-Flory-Anderson (SFA) polymerization kinetics [4].

Currently there is significant commercial interest in producing diesel-fuel range middle distillates (C_{10}-C_{20} paraffins) from natural gas-derived syngas [5]. Increasing the selectivity of FTS to desired products such as diesel (C_{10}-C_{20}) or gasoline (C_5-C_{11}) by altering the SFA distribution is economically attractive. Use of bifunctional catalysts (FT-active metals on zeolite, e.g. ZSM-5) to produce high-octane gasoline-range hydrocarbons (explored in the past 2 decades), has been economically unsuccessful [6-9]. The zeolite cracking activity lowers the chain-growth probability (α), producing gasoline-range products in excess of 48wt% of the total hydrocarbon, but it also produces a significant amount of undesirable C_1-C_4 gases (Figure 1.1).

The present emphasis has shifted towards maximizing the yield of high-cetane C_{10}-C_{20} products from FTS. Increased worldwide demand for low-sulfur diesel has further stressed the importance of development of zero-sulfur FT-diesel products. An alternative approach to the use of bifunctional catalysts to alter selectivity is periodic FT reactor operation (pulsing) [3]. It entails alternatively switching between two predetermined input compositions over the FT catalyst to promote time-average rate, selectivity, and catalyst life [10-12].
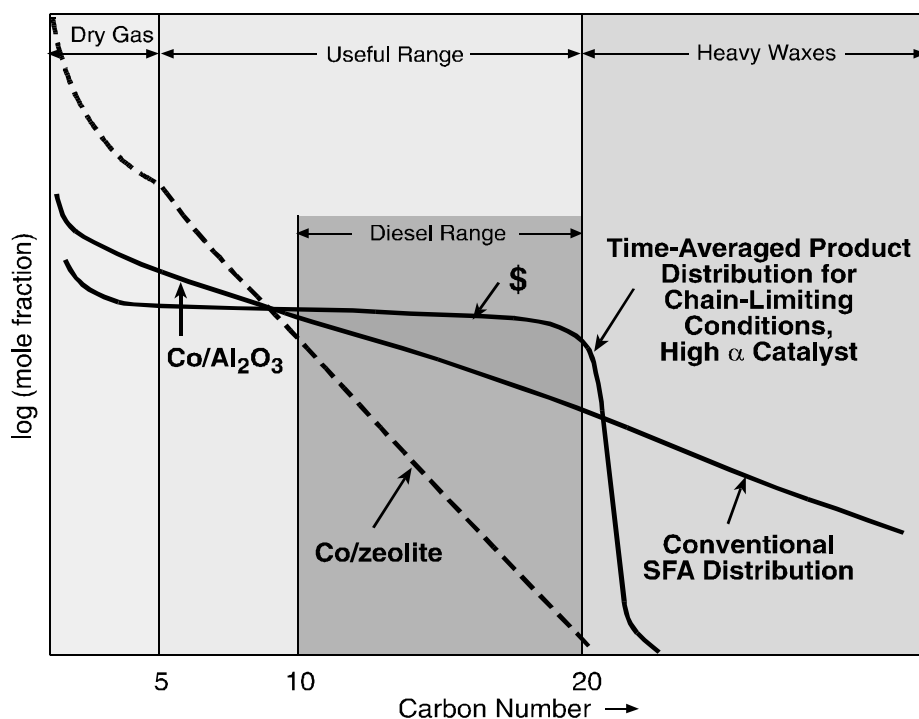
Figure 1.1.   Product distribution (α-plot) for FT synthesis

Periodic pulsing of H_2 has been examined so as to limit chain growth by removing the growing hydrocarbon chain from the catalyst surface [13-15]. Experimental studies have shown the potential to alter the SFA distribution [16,17]; they were performed, however, at conditions of limited industrial interest.

The chain-limiting concept using pulsing to maximize the diesel yield is shown in a plot of carbon number vs. mole fraction (Fig. 1.1). The slope of the curve is determined by the chain-growth probability, **α**. Periodic operation on a high-**α** catalyst may result in removal of the growing chain from the surface at the desired C_{10}-C_{20} length, thereby maximizing diesel yield without increasing the dry gas.

The objective of this study was to investigate the effect of pulsing on the activity and product distribution of high-**α** FT synthesis catalysts, in an attempt to maximize the C_{10}-C_{20} product yield.

2. EXPERIMENTAL

2.1. Fixed-Bed Reactor (FBR) Set-Up

The reaction system consisted of the gas-feed, a fixed-bed reactor, and a sampling & analysis system for the gas and liquid products. This system has been designed to operate continuously (24 h/day, 7 days/week) at a pressure of up to 600 psig and a temperature of up to 500°C (932°F). Up to 18 cm^3 of catalyst can be loaded into the 3/8-inch o.d. (0.305-inch i.d.) reactor, with a bed height of up to 15 inches. The process flow diagram for the fixed-bed reaction system is shown in Figure 2.1.1.

The feed system blended CO/Ar, H_2, N_2, other premixed gases, and steam (as needed) in desired concentrations. Ar was used as internal standard, to provide information on the outlet flow rate and conversion. The feed streams entered through the top of the reactor at space velocities from 300 up to 9000 scc per cc catalyst per h. Mass flow controllers (Brooks) were used to control the flow rate of the feed streams. They were rated from zero to 200 scc/min, except that for CO, which was rated up to 100 scc/min. They operated in a fail-closed mode in order to stop the flow of the feed gases to the reactor in the event of a power/controller failure.

V-151	T-150	P-152	HTR-201	R-200	V-321	V-311	V-312	V-322
Water Tank	Carbonyl Trap	Water Pump	3-Zone Furnace	Reactor	Left Water Trap	Left Wax Trap	Right Wax Trap	Right Water Trap
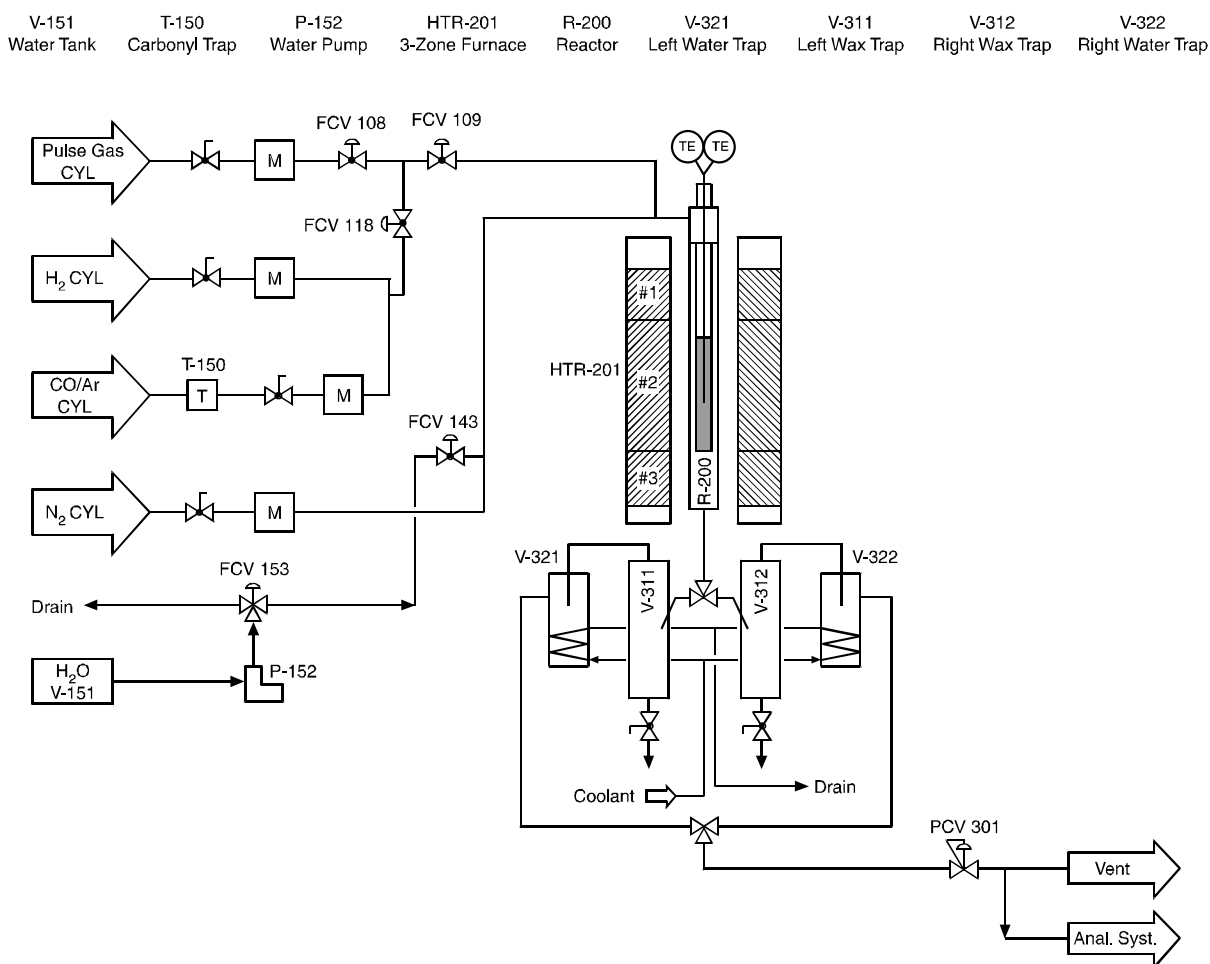
Figure 2.1.1. Process flow diagram of the fixed-bed reaction system

The addition of steam was accomplished by vaporizing water fed at a constant liquid flow rate, using a high-performance liquid chromatography pump. This pump could be set to deliver flows down to 0.001 mL/min. The water was fed into a heated N_2 line where it was converted to steam. The N_2 mixed with the steam and carried it to the reactor. The entire steam line (after mixing with N_2) was maintained at 155°C (311°F). The water vapor pressure at this temperature corresponded to 20% steam in the feed gas to the reactor at 375 psig.

A time-programmable interface system (Carolina Instrumentation Co.) was used to control a series of actuated valves, so that a (reactant or inert) flow opened / closed automatically and independently of the others. Appropriate periodic switch of these valves offered the capability to perform various pulsing-type experiments with this configuration. Pulse time could be varied from 1 min to 48 hours. All valves automatically switched to their respective fail-safe position (N_2 flow open, all others closed) in the event of power failure.

Except for the ¼-inch lines that connected the reactor outlet to the two wax traps (placed in parallel, Fig. 2.1.1), 1/8-inch stainless steel lines were used throughout the unit for the flow of the feed gases and for removing the light gas products. These lines were heated with heating tapes and were insulated to provide sufficient temperature control. The surface temperature of these lines (which was monitored by thermocouples) was quite stable. The lines exiting the two wax traps were maintained at a higher temperature than the traps themselves to prevent any condensation in the lines.

The stainless steel downflow reactor was enclosed in a three-zone programmable furnace. The reactor itself consisted of two annular tubes. The outer tube was 0.5-inch o.d. with a 0.049-inch wall thickness. The inner reactor tube, which housed the catalyst bed, had a 3/8-inch o.d. and 0.035-inch wall thickness (0.305-inch i.d.). A 90-μm sintered stainless-steel frit, held in place by a welded cap, was placed at the bottom of the insert. It supported the catalyst bed and prevented the removal of catalyst fines from the catalyst bed into the liquid product stream.

The three controllers corresponding to each one of the three zones of the furnace were temperature programmable. An "empty reactor test" was carried out to determine the set points of the three-zone furnace to maintain a minimum temperature differential axially down the bed. These were: a) top zone: T+2, b) middle zone: T, and c) bottom zone T-3 (all in °C). Each of the three zones had two thermocouples (one for control and one for high limit) touching the outer wall of the 0.5-inch reactor housing. The entire catalyst bed was located in the middle zone. A "dual-profile" internal bed thermocouple measured the bed temperature at two points: 1 inch from the top of the bed and 3 inches from the bottom of the bed.

Two wax traps, maintained at 140°C (284°F), were used for collecting the wax product. They were placed in parallel, to ensure continuous operation. Each of these traps could hold up to 13 cm^3 of liquid, allowing the reactor to operate typically for 24 to 48 hours before switching from one trap to the other. The inclined lines from the reactor outlet to these traps allowed for the wax to drip downwards and collect in the traps. This design provided for continuous downflow of the wax by eliminating horizontal sections that might lead to wax buildup in the lines. Heating these downflow lines also eliminated the chance for condensation of the wax.

Two water traps were also placed in parallel after the wax traps, to allow for continuous operation. The condensables, mainly water and some hydrocarbons, condensed in the water traps, which were maintained at system pressure. The water traps were cooled down to ca. 20°C (68°F) using a coolant flowing through tubing coils attached to the cylindrical surface of the traps. A recirculator was used for continuous constant coolant flow.

A Kammer back-pressure-control valve, located down-stream of the traps, controlled the reactor and trap pressure. The valve maintained the set pressure even when the flow changed rapidly. The valve was kept at 85°C (185°F) to prevent hydrocarbon condensation due to expansion cooling. To ensure safe operation the valve opened up fully in the event of an actuator air pressure loss or power failure.

The typical procedure for loading the catalyst into the reactor was as follows: first, 3.6 cm^3 of a low surface-area (~0.2 m^2/g) high-purity α-alumina (SA 5397, Norton) were loaded into the reactor, forming a 3-in.-high bed. Then, typically 2 cm^3 of catalyst was physically mixed with 10 cm^3 of the α-alumina and loaded into the reactor. This mixing was performed in three steps, each involving one third of the amounts of catalyst and α-alumina being homogeneously mixed in each one of three vials. The contents of the vials were sequentially loaded into the reactor under mild tapping, to ensure good settling of the bed without separation of the catalyst and the alumina. Finally, 2.4 cm^3 of α-alumina were added to form a preheat zone of 2 inches at the top of the bed. Thus, the catalyst bed was placed between two zones of α-alumina. A schematic of the reactor and catalyst bed configuration is shown in Figure 2.1.2.
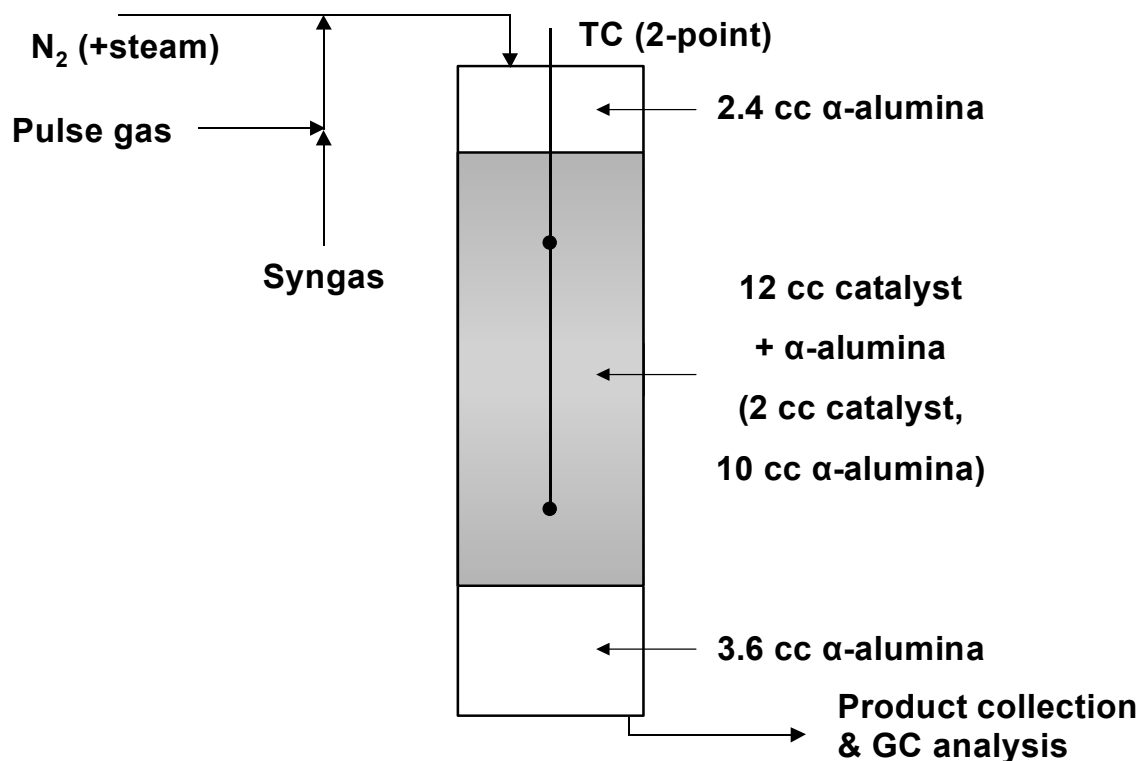
Figure 2.1.2. Schematic diagram of the fixed-bed reactor

2.2.   Continuous Stirred-Tank Reactor (CSTR) Set-Up

The CSTR reaction system included the gas feed, the 1-liter continuous stirred-tank reactor, and the sampling and analysis system for the gas and liquid products. The process flow diagram for the fixed-bed reaction system is shown in Figure 2.2.1.

The feed system blended CO/Ar and H_2 (or N_2) in desired concentrations, using a set of two mass-flow controllers (Brooks). The mass-flow controllers operated in a fail-closed mode in order to stop the flow of the feed gases to the reactor in the event of a power/controller failure. With the use of 3-way valves, high-pressure high-purity N_2 could flow through either one or both of the two mass-flow controllers. This feed system was constructed as a partial extension of the fixed-bed reactor feed system (Fig. 2.1.1) but by-passing the actuated valves that were used for the pulsing experiments in the fixed-bed reaction system.

The reactor was a 1-liter stainless-steel bolted-closure continuous stirred-tank reactor (CSTR, from Autoclave Engineers), with a 4.9-inch diameter and 8.7-inch height, positioned in a single-zone furnace. It was rated at 5800 psig (395 atm) at 650°F (343°C). A stainless-steel liner was positioned inside the reactor, to facilitate loading and unloading the hydrocarbon liquid medium and the catalyst. The contents of the reactor were stirred using a (MagneDrive) magnetically actuated packless impeller system with a straight-blade turbine. The impeller speed was controlled by a motor (achieving stirring speeds of up to 3300 RPM) and indicated by an analog tachometer. A stirring speed of 800 RPM was typically applied. The impeller head containing the driver magnets was cooled by flowing water.

HTR-550	R-540	M-541	V-560	V-570	V-580
RXTR HEATER	STIRRED-TANK REACTOR	AGITATOR DRIVE	WAX RECEIVER	HOT TRAP	COLD TRAP
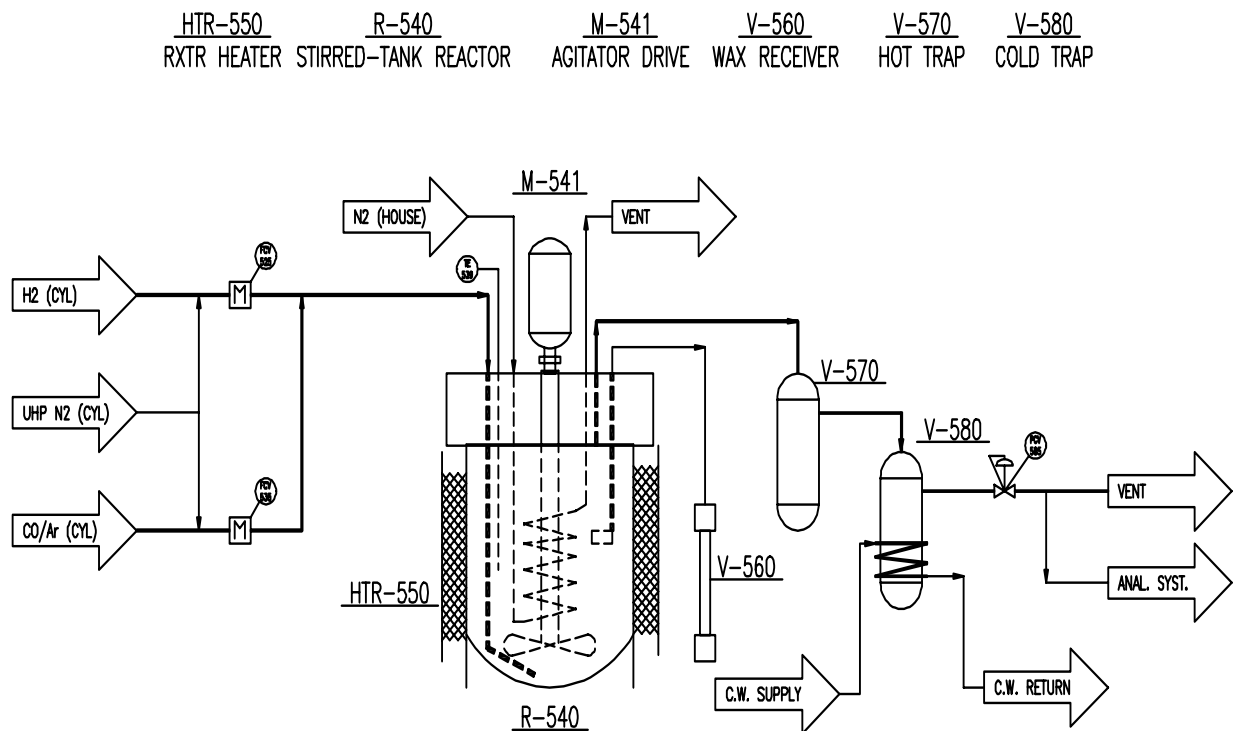
Figure 2.2.1. Process flow diagram of the continuous stirred-tank reaction system

The reactor also included: a thermowell, containing a K-type thermocouple, to indicate the reaction temperature, a port connected to pressure gage, to indicate the reaction pressure, a blow pipe, for feeding the reactant gases, an exit port, for the exiting gases, and a liquid sample tube, for removing liquid samples into a liquid receiver. It also included a sparge tube and a cooling coil that were not used.

The liquid receiver was a 50mL sample cylinder (1-inch outside diameter and 6.25-inch height) maintained at 130°C. The exiting gases passed through a hot trap (also a 50mL sample cylinder, 1-inch outside diameter and 6.25-inch height) maintained at 130°C, to collect droplets of liquid that may be entrained by the gases, and through a cold trap (a 150mL sample cylinder, 2-inch outside diameter and 5.25-inch height) maintained at 25°C by external cooling with flowing water, to condense the produced steam.

Again, in a manner similar to that applied for the fixed-bed reaction system, 1/8-inch stainless steel lines were used throughout the unit for the flow of the feed gases and for removing the light gas products. These lines were heated with heating tapes and were insulated to provide sufficient temperature control. The surface temperature of these lines (which was monitored by thermocouples) was quite stable. The lines exiting the two wax traps were maintained at a higher temperature than the traps themselves to prevent any condensation in the lines.

A back-pressure regulator (Tescom) located downstream of the traps, controlled the reactor and trap pressure. After passing through the back-pressure regulator, the outlet gases were sent to the vent and the analytical system (described in the next section).

The typical procedure for loading the catalyst into the reactor was as follows: first, the stainless-steel liner was filled with 225 cc (186.75 g, density of 0.83 g/cc) of Oronite Synfluid PAO 8 cSt (CAS 68037014). This is a clear, colorless, odorless liquid, which is a hydrogenated 1-decene-based homo-polymer with vapor pressure of 0.1 mm Hg at 232°C (450°F). Then, 15 cc (15 g) of catalyst were typically added, and the liner containing the catalyst and the synfluid was positioned inside the reactor vessel. The reaction system was pressurized under N_2 and the stirrer was typically set to 800 RPM.

2.3.   Analytical System

The analytical system included two on-line gas chromatographs and one off-line gas chromatograph for the analysis of the permanent gases and light hydrocarbons, and the waxes, respectively. It was used for the analysis of the products of either of the two reaction systems described in the previous sections, namely the fixed-bed reactor and the CSTR.

An on-line Carle GC equipped with a thermal conductivity detector (TCD) analyzed the permanent gases (H_2, CO_2, Ar, N_2, CH_4, CO). Argon was used as internal standard. Separation of these species was achieved using a combination of a porous polymer, molecular sieve column, and a palladium membrane (which acted as a hydrogen transfer tube, for hydrogen separation). Helium was used as the carrier gas with a flow of 30 cc/min, while nitrogen was used for the hydrogen transfer line. A typical chromatogram from the Carle GC is shown in Figure 2.3.1.

An on-line HP5890 GC equipped with a flame ionization detector (FID) analyzed the light hydrocarbons (C_1-C_{15}). It used a Petrocol column, which is essentially a boiling point separator. The column was 100 m by 0.25 mm, with a film thickness of 0.50 μm. The thick film helped in the separation of the light hydrocarbons. The column was temperature-programmed from -25°C (-13°F) to 300°C (572°F). A helium flow of 1.28 cc/min gave optimum separation. Calibration standards of n-paraffins, olefins, and iso-paraffins were used to identify the retention times and response factors for the species of interest. The total analysis time was 70 minutes. A typical chromatogram from the HP5890 GC is shown in Figure 2.3.2.
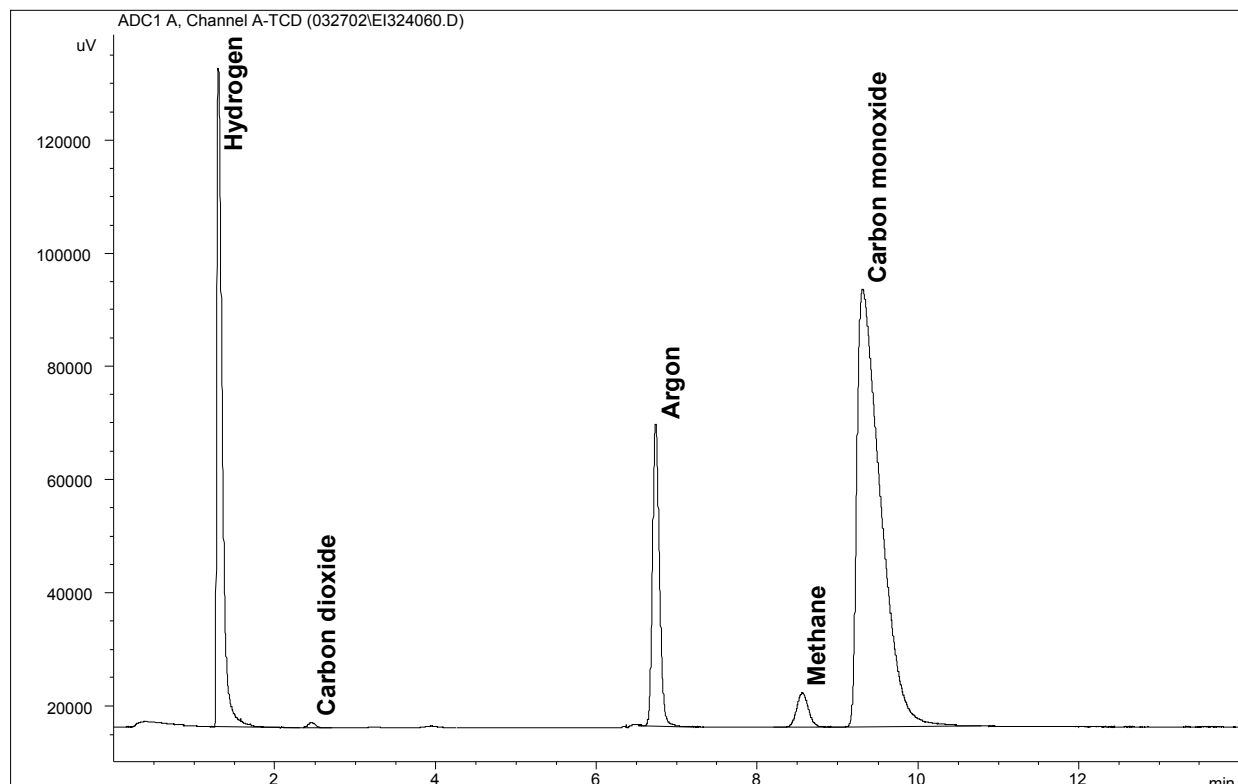
Figure 2.3.1.   On-line GC analysis of the permanent gases – TCD signal
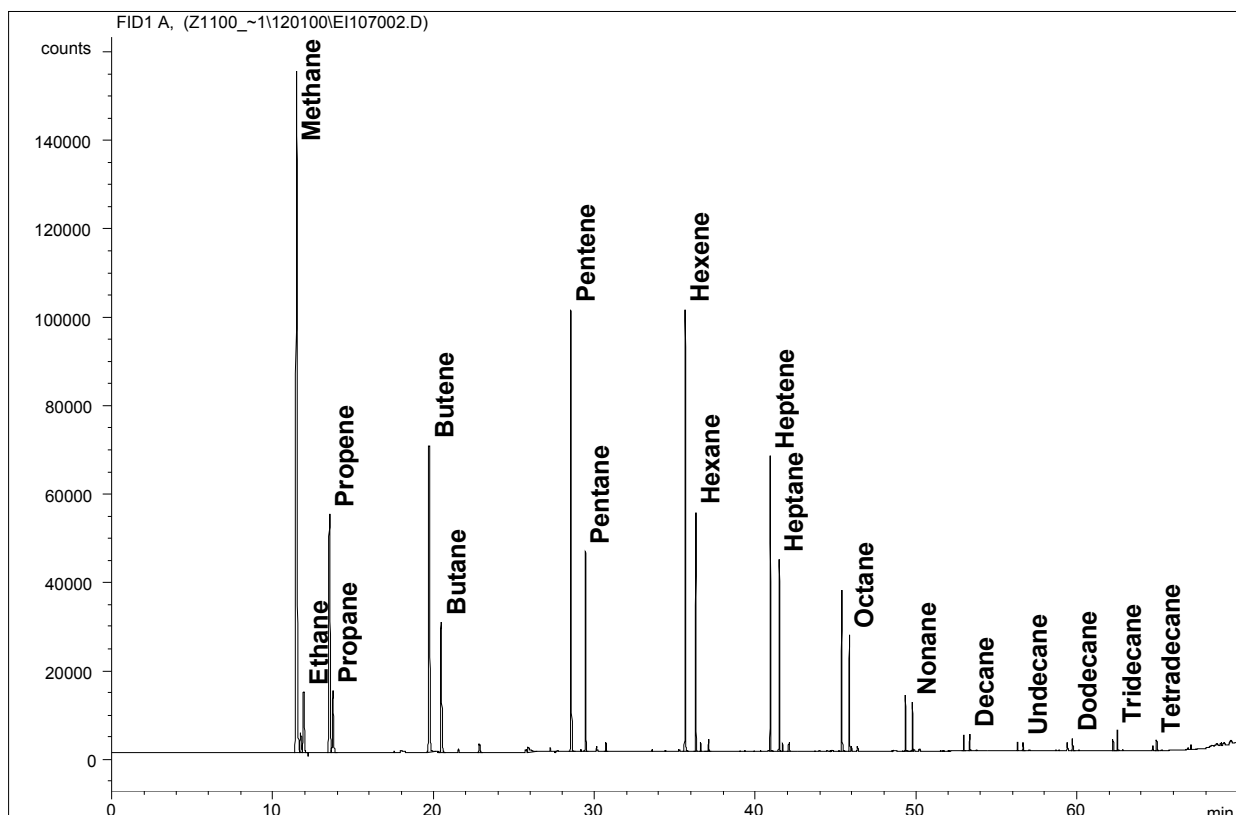
Figure 2.3.2. On-line GC analysis of the light hydrocarbons (C_1-C_{15}) – FID signal

An off-line HP6890 GC equipped with a flame ionization detector (FID) was used for analyzing the wax collected in the wax traps and the oil phase over the water collected in the water traps. The oil was added into the vial containing the collected wax and they were heated beyond the melting point of the wax until forming a homogeneous liquid phase. Two droplets of this liquid were transferred into a 5-ml vial and dissolved with carbon disulfide. A micro-syringe was used to draw 1 µL of sample and inject directly into the GC.

The GC contained a thin-film capillary column (SPB-1, with a 0.10-µm thickness and 15 m in length). Due to its short length, there was very little retention in this column. Hence, waxes up to C_{60+} could be separated easily. The column was temperature-programmed from 40°C (104°F) to 350°C (662°F). The complete analysis time was 40 min. Calibration standards from C_{12} to C_{60} were run to identify the retention times of the various hydrocarbon species of interest. Helium was used as the carrier gas. A typical chromatogram from the HP6890 GC is shown in Figure 2.3.3.
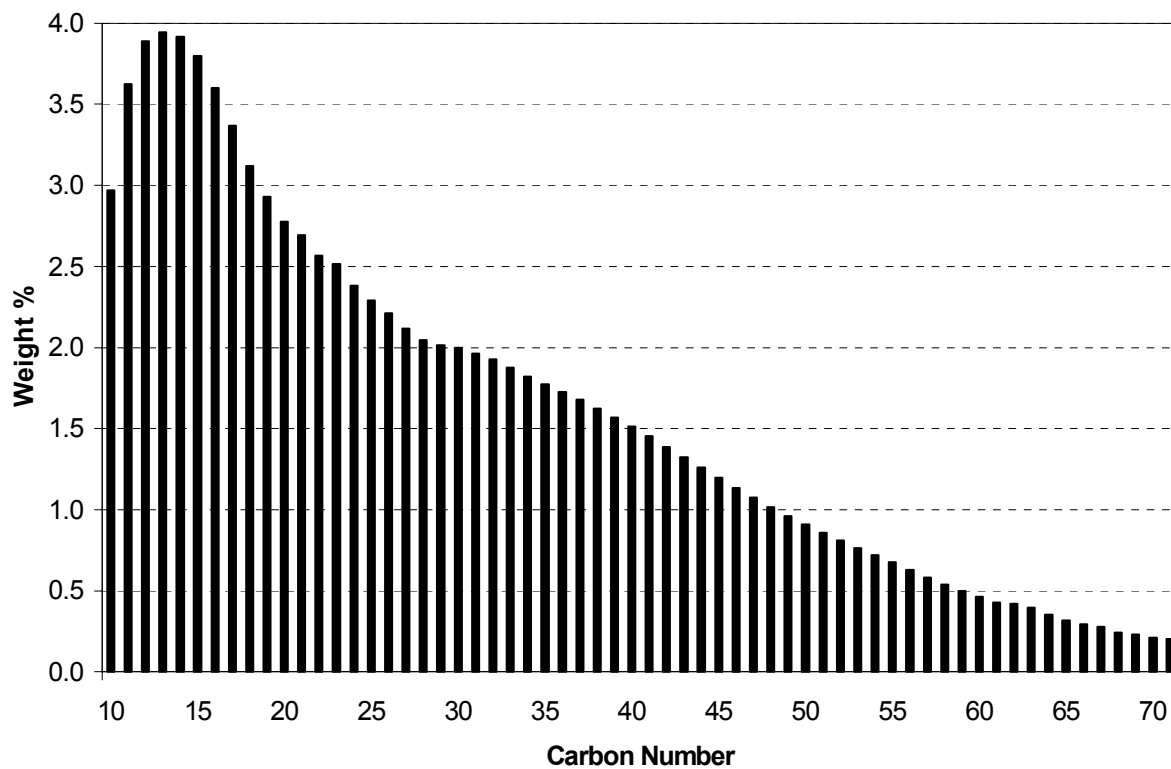
Figure 2.3.3. Off-line GC analysis of the wax hydrocarbons (C_{10}-C_{70}) – FID signal

2.4.   Catalytic Materials

The following catalysts were examined in terms of their activity and product selectivity with respect to the application of various pulse schemes in the fixed-bed reactor:

a) A high-purity, low-surface-area ($0.2\text{-}m^2/g$) α-alumina (SA 5397, Norton), which was used as a baseline; it was also used for diluting the other examined FT catalysts.

b) A high **α** (~0.9) 25pbw Co-18pbw Zr-100pbw SiO_2 (14.5wt% Co − ZrO_2/SiO_2) catalyst, synthesized at RTI (from Ref. [18]).
c) A high-**α** (~0.9) 20wt% $CoOx/Al_2O_3$ (14wt% Co/Al_2O_3) catalyst, synthesized by Energy International.

d) A potentially very-high-**α** (0.95 or more) 0.5wt% Ru/Al_2O_3 catalyst (synthesized at North Carolina State University, in sub-contract to RTI), and

e) A very-high-**α** (~0.95) $Fe/K/Cu/SiO_2$ catalyst (HPR-43), synthesized by the Hampton University, RTI, University of Pittsburgh team under another DOE contract (DE-FG22-96PC96217).

3. RESULTS AND DISCUSSION

3.1. FT Reaction on α-Alumina in a Fixed-Bed Reactor (FBR)

A preliminary FT reaction run was performed on a low surface-area (~0.2 m^2/g) high-purity α-alumina sample (SA 5397, Norton). This alumina was also used for diluting the other examined FT catalysts included in this report. The objective of this experiment was to establish a "blank-run" activity in the absence of a metal-supported FT catalyst.

The fixed-bed reactor was loaded with 17.7 cc (28.32 g) of α-alumina. The sample was *in-situ* exposed to H$_2$ at 350°C for 14 h, and was cooled and pressurized to ca. 300 psig (21.4 atm). The FT reaction started by feeding a 10%Ar/CO gas mix, thus establishing the following base reaction conditions:

> Reactants (50%): H$_2$ = 33.3%, CO = 16.7% (H$_2$:CO = 2.0)
> Inerts (50%): N$_2$ = 48.3%, Ar = 1.7%
> P = 300 psig (21.4 atm), F = 200 scc/min, SV=6000 h^{-1}

The reaction temperature was stabilized at 208°C, thus allowing the reaction to reach a "pseudo-steady state". Under these reaction conditions a moderate (<10%) CO conversion was observed initially (Figure 3.1.1). Then, the α-alumina showed no FT activity, thus establishing a true "blank" run at 208°C.
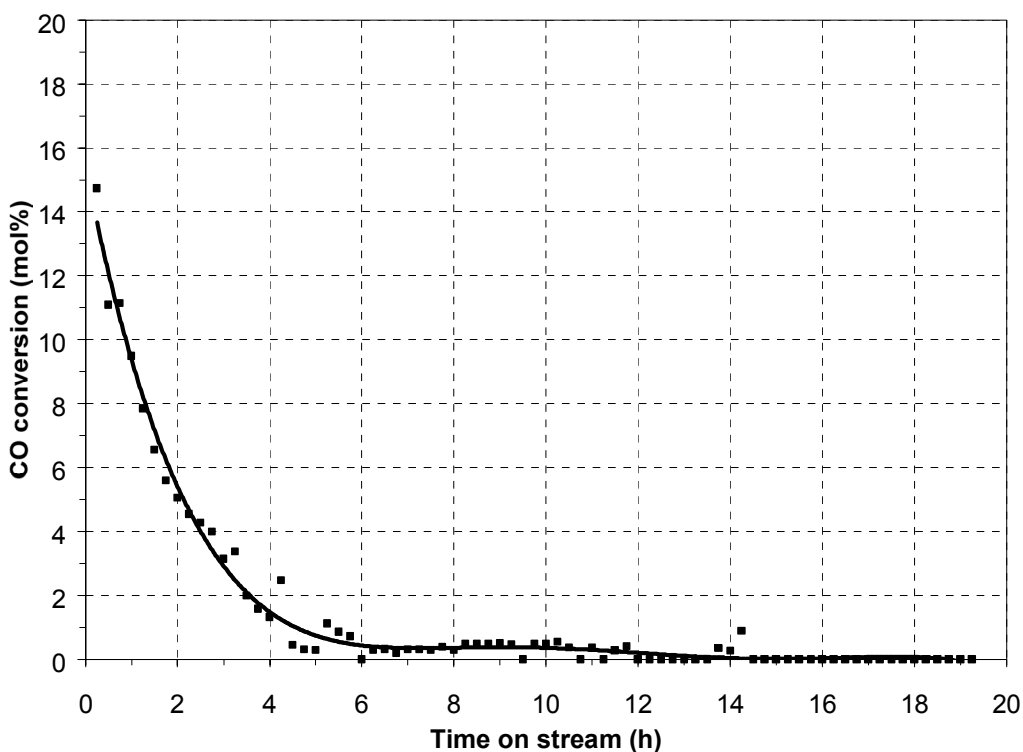
Figure 3.1.1. CO conversion of α-alumina @208°C; P=300 psig; SV=6000 h^{-1}

The reaction temperature was then gradually increased to 270°C (maximum temperature for Fe-FT reaction). The measured CO conversion also remained essentially zero at this reaction temperature. After 4 hours on stream a 1-min H_2 pulse per 1 hour was applied, so as to establish any background activity when pulses are used. Pulse runs involved substituting the reactant feed flow (H_2+CO/Ar) with an equal molar flow of a pulse gas. The total molar flow and the reaction pressure were kept constant between base and pulse runs. Seventeen such H_2 pulses (in a period of 17 hours) were applied. The effect on the outlet H_2:CO ratio is shown in Figure 3.1.2.

Due to the 15-min analysis time of the permanent gases (H_2, CO_2, Ar, N_2, CH_4, CO), only 4 data points could be obtained for every 1-hour pulse cycle. In order to better observe the effect of a given pulse, a "delay time" is defined as the time difference between the end of a pulse and the following GC data point. The need for applying a delay time arises from the fact that a step change in the reactant feed cannot be instantaneously detected due to the dead volume of the reaction/analysis system. A delay time of 5 min was used, i.e., the first 1-min H_2 pulse was completed at 4 hours and 55 min on stream and the next data point was obtained at 5 hours on stream, as shown in Figure 3.1.2.

The results of Fig. 3.1.2 indicate that the applied H_2 pulses caused an increase in the outlet H_2:CO ratio (up to ca. 2.4), but this ratio was quickly restored to a value of ca. 2. A minimal reactor pressure variation (ca. 3 psi, i.e., ca. 1% of the measured pressure) was observed during each pulse. The measured CO conversion was also essentially zero throughout this run, thus establishing a zero-activity baseline for the FT reaction at 270°C even under a typical H_2 pulse sequence.
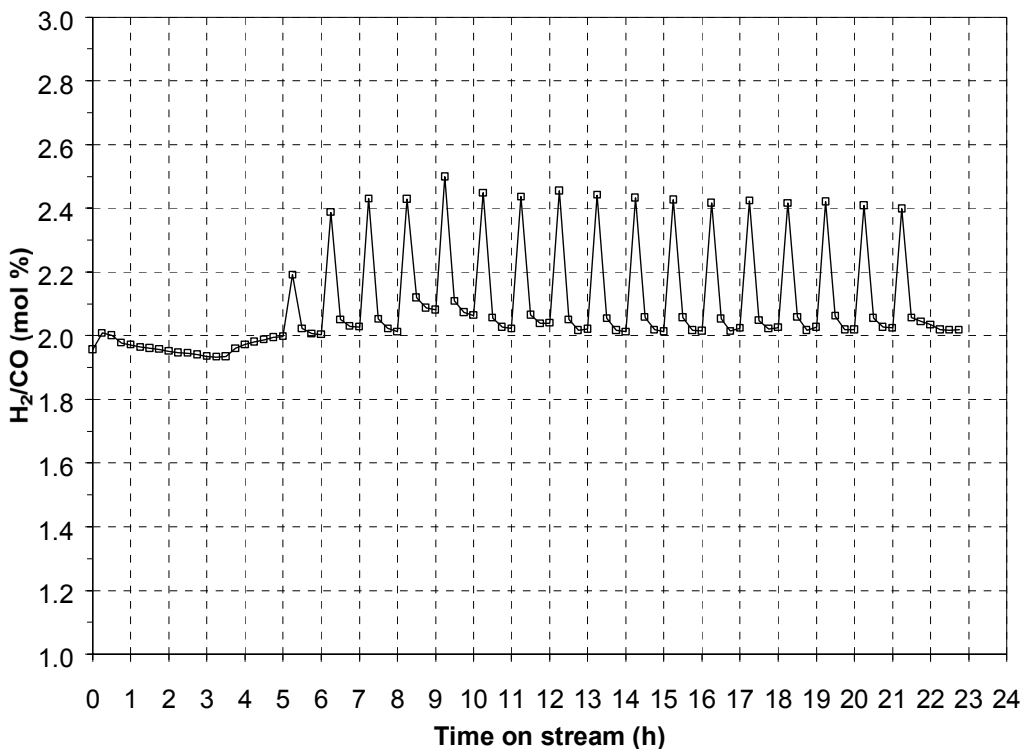
Figure 3.1.2. Effect of H_2 pulse (1 min per 1 hour) on the outlet H_2:CO ratio of α-alumina at 270°C; P=300 psig; SV=6000 h^{-1}

3.2. FT Reaction on 25pbw Co-18pbw Zr-100pbw SiO$_2$ in a Fixed-Bed Reactor (FBR)

A 25pbw Co-18pbw Zr-100pbw SiO$_2$ catalyst (pbw: parts by weight) was synthesized by sequential incipient wetness impregnation of a high-purity, high-surface-area (144-m^2/g) silica support (XS 16080, Norton) [18]. The support was crushed and sieved to a particle size of 100-150 μm) and was degassed in vacuum and then heated to 80°C. A zirconium tetrapropoxide (Zr(OCH$_2$CH$_2$CH$_3$)$_4$) solution in 1-propanol (Aldrich) was used for the incipient wetness impregnation, which was performed in two steps. After each impregnation step, the product was dried (at 120°C, for 2 h) and calcined in air (at 500°C, for 1 hour). The produced material had a nominal loading of 18pbw Zr/silica.

Cobalt was impregnated on the zirconia/silica support using a cobalt nitrate hexahydrate precursor (Co(NO$_3$)$_2$.6H$_2$O, Aldrich). The hexahydrate was dissolved in water and the formed solution was added in a controlled manner to the zirconia/silica support, forming the catalyst with a nominal composition of 25pbw Co-18pbw Zr-100pbw SiO$_2$. Finally, the catalyst was calcined in air at 350°C for 1 hour.

The surface area of the Co-ZrO$_2$/SiO$_2$ catalyst was measured (by BET method) to be 102±3 m^2/g. Its pore volume was estimated at 0.40±0.01 cc/g (by mercury porosimetry). Its crystalline structure was examined by X-ray diffraction (XRD). The predominant phase was Co$_3$O$_4$, with no other Co-O or Zr-O crystalline phases or cobalt silicate present in the diffraction pattern.

A physical mixture of 2 cc (1.55 g) of the calcined Co-ZrO$_2$/SiO$_2$ catalyst and 10 cc (15.91 g) of a low-surface-area (0.2 m^2/g) α-alumina (SA5397, Norton) was loaded into the reactor. The catalyst was reduced *in-situ* under H$_2$ at 350°C for 14 h, and was cooled and pressurized to ca. 300 psig (21.4 atm). The FT reaction was initiated by feeding a 10%Ar/CO gas mix, thus establishing the following base reaction conditions:

> Reactants (50%): H$_2$ = 33.3%, CO = 16.7% (H$_2$:CO = 2.0)
> Inerts (50%): N$_2$ = 48.3%, Ar = 1.7%
> P = 300 psig (21.4 atm), F = 200 scc/min, SV=6000 h^{-1}

The reaction temperature was increased (by 0.5°C/h or less) to 220°C and was stabilized at this value, thus allowing the reaction to reach a "pseudo-steady state". Pulse runs involved substituting the reactant feed flow (H$_2$+CO/Ar) with an equal molar flow of a pulse gas. The total molar flow and the reaction pressure were kept constant between base and pulse runs.

A "blank" pulse run (i.e., switching between two equal flows of H$_2$/CO/Ar reactant mix) was performed in order to identify the possible effect of the periodic pressure disturbance (directly related to the applied pulse) due to non-ideal switching of the actuated valves. This run gave no measurable variation in CO conversion, in the outlet H$_2$:CO ratio, or in the product distribution (α-value, C$_{10}$-C$_{20}$ yield), as seen in Table 3.2.1. Therefore, pulse runs involving no variations in the feed composition have apparently no effect on measurements of the progress of the FT reaction.

Table 3.2.1. Effect of "blank" pulse on the performance of Co-ZrO$_2$/SiO$_2$; T = 220°C

Run type	Pulse gas	T (°C)	X(CO) (%)	S(CH$_4$) (mol%)	Alpha (-)	Y(CH$_4$) (cc/cc/h)	Y(C$_{10}$-C$_{20}$) (cc/cc/h)
Base run	-	220	13.0	14.5	0.89	0.014	0.025
Blank pulse	H$_2$+CO/Ar	220	13.0	15.0	0.89	0.014	0.021

A 1-min N$_2$ (inert) pulse per 1 hour (i.e., substituting the H$_2$/CO/Ar flow, which is 51.7% of the total, with an equal flow of N$_2$ for 1 min every hour) was applied, to examine the effect of inert pulsing on the reaction progress. The N$_2$ pulse gave only minimal variations in activity (CO conversion) or product selectivity (**α**-value, CH$_4$ yield, C$_{10}$-C$_{20}$ yield) as shown in Table 3.2.2, implying that short (1-min) disruptions in reactant flow do not substantially affect the FT reaction.

Table 3.2.2. Effect of inert (N$_2$) pulse on the performance of Co-ZrO$_2$/SiO$_2$; T = 224°C

Run type	Pulse gas	T (°C)	X(CO) (%)	S(CH$_4$) (mol%)	Alpha (-)	Y(CH$_4$) (cc/cc/h)	Y(C$_{10}$-C$_{20}$) (cc/cc/h)
Base run	-	224	15.0	14.5	0.89	0.016	0.027
Inert pulse	N$_2$	224	15.0	14.5	0.89	0.018	0.022
Base run	-	224	15.5	14.0	0.88	0.017	0.027

In contrast to the inert pulse, a 1-min H$_2$ (reactant) pulse caused significant variations in CO conversion and CH$_4$ selectivity. Effects of varying the H$_2$ pulse frequency (1-min H$_2$ per 1, 2, and 4 hours) on the CO conversion and the C$_1$ (CH$_4$ and CO$_2$) selectivity are shown in the composite plots of Figures 3.2.1 and 3.2.2, respectively. These plots are composed of 10-hour segments of a series of sequential runs (typically lasting 48 hours, to collect sufficient amounts of oil + wax for the analysis), starting and ending with a base (no pulse) run. The data points correspond to measurements of the reactor effluent gas every 15 minutes.

A 1-min H$_2$ pulse per 1-hour (10-20-hour segment in Figs. 3.2.1 and 3.2.2) caused a significant increase in CO conversion (from 16% to ca. 30%). The measured temperature of the catalyst bed also increased to 226°C, indicating a strong reaction exotherm. The conversion of CO decreased *gradually* until the next H$_2$ pulse. A less-pronounced increase in CO conversion was also observed for the 1-min H$_2$ pulse per 2-h and 4-h runs. The observed decrease in CO conversion after the pulse indicates that the activity tends to return to its steady state (comparing also the base runs before and after the 3 pulse runs). The measured changes in CO conversion cannot be attributed to variations in the inlet CO concentration since the conversion was based on comparing the inlet and outlet *ratios* of CO to the inert Ar (fed at a fixed ratio from a single gas cylinder).

Figure 3.2.1. Effect of H_2 pulse frequency on the CO conversion of Co-ZrO_2/SiO_2; P = 300 psig; SV = 6000 h^{-1}
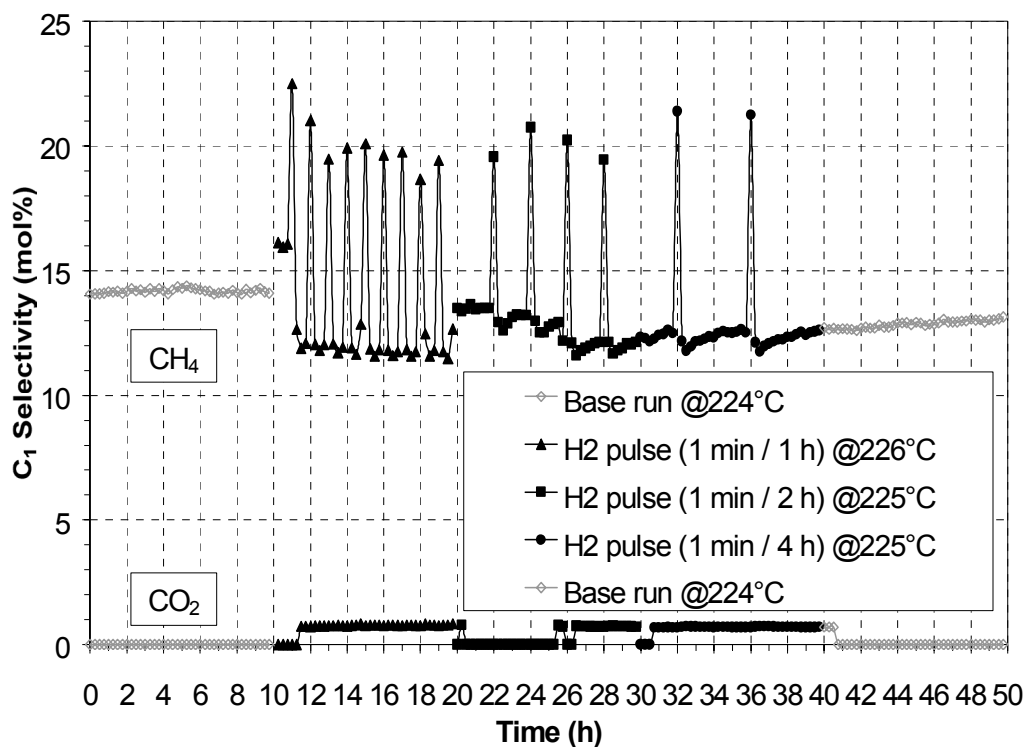
Figure 3.2.2. Effect of H_2 pulse frequency on the C_1 selectivity of Co-ZrO_2/SiO_2; P = 300 psig; SV = 6000 h^{-1}

The selectivity to CH_4 was observed to increase *instantaneously* after each H_2 pulse (from 13-14% to ca. 20% for all examined pulse runs). It was then quickly restored to its base value (Fig. 3.2.2). Thus, H_2 pulsing increased the catalytic activity while only briefly increasing the undesirable formation of CH_4.

The effect of varying H_2 pulse frequency on the desired C_{10}-C_{20} yield vs. the undesired CH_4 yield is shown in Figure 3.2.3. Pulse frequencies of 1, 0.5, and 0.25, h^{-1} correspond to a 1-min H_2 pulse per 1, 2, and 4 hours, respectively. The zero pulse frequency corresponds to the average of the two no pulse (base) runs before and after the 3 pulse runs.

Both C_{10}-C_{20} and CH_4 yields increased with H_2-pulse frequency (and so did the yield of C_{21+}), obviously due to the enhancement in catalytic activity caused by the pulsing (Fig. 3.2.1). As seen in Fig. 3.2.3, the effect of the 1-min H_2 pulse per 1 hour compared to the (average) base run was to increase the C_{10}-C_{20} yield by ca. 57%, while the CH_4 yield only increased by ca. 34%. Although this comparison entails a temperature change (from 224°C to 226°C), the increase in the C_{10}-C_{20} yield is more than what could be accounted for solely by a 2°C increase in reaction temperature.

The CH_4 selectivity in the pulse runs (13-14% on molar basis) was lower than that of the base runs (15.5%), whereas the selectivity to C_{10}-C_{20} and C_{21+} compounds was higher (28-32% vs. 27%, and 23-24% vs. 20%, respectively). The α-values of the pulse runs (based on the molar fractions of C_{10}-C_{65} products) were found to be essentially identical to that of the base runs (0.890±0.005). Thus, the applied H_2 pulsing apparently does not alter the SFA distribution.
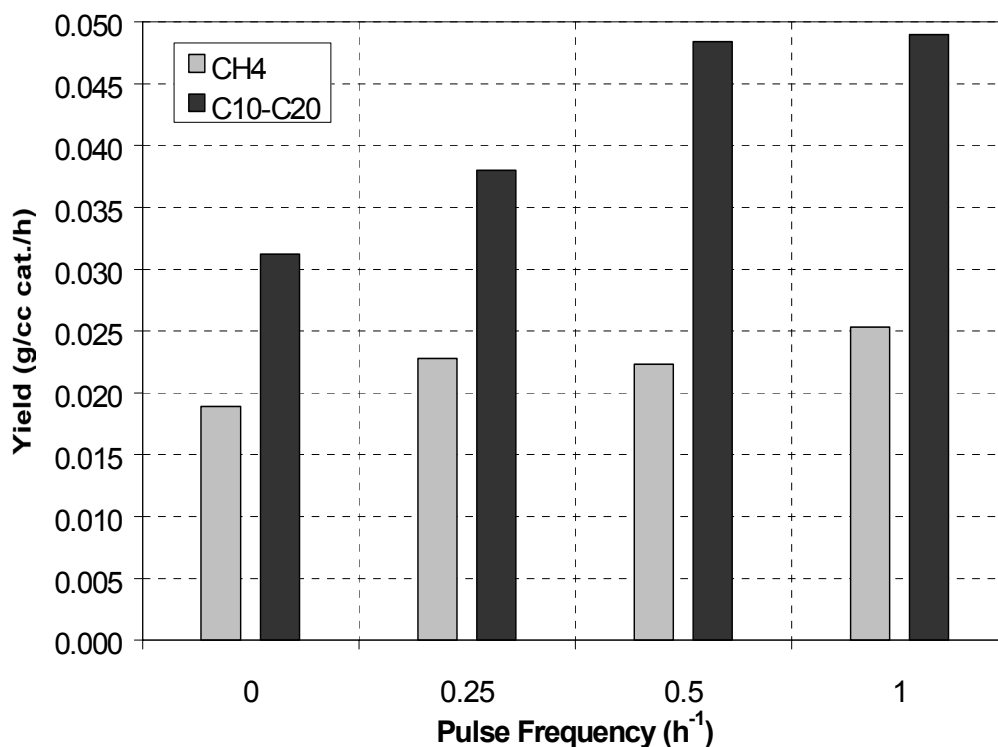
Figure 3.2.3. Effect of H_2 pulse frequency on the product yield of Co-ZrO$_2$/SiO$_2$; P = 300 psig; SV = 6000 h^{-1}

Within the examined pulse frequency range, the greater difference between the yields of the desirable C_{10}-C_{20} and the undesirable CH_4 was obtained at the *intermediate* pulse frequency of 0.5 h^{-1} (1-min H_2 per 2 hours). Also, upon extrapolating to higher H_2-pulse frequencies, we could expect a stronger reaction exotherm and thus an increase in reaction temperature, which is known to cause a shift in FTS product distribution to lower molecular weight compounds and to enhance the methanation reaction [4]. Higher pulse frequencies would thus tend to increase the CH_4 yield much more than the C_{10}-C_{20} yield. An optimum H_2-pulse frequency (depending on catalyst and reaction conditions) would therefore be required for maximizing the C_{10}-C_{20} yield without substantially increasing the CH_4 yield.

Another series of H_2-pulse runs on the Co-ZrO$_2$/SiO$_2$ catalyst examined the effect of H_2-pulse duration on the outlet H_2:CO ratio, the activity, and product distribution, by varying the pulse duration (1, 2, 4-min of H_2) at a fixed pulse frequency (0.5 h^{-1}). The results of this study are given in the plots of Figures 3.2.4, 3.2.5, and 3.2.6, respectively, composed of superimposed 10-hour segments of sequential runs (typically lasting 48 hours), starting and ending with a base (no pulse) run.

As seen in Fig. 3.2.4, an increase in the H_2 pulse duration (1 min, 2 min, 4 min) increased the outlet H_2:CO ratio (from a base value of 1.9 to 2.2, 2.8, and 4.1, respectively). However, this ratio was very quickly restored to its base value of 1.9 (within 20 min, as indicated by the 2nd data point after each pulse). Thus there appears to be no impact of the system "dead" volume (from the catalyst bed to the GC sample loop) on the measured parameters within the examined pulse duration (4 min or less).
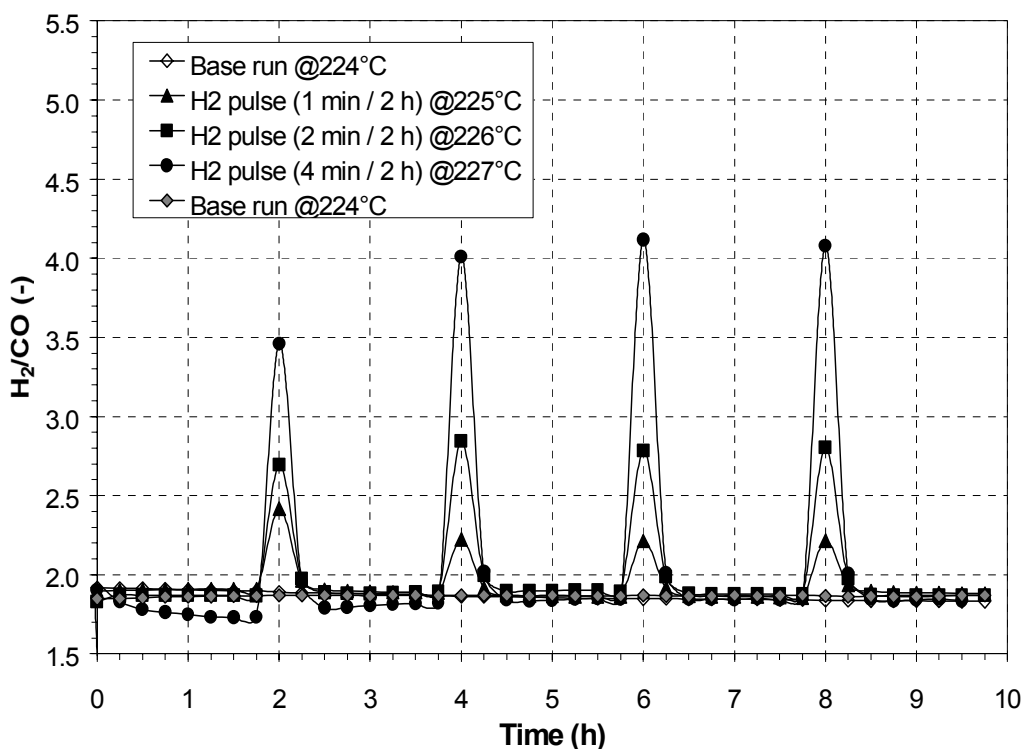
Figure 3.2.4. Effect of H_2 pulse duration on the outlet H_2:CO ratio of Co-ZrO$_2$/SiO$_2$; P = 300 psig; SV = 6000 h^{-1}
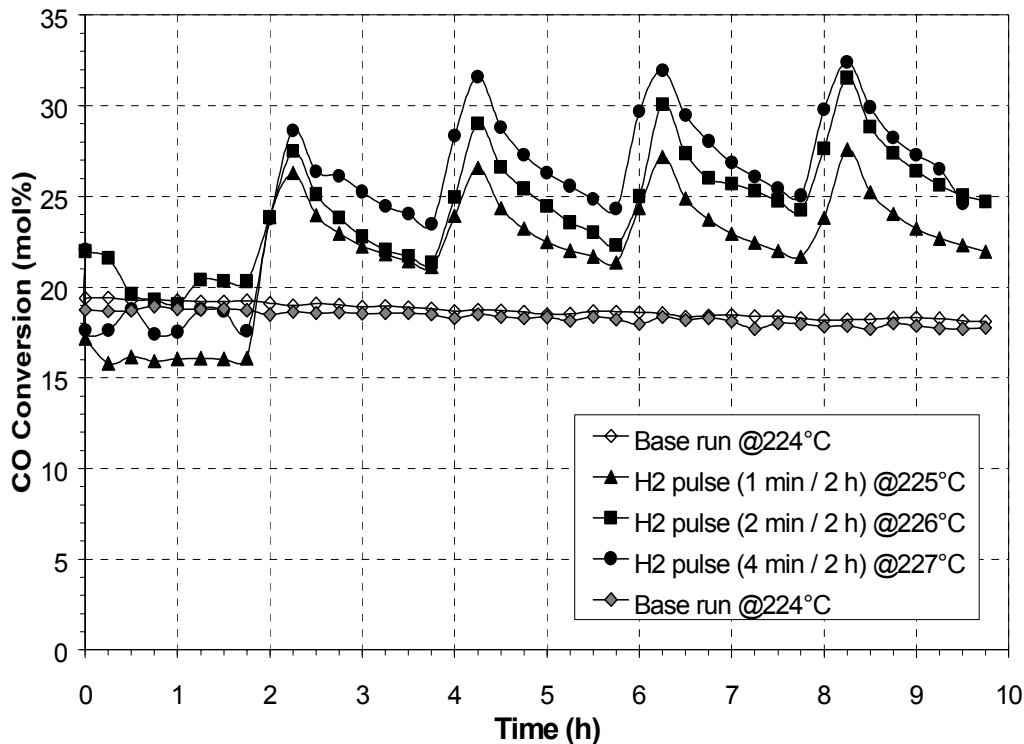
Figure 3.2.5. **Effect of H_2 pulse duration on the CO conversion of Co-ZrO$_2$/SiO$_2$; P = 300 psig; SV = 6000 h^{-1}**
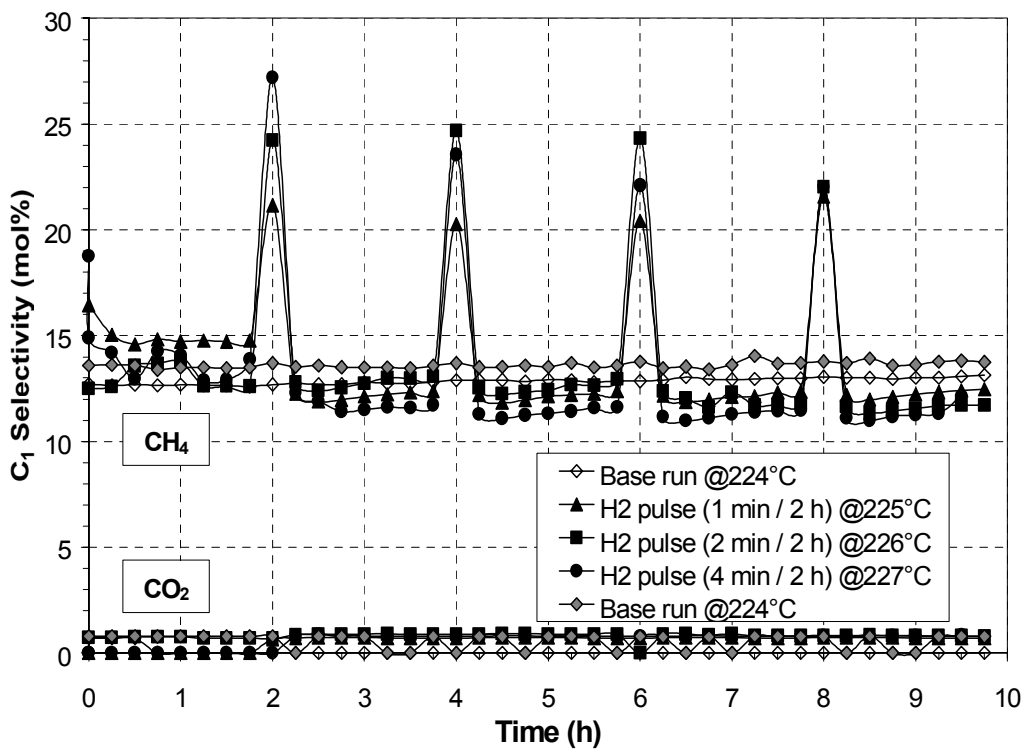
Figure 3.2.6. **Effect of H_2 pulse duration on the C$_1$ selectivity of Co-ZrO$_2$/SiO$_2$; P = 300 psig; SV = 6000 h^{-1}**

As expected, application of a H_2 pulse caused an increase in the measured CO conversion (Fig. 3.2.5). An increase in the H_2 pulse duration (1 min, 2 min, 4 min) increased the maximum obtained CO conversion (from a base value of 18.5% to 27%, 31%, and 32%, respectively). The measured temperature of the catalyst bed also increased (from 224°C to 227°C) indicating a strong reaction exotherm. The conversion of CO decreased *gradually* until the next H_2 pulse (in clear contrast to the observed rapid decrease in the outlet H_2:CO ratio, Fig. 3.2.4). The observed decrease in CO conversion after the pulse indicates that the activity tends to return to its steady state (comparing also the base runs before and after the 3 pulse runs).

The selectivity to CH_4 was observed to increase *instantaneously* after each H_2 pulse and to eventually stabilize to a common maximum value (from 12-14% to ca. 22% for all 3 examined pulse runs). It was then quickly restored to its base value (Fig. 3.2.6). On the other hand, the CO_2 formation remained very low (selectivity below 1%) for both base and pulse runs. The similar time-dependence of the measured outlet H_2:CO ratio and selectivity to CH_4 (Figs. 3.2.4 and 3.2.6) imply a correlation between the increase in H_2 concentration (caused by pulsing) and the extent of the methane formation reaction. The FT reaction, however, appears to have a different dependence on the inlet H_2 concentration compared to the undesirable CH_4 formation, since it progresses within a different time-frame (Fig. 3.2.5).

The effect of H_2 pulse duration on the product distribution of the $Co-ZrO_2/SiO_2$ catalyst is shown in the form of the logarithm of the molar fraction of the hydrocarbon products (C_1-C_{65}) vs. the corresponding carbon number (**α**-plot) in Figure 3.2.7. Only the **α**-plots produced by the initial base run and two H_2 pulse runs are shown for purposes of clarity. A straight line with a slope that corresponds to α = 0.9 is also shown for comparison.
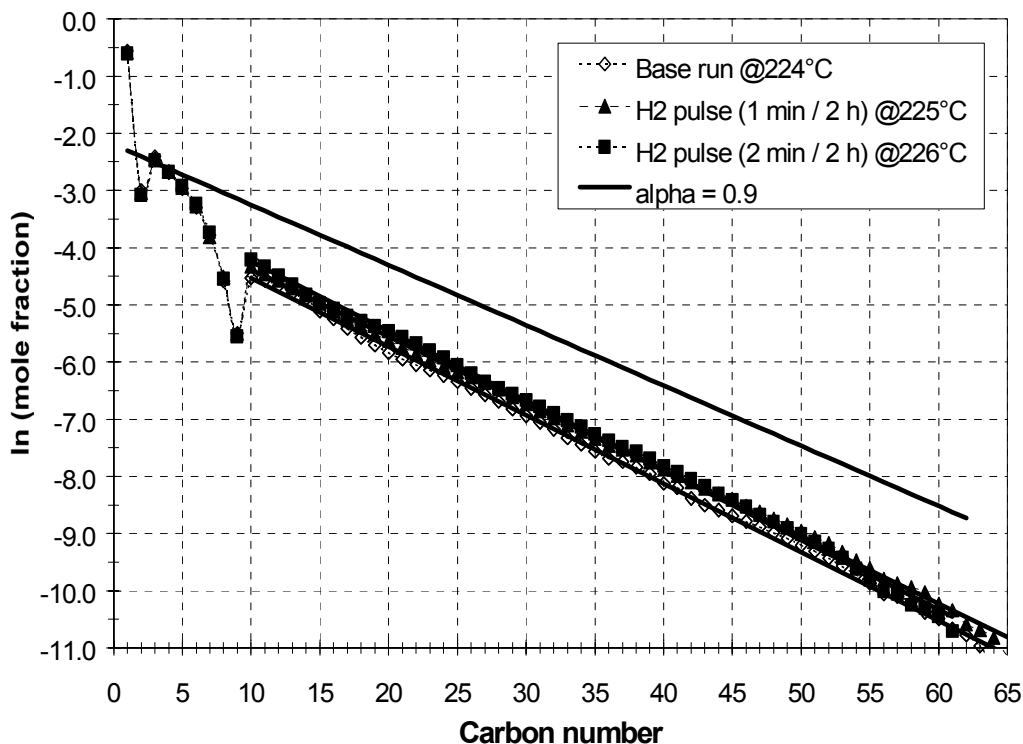
Figure 3.2.7. Effect of H_2 pulse duration on the product distribution (α-plot) of Co-ZrO_2/SiO_2; P = 300 psig; SV = 6000 h^{-1}

The produced curves of Fig. 3.2.7 appear to be almost overlapping, indicating only minor variations in the product distribution between base and pulse runs, as well as between two pulse runs of different H_2 pulse duration (1 min vs. 2 min). The slopes of these curves (based on the molar fractions of the C_{10}-C_{65} range) were very similar to each other and to that of the $\alpha = 0.9$ curve. Indeed, the α values of these runs (as well as those of the other base and pulse runs not included in the graph of Fig. 3.2.7) were equal to 0.890±0.005. Therefore, the applied variable-duration H_2 pulsing apparently did not alter the SFA distribution, similar to the applied variable-frequency H_2 pulsing.

The effect of varying H_2 pulse duration on the desired C_{10}-C_{20} yield vs. the undesired CH_4 yield is shown in Figure 3.2.8. The zero pulse duration corresponded to the average of the two no pulse (base) runs before and after the 3 pulse runs. Both the C_{10}-C_{20} and CH_4 yields increased with H_2-pulse duration (and so did the yield of C_{21+}), obviously due to an enhancement in catalytic activity caused by the pulsing (Fig. 3.2.5). As seen in Fig. 3.2.8, the effect of the 4-min H_2 pulse per 2 hours compared to the (average) base run was to increase the C_{10}-C_{20} yield by ca. 45%, while the CH_4 yield only increased by ca. 28%. This comparison entailed a temperature change (from 224°C to 227°C); however, the increase in the C_{10}-C_{20} yield was more than what could be accounted for solely by a 3°C increase in reaction temperature.

Within the examined pulse duration range, the greater difference between the yields of the desirable C_{10}-C_{20} and the undesirable CH_4 is obtained at the *intermediate* pulse duration of 2-min H_2 per 2 hours. In addition, upon extrapolating to higher H_2-pulse duration, we could expect a stronger reaction exotherm and thus an increase in reaction temperature.
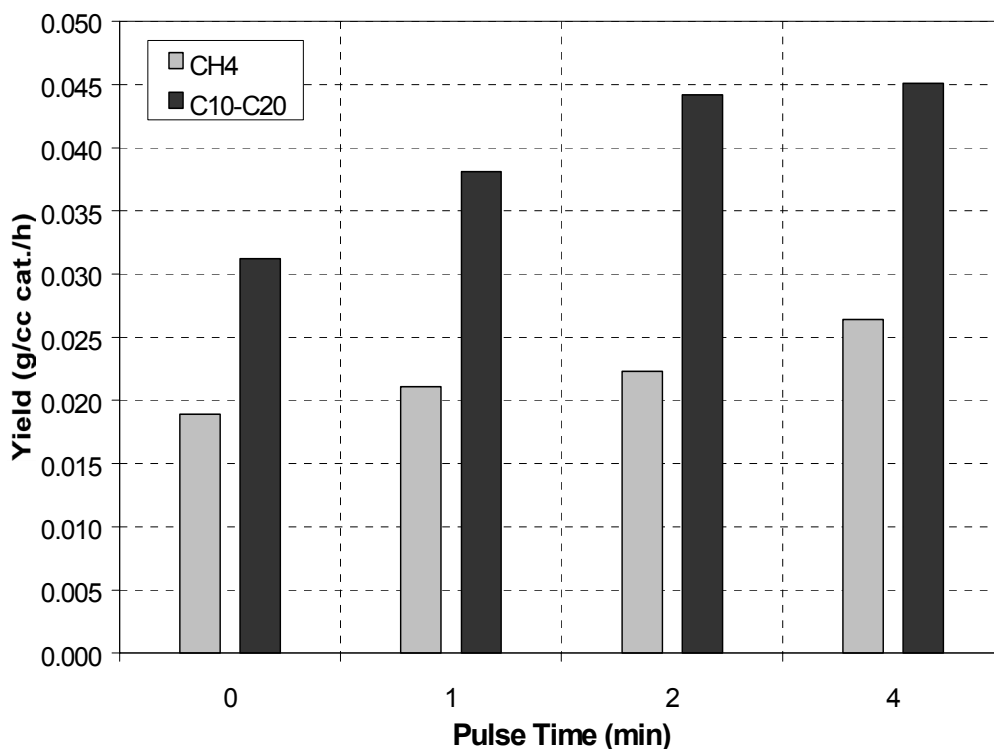
Figure 3.2.8. Effect of H_2 pulse duration on the product yield of Co-ZrO$_2$/SiO$_2$; P = 300 psig; SV = 6000 h^{-1}

Such an increase in temperature is known to cause a shift in FTS product distribution to lower molecular weight compounds and to enhance the methanation reaction [4]. Higher pulse duration would thus tend to increase the CH_4 yield much more than the C_{10}-C_{20} yield, in a similar manner to the effect of increasing pulse frequency. Therefore, an optimum set of both H_2-pulse parameters (pulse frequency and pulse duration) would be required for maximizing the formation of diesel-range FT products.

Additional runs included studying the effect of pulsing (at 1 min per 1 hour) with a pulse gas other than H_2 (namely, 50%H_2/N_2 and 24%CO_2/N_2). The dilute-H_2 pulse had minimal impact on CO conversion and C_{10}-C_{20} yield compared to the full H_2 pulse. The CO_2 pulse had a minimal effect on CO conversion and a positive effect on the selectivity to CH_4 (from 18% to 24%), resulting in low C_{10}-C_{20} yield. Despite some increased uncertainty on the obtained data, the effect of CO_2 pulsing appeared to be not promising (or minimal at best).

A new experiment was performed by loading a physical mixture of 1.7 cc (1.32 g) of the Co-Zr/SiO_2 catalyst and 10 cc (16.0 g) of the low-surface-area-area α-alumina into the reactor between two layers of α-alumina (2.4 cc top, 3.6 cc bottom). The catalyst was reduced *in-situ* under H_2 at 350°C for 8 h, and was cooled to 175ºC and pressurized to ca. 300 psig (21.4 atm). The FT reaction started by feeding CO+H_2 under the following base reaction conditions:

Reactants (50%): H_2 = 33.3%, CO = 16.7% (H_2:CO = 2.0)
Inerts (50%): N_2 = 48.2%, Ar = 1.8% (CO:Ar = 9)
P = 300 psig (21.4 atm), F = 200 scc/min, SV = 7000 h^{-1}

The reaction temperature was increased to 205°C (by 2°C/h), then to 215°C (by 1°C/h) and finally to 225°C (by 0.5°C/h) where it stabilized. The effect of temperature on the measured rate of CO conversion is shown in the form of an Arrhenius plot in Figure 3.2.9. Using the data in the 205-225°C temperature range, the measured apparent activation energy was 113 kJ/mol.

A 24-hour run segment performed isothermally at 225°C allowed the reaction to reach a pseudo steady state. The measured CO conversion was ca. 19.5% (CO productivity of ca. 230 cc CO / cc catalyst / hour), and the selectivity to CH_4 and CO_2 was ca. 9% and 0.7%, respectively. The reactant partial pressure was then decreased from 50% syngas (150 psig) to 16.7% syngas (50 psig) under constant feed flow (200 scc/min) and total reaction pressure (300 psig), where a new pseudo steady state was attained (the reaction temperature decreased by 1°C to 224°C). As a result of the lower reactant partial pressure, the CO conversion increased to ca. 37%, while the CO productivity decreased to ca. 145 cc CO / cc cat / h (i.e., a decrease of ca. 37%). The selectivity to CH_4 and CO_2 increased to ca. 12% and 1.0%, respectively.

The effect of decreasing the reactant partial pressure on the amount of formed hydrocarbons within the C_1-C_9 range (as measured by GC-FID) is given in Figure 3.2.10. Hydrocarbons in the C_{10}-C_{14} range were also detected qualitatively, but their amounts were quantitatively uncertain (due to lower fractions of these species in the gas phase) and were thus not included. Two sets of data for the low (16.7%, or 50 psig) syngas partial pressure are included in Fig. 3.2.10, the second set taken at ca. 22 hours after the first one. There were only minor deviations between these two data sets, thus establishing the good reproducibility of these measurements.
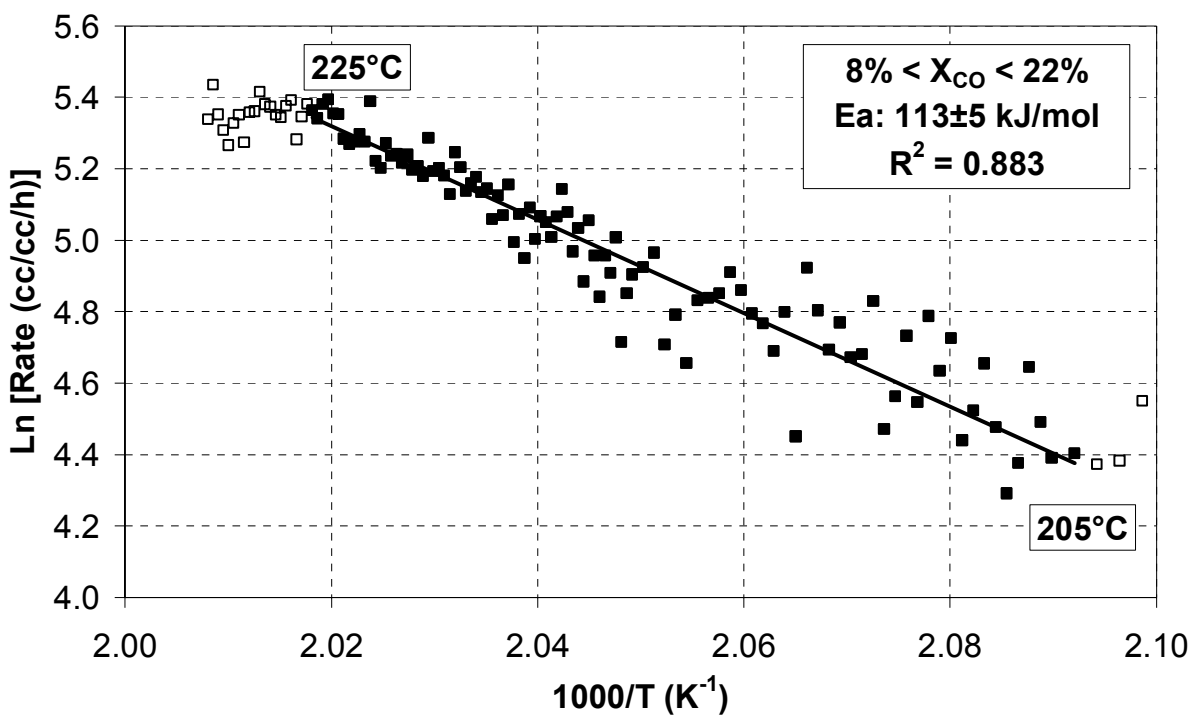
Figure 3.2.9. Effect of temperature on the rate of CO conversion of Co-ZrO$_2$/SiO$_2$; P = 300 psig, SV = 7000 h^{-1}
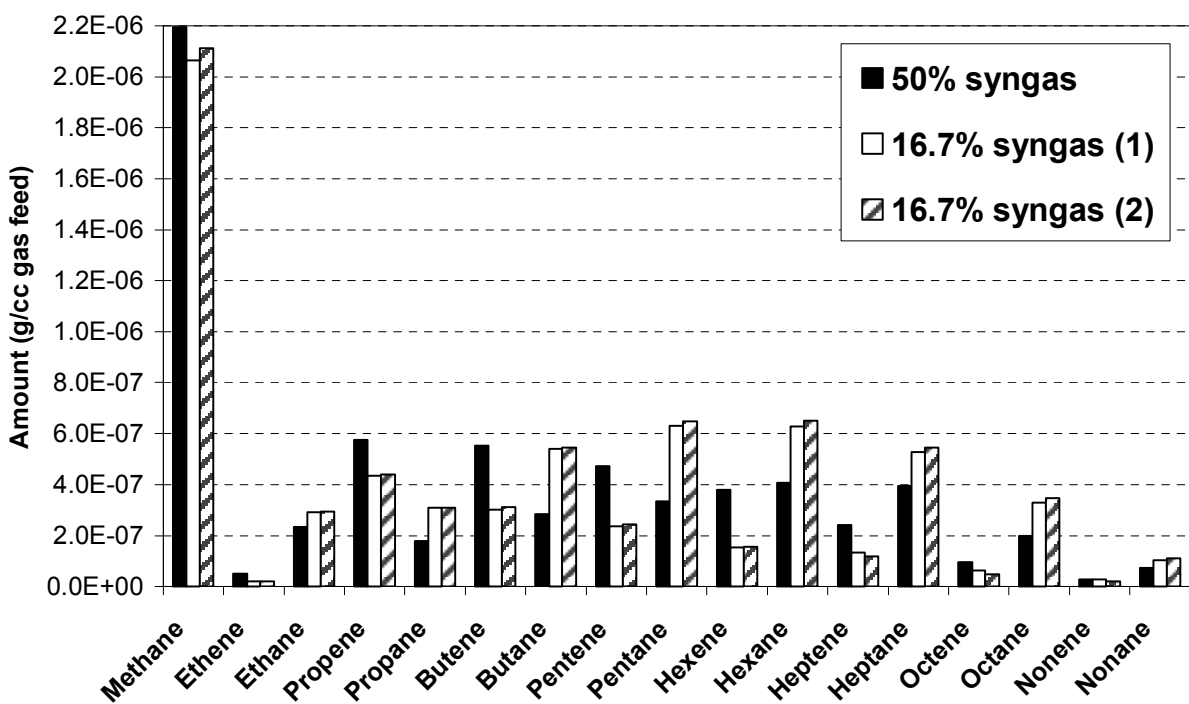
Figure 3.2.10. Effect of reactant partial pressure on the C$_1$-C$_9$ hydrocarbon amounts of Co-ZrO$_2$/SiO$_2$; T = 225/224°C, P = 300 psig, SV = 7000 h^{-1}

A decrease in syngas partial pressure to 1/3 of its initial value (from 50% to 16.7%, or from 150 psig to 50 psig) had only a minor effect on the formation of methane (<10% deviation). Thus, methanation appears to be only weakly dependent on syngas partial pressure within the examined range, in clear contrast to its strong dependence on reaction temperature.

On the other hand, this decrease in syngas partial pressure caused a measurable decrease in the C_2-C_9 olefins but also a significant increase in the C_2-C_9 paraffins. Therefore, variations in syngas partial pressure appear to have a strong impact (in opposite directions) on the rates of formation of light paraffins and olefins.

As a result of the reduction in the amount of light olefins and enhancement in that of the light paraffins, this decrease in syngas partial pressure would have a strong suppressing effect in the olefin/paraffin ratio for the examined C_2-C_9 hydrocarbon species. This is clearly shown in Figure 3.2.11, with the C_3 ratio exhibiting the greatest deviation (a decrease by more than 50%). This deviation appears to decrease in magnitude with increasing carbon number.

The next run segment (a 30-hour run) involved the application of a 1-min H_2 pulse per hour at 224°C and low (50 psig) reactant partial pressure conditions. Then, a 40-hour post-pulse run under the same reaction conditions followed. This series of runs allowed evaluation of the effect of H_2 pulsing under low (50 psig) syngas partial pressure in comparison to the effect under the "base" 150-psig syngas partial pressure (Figs. 3.2.1 – 3.2.3).
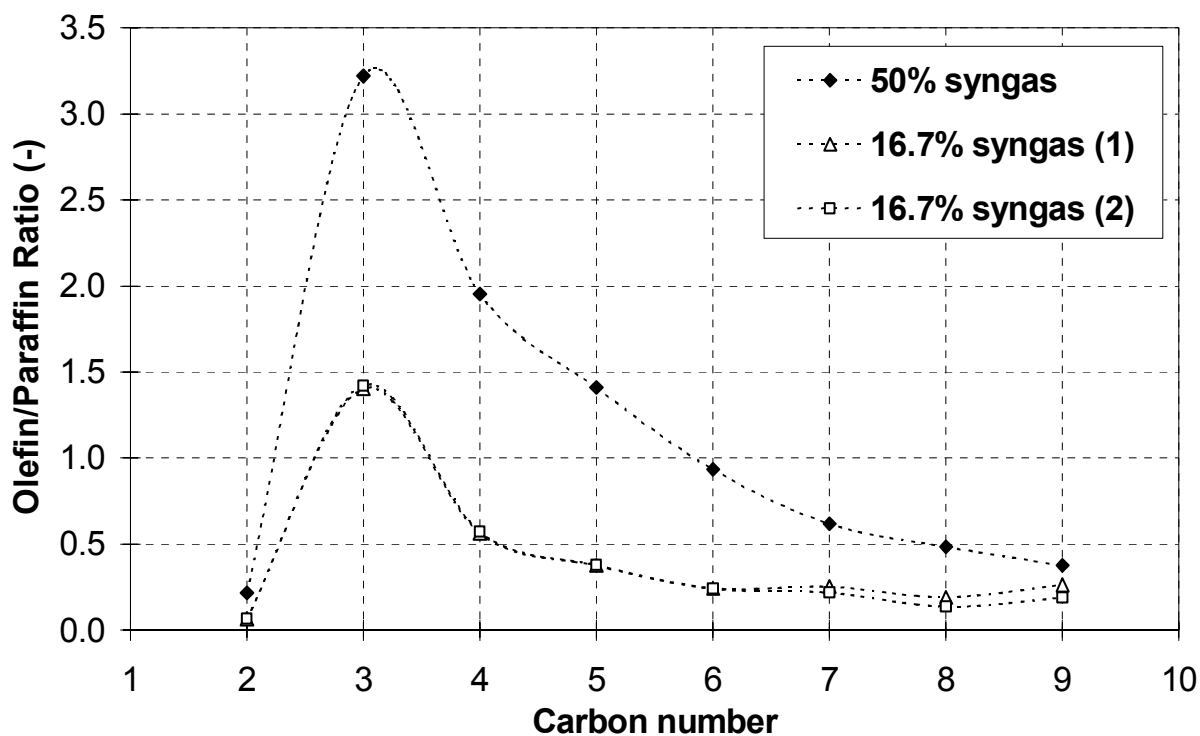
Figure 3.2.11. Effect of reactant partial pressure on the C_2-C_9 olefin/paraffin ratio of Co-ZrO$_2$/SiO$_2$; T = 225/224°C, P = 300 psig, SV = 7000 h^{-1}

As a result of the applied 1-min H_2 pulse per hour, the CO conversion increased in a manner similar to that seen previously (Fig. 3.2.1), i.e., an increase after the pulse followed by a gradual decrease until the next pulse. The CO conversion increased from ca. 37% (CO productivity of ca. 145 cc CO / cc cat / h) to a maximum of ca. 48% (CO productivity of ca. 190 cc CO / cc cat / h), i.e., an increase of ca. 30%.

In contrast, the corresponding activity increase using the same H_2 pulse sequence but with 150 psig of syngas partial pressure was ca. 87% (Fig. 3.2.1). This deviation is most likely the result of exposing the catalyst to different concentrations of H_2 during the pulse (different by a factor of 3, matching the 3-to-1 syngas partial pressure analogy).

The selectivity to CH_4 also increased *instantaneously* after each H_2 pulse, from ca. 12% to ca. 23% at 5 min after the pulse (a 90% increase) and was quickly restored to its base value of ca. 12%. The selectivity to CO_2 appeared to be only marginally affected by the H_2 pulsing, and was maintained at 0.7-1.4% throughout the pulse run. Therefore, the formation of CH_4 appears to be significantly enhanced as a result of H_2 pulsing, whereas the formation of CO_2, i.e., the water-gas shift reaction, appears to be practically unaffected, in agreement with previous observations (Fig. 3.2.2).

In order to identify the direct effect of a given pulse on the formation of the various FT products, the evolution in the rate of formation of these species with time after the pulse would be required. The frequent GC analysis of the permanent gases (every 15 min) allows for essentially continuous monitoring of CO conversion and C_1 selectivity during the time after a pulse. Conversely, the oil+wax analysis corresponds to a statistical average within a run. The GC analysis of the light (C_1-C_8) hydrocarbons can be used to monitor the desired evolution.

The variation in the amount of formed C_1-C_8 paraffins and olefins with respect to the time after a 1-min H_2 pulse is shown in Figures 3.2.12a and 3.2.12b. The data came from measurements at 5, 10, 15, 30, and 55 min after the pulse, in comparison to pre-pulse and post-pulse data. The two figures contain the same data but *zoom in* at different amount levels to facilitate the analysis.

The formation of CH_4 showed a maximum at 5 min after the pulse (Fig. 3.2.12a) and then decreased with time, tracking the decrease in CO conversion (constant selectivity to CH_4). The formation of C_2-C_8 paraffins followed the trend of CH_4, also exhibiting a maximum with time after the pulse (Fig. 3.2.12b). However, that maximum appeared to shift to *longer times* with increasing carbon number. Indeed, the ethane and propane showed a maximum at 10 min, the butane at 10 or 15 min, the pentane at 15 min, the hexane and heptane at 30 min, and the octane at 55 min after the applied 1-min H_2 pulse.

On the other hand, the C_2-C_8 olefins showed a much less prominent and more "random-like" variation in their corresponding amounts with respect to the time after the pulse (Fig. 3.2.12b). Finally, the measured pre-pulse and post-pulse amounts were essentially the same for every species in the examined C_1-C_8 range, implying full reversibility upon completion of the applied pulse sequence.
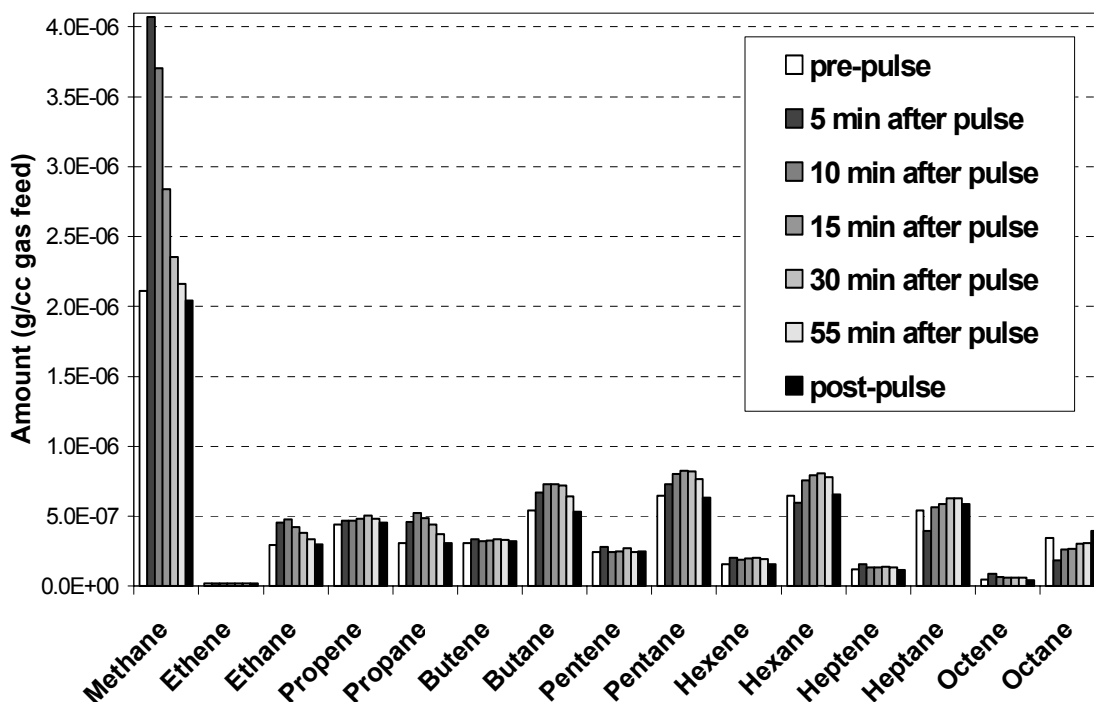
Figure 3.2.12a. Effect of time after a 1-min H_2 pulse on the amount of C_1-C_8 formed on Co-ZrO_2/SiO_2; T = 224/225°C, P = 300 psig, SV = 7000 h^{-1}
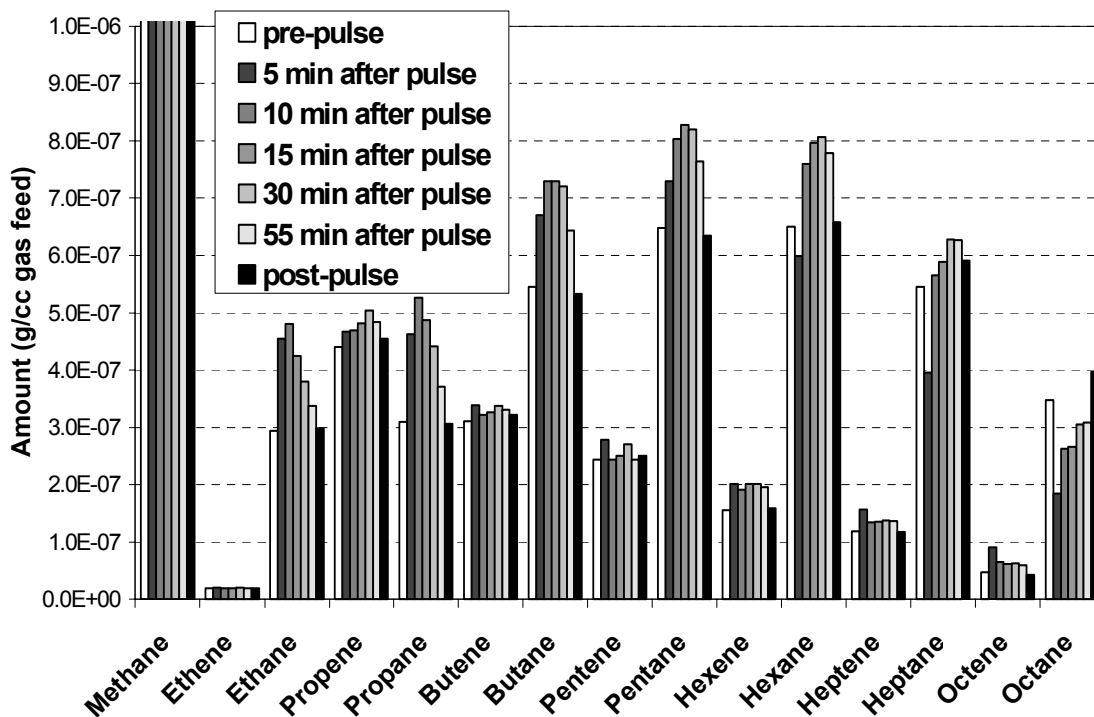
Figure 3.2.12b. Effect of time after a 1-min H_2 pulse on the amount of C_2-C_8 formed on Co-ZrO_2/SiO_2; T = 224/225°C, P = 300 psig, SV = 7000 h^{-1}

These very interesting observations lead to the conclusion that the effect of the applied H_2 pulse is like a *rippling* phenomenon. The formation of paraffinic (and apparently olefinic also) hydrocarbons exhibits a local maximum with respect to the time after the pulse, whereas this maximum shifts to longer times with increasing carbon number. In addition, the magnitude of the observed increase in formation is greater for the paraffins than for the corresponding olefins, and appears to decline with increasing carbon number.

After establishing a new pseudo steady state at the low reactant partial pressure of 50 psig and at 224°C, 10% steam was added to the reactant feed while maintaining a constant total feed flow and reaction pressure. The purpose of this run was to simulate in a fixed-bed reactor system the higher conversion (i.e., lower reactant partial pressure in the reactor outlet) and presence of excess concentration of steam (a reaction by-product) typically encountered for FT synthesis in a slurry bubble column reactor (SBCR). Following this run, a 1-min H_2 pulse per hour run in the presence of 10% added steam was performed, so as to evaluate the effect of a well-known pulse sequence on the performance of the examined catalyst in the presence of excess steam. Finally, the same pulse sequence after stopping the addition of steam was performed for comparison.

As shown in Table 3.2.3, the addition of 10% steam caused a decrease in CO conversion (and productivity) of ca. 17% (from 37% to 30%). It also strongly suppressed the formation of CH_4 while enhancing (actually doubling) the formation of CO_2 by enhancing the extent of the water gas shift reaction, as expected. A 1°C drop in the reaction temperature was also observed.

Application of a 1-min H_2 pulse in the presence of added steam resulted in a significant enhancement in CO conversion (maximum of ca. 40%) followed by a gradual decline in activity until the next pulse, as observed previously. The selectivity to CH_4 increased *instantaneously* (maximum of ca. 20%) and quickly returned to its steady state value of ca. 8%. The selectivity to CO_2 increased also. Upon stopping the addition of steam, the H_2 pulsing maintained its positive effect on CO conversion and selectivity to CH_4, while the selectivity to CO_2 returned to its previously measured value of ca. 1.0%, i.e., the water gas shift reaction was not significantly affected by the application of the H_2 pulse alone.

Table 3.2.3. Effect of steam addition and H_2 pulse on the activity/selectivity of Co-ZrO_2/SiO_2; T=224/223°C; P=300 psig; SV=7000 h^{-1}

Run type	CO conversion (mol%)	CO productivity (cc CO/cc cat/h)	CH₄ selectivity (mol%)	CO₂ selectivity (mol%)
Pre-pulse	37	145	13	1.2
+ 10% steam	30	120	8.0	3.0
Pulse + 10% steam	30-40	120-157	8.0-20	3.0-3.5
Pulse (no steam)	32-38	125-150	10-19	0.9-1.0

The effect of this series of runs (pre-pulse run, addition of 10% steam, 1-min H_2 pulse in the presence of added steam, 1-min H_2 pulse with no steam added) on the formation of C_1-C_8 species is shown in Figure 3.2.13. The addition of 10% steam caused a decrease in the amount of CH_4 and C_2-C_8 paraffins, to about or less than half their corresponding value prior to the addition of steam. In terms of the olefins, propene and butene decreased also, whereas for C_5-C_8 there was an increase in the amount formed by adding steam.

Application of a 1-min H_2 pulse per hour in the presence of added steam caused a moderate increase in the amount of all paraffins and of the C_2-C_6 olefins (C_7 and C_8 olefins showed a slight decrease which may be within the experimental uncertainty of these measurements). Upon stopping the addition of steam, the same H_2 pulse sequence resulted in a further increase in the amount of CH_4 and C_2-C_6 paraffins, but also in a slight decrease in the amount of C_7-C_8 paraffins and C_3-C_8 olefins.

Another way to examine the effect of these runs on the formation of light hydrocarbons is by plotting the olefin/paraffin ratio for the C_2-C_9 species, as shown in Figure 3.2.14. The addition of steam significantly increased the olefin/paraffin ratio for all species in the C_2-C_9 range. This was due to the decrease in paraffin formation, in addition to an increase in the higher (>C_5) olefin formation, as already shown in Fig. 3.2.13. Application of the H_2 pulse in the presence of added steam decreased the olefin/paraffin ratio, but nowhere near the values obtained prior to the addition of steam. Thus, steam addition and H_2 pulsing appear to have opposite effects on the olefin/paraffin ratio within the examined C_2-C_9 range.
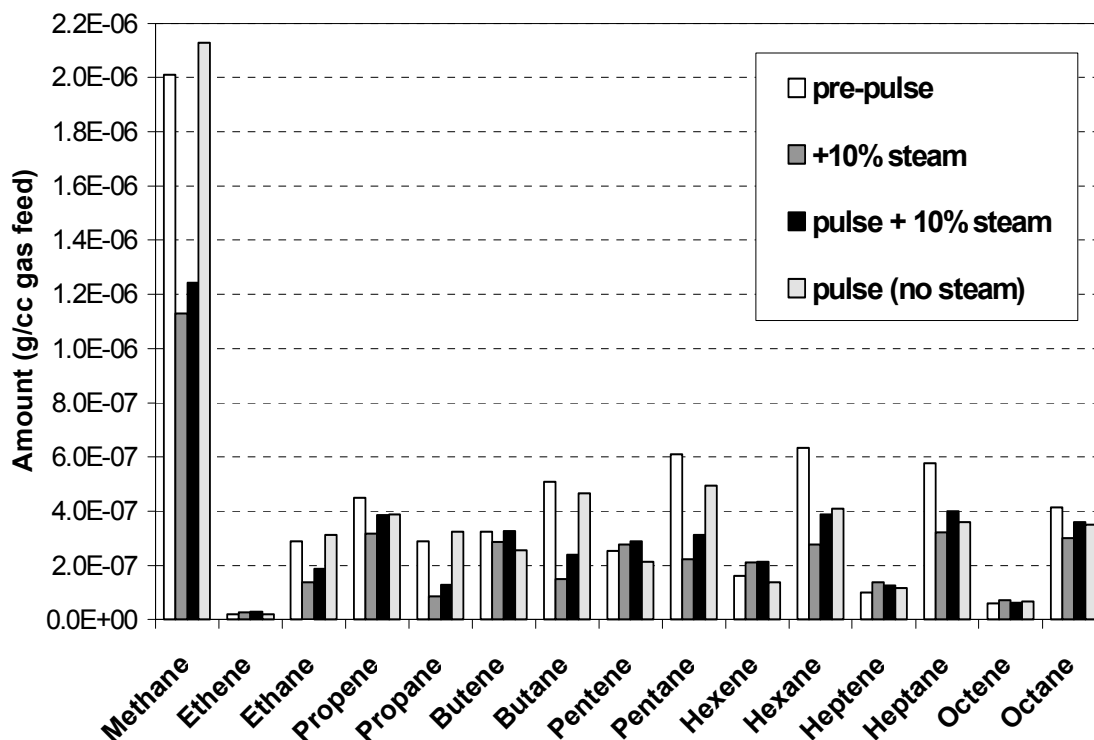
Figure 3.2.13. Effect of steam addition and 1-min H_2 pulse on the amount of C_1-C_8 formed on Co-ZrO$_2$/SiO$_2$; T=223/224°C; P=300 psig; SV=7000 h^{-1}
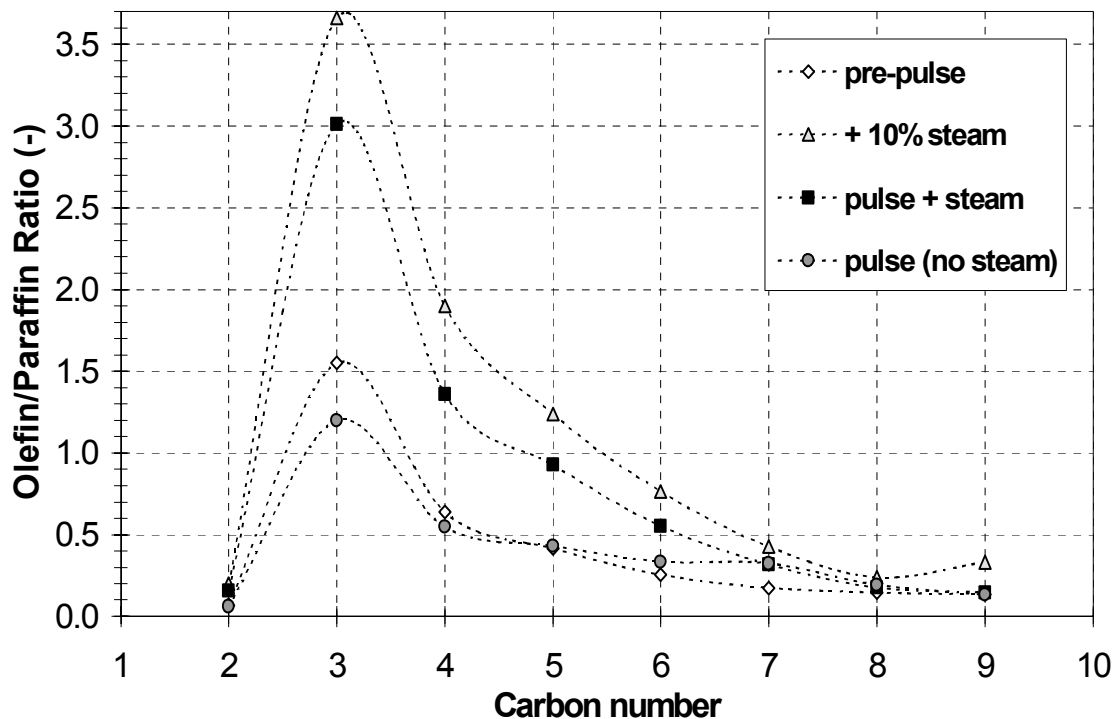
Figure 3.2.14. Effect of steam addition and 1-min H$_2$ pulse on the C$_2$-C$_9$ olefin / paraffin ratio of Co-ZrO$_2$/SiO$_2$; T=223/224°C; P=300 psig; SV=7000 h^{-1}

Upon stopping the addition of steam, the C$_2$-C$_9$ olefin/paraffin ratio decreased further, clearly indicating that H$_2$ pulsing enhances olefin hydrogenation. The resulting olefin/paraffin ratios were quite similar to those obtained prior to the addition of steam. Therefore, H$_2$ pulsing is a simple method to counterbalance the negative effect on activity (CO productivity, Table 3.2.3) and selectivity (paraffin vs. olefin, Fig. 3.2.14) caused by the addition of excess steam.

3.3. FT Reaction on 20% CoOx/Al$_2$O$_3$ (EI catalyst) in a Fixed-Bed Reactor (FBR)

A 20% CoOx/Al$_2$O$_3$ catalyst (14wt% Co, Energy International) was tested for the FT reaction under periodic pulsing. This fine powder (90-150 µm) material has a BET surface area of 156 m^2/g. Its actual metal loading was verified as 14% Co by elemental analysis (ICP-OES).

A physical mixture of 2 cc (1.91 g) of the 20% CoOx/Al$_2$O$_3$ catalyst and 10 cc (16.01 g) of a low-surface-area (0.2 m^2/g) α-alumina (SA5397, Norton) was loaded into the reactor between two layers of α-alumina (2.4 cc top, 3.6 cc bottom). The catalyst was reduced *in-situ* under H$_2$ at 350°C for 8 h, and was cooled to 125°C and then pressurized to ca. 300 psig (19.4 atm). The FT reaction started by feeding a 50% CO+H$_2$ mixture under the following base reaction conditions:

> Reactants (50%): H$_2$ = 33.3%, CO = 16.7% (H$_2$:CO = 2.0)
> Inerts (50%): N$_2$ = 48.2%, Ar = 1.8% (CO:Ar = 9)
> P = 300 psig (21.4 atm), F = 200 scc/min, SV = 6000 h^{-1}

The reaction temperature was increased to 185°C (by 4°C/h) and then to 205°C (by 1°C/h). Due to the strong reaction exotherm the bed temperature exceeded the target value by ca. 10°C, resulting in a max CO conversion of ca. 64%. The bed was then cooled to 204°C and the CO conversion was stabilized at ca. 24%. The effect of temperature on the measured rate of CO conversion is given in the form of an Arrhenius plot in Figure 3.3.1. Excluding low-T (<187°C, wide data dispersion) and high-T data (>202°C, strong heat transfer effects due to insufficient heat dissipation, commonly observed for strong exothermic reactions in a fixed-bed reactor), the measured apparent activation energy was ca. 120 kJ/mol (in agreement with Fig. 3.2.9).
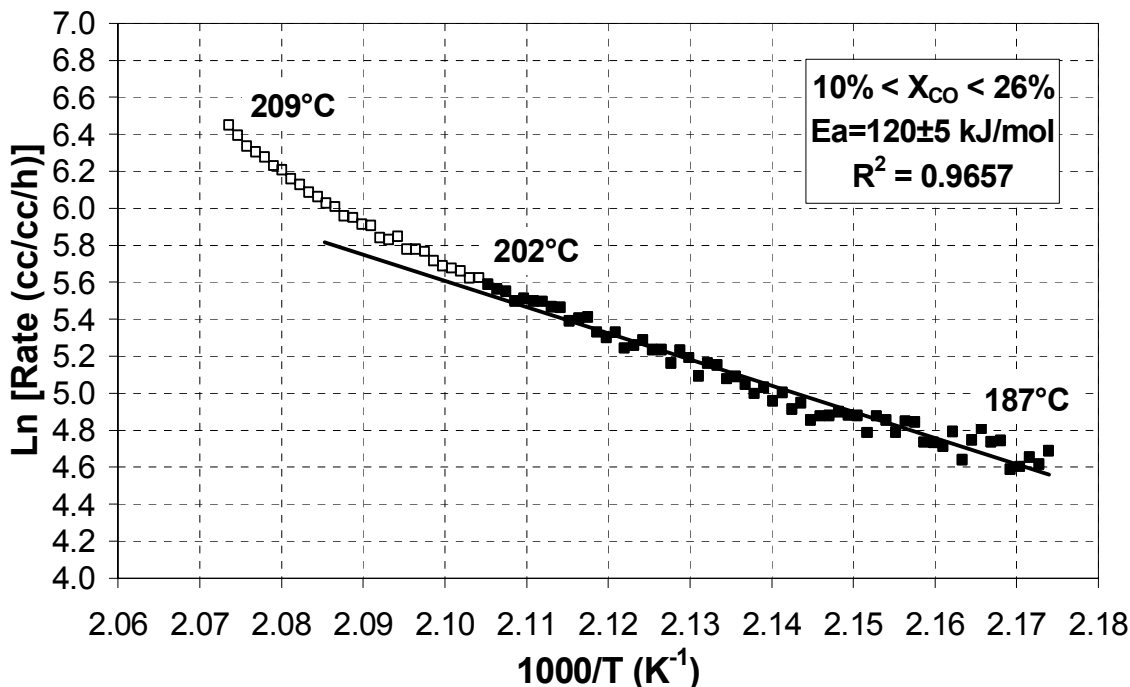
Figure 3.3.1. Effect of temperature on the rate of CO conversion of Co /Al$_2$O$_3$; P = 300 psig, SV = 6000 h^{-1}

Effect of Space Velocity

After establishing a "pseudo steady state" at 204°C and 6000 h^{-1} the effect of space velocity variation on the activity and selectivity of the Co/Al$_2$O$_3$ catalyst was examined. The space velocity was increased (9000 and 12000 h^{-1}), decreased (6000, 4500, 3000 h^{-1}) and then returned to 6000 h^{-1}, by varying the total feed flow while keeping constant total pressure and reactant concentration.

The CO conversion was a decreasing function of space velocity (ca. 38% at 3000 h^{-1}, ca. 13% at 12000 h^{-1}). The effect of space velocity on the measured chain growth probability, **α**, and on the CO productivity (expressed as cc CO converted per cc catalyst per hour) is shown in Figure 3.3.2. The CO productivity decreased moderately with decreasing space velocity (from ca. 250 to ca. 190 cc CO/cc cat/h). This suggests that at lower feed flows the activity data become influenced by external mass transfer limitations. A lower space velocity appears to enhance the formation of heavy products, thus increasing the chain growth probability **α** at least somewhat (from 0.918 to 0.928, Fig. 3.3.2).

The effect of space velocity on product distribution can also be seen in Figure 3.3.3. The reaction products were divided into four groups: C$_1$ (methane), C$_2$-C$_9$ (lights), C$_{10}$-C$_{20}$ (intermediates, diesel range), and C$_{21+}$ (heavy oils + waxes), and their fractions (in wt%) were plotted vs. the space velocity. An increase in the feed flow appears to enhance the selectivity to the undesirable light products (methane and C$_2$-C$_9$) and to decrease the selectivity to the intermediate and heavy ones (C$_{10}$-C$_{20}$ and C$_{21+}$).
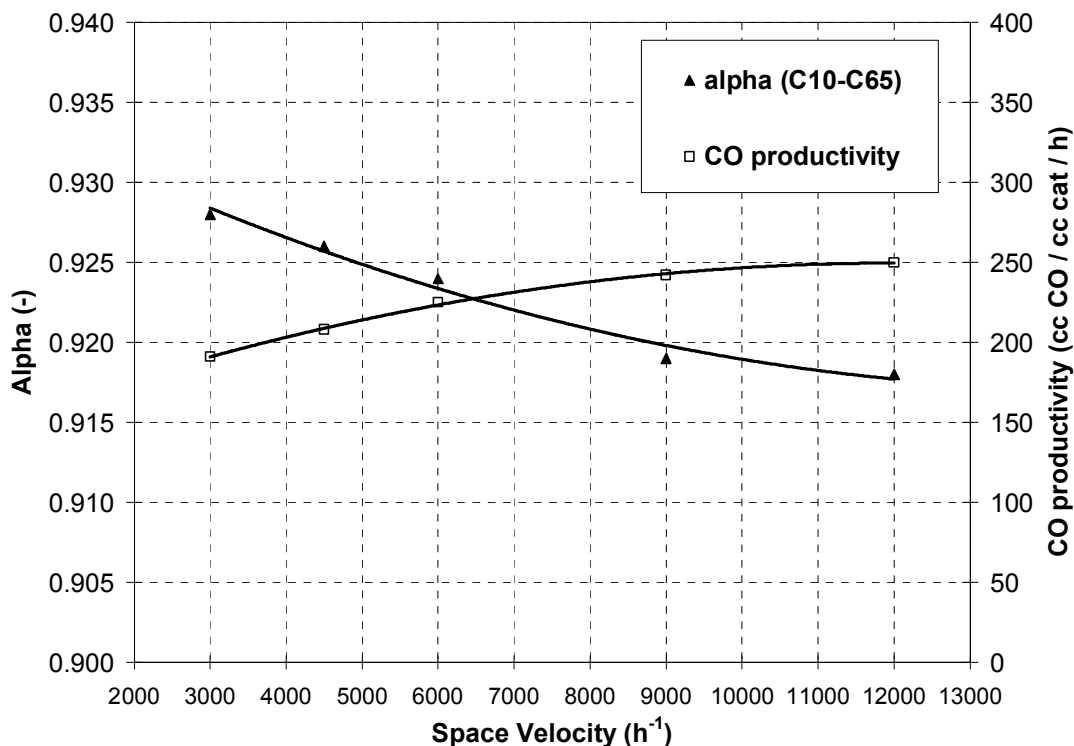
Figure 3.3.2. **Effect of space velocity on the chain growth probability (α) and on the CO productivity of Co/Al$_2$O$_3$; T = 204°C; P = 300 psig**
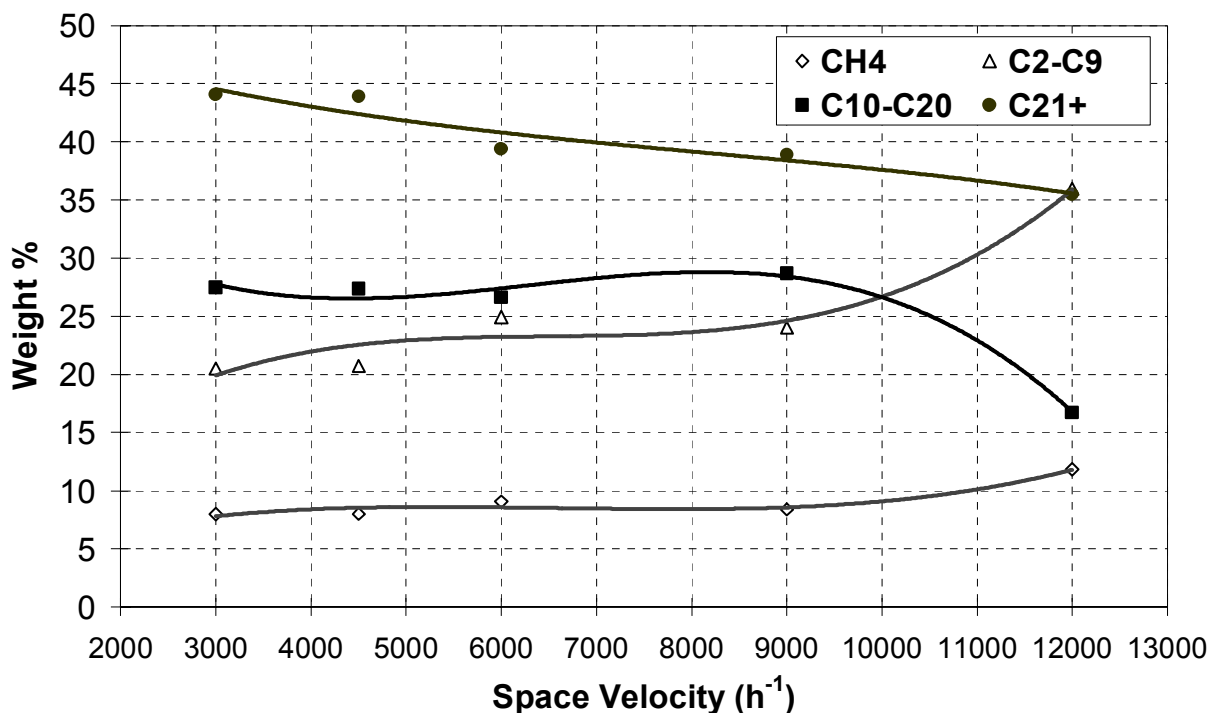
Figure 3.3.3. **Effect of space velocity on the wt% product fraction of Co/Al₂O₃; T = 204°C; P = 300 psig**

The effect of increasing and decreasing space velocity on the olefin/paraffin ratio of the light (C_2-C_9) hydrocarbon products is presented in Figures 3.3.4a and 3.3.4b, respectively. The order within the legends in these figures corresponds to the order in which the space velocity variation runs were performed. The last data set of Fig. 3.3.4a and the first of Fig. 3.3.4b (6000 h^{-1}) correspond to a single run and thus are identical (they are presented twice for facilitating comparison of the other data). Olefins higher than C_9 were detected qualitatively (typically up to C_{12}) but the amounts were quantitatively uncertain (close to or below the detection limit of the Flame Ionization Detector).

The olefin/paraffin ratio of C_3 and higher is a decreasing function of carbon number (at every examined space velocity), something well established in the literature. The ethylene/ethane ratio is the exception to this rule, apparently due to the enhanced activity of ethylene for secondary reaction (re-insertion) to form a longer chain. Thus, its exit concentration and the ethylene/ethane ratio are significantly lower.

The results of Figs. 3.3.4a and 3.3.4b clearly demonstrate that the olefin/paraffin ratio is an increasing function of space velocity for every carbon number within the examined range (C_2-C_9). This is in good agreement with the literature [19], where an increase in space velocity increases the selectivity towards olefins while the paraffin selectivity remains unchanged. The olefin/paraffin ratio data of the last run in Fig. 3.4.4b match very closely the ones of the first run in this figure (both performed at 6000 h^{-1}). This suggests that the obtained data were apparently not influenced by the order in which these runs were performed or by the exposure of the catalyst to these feed flow conditions.
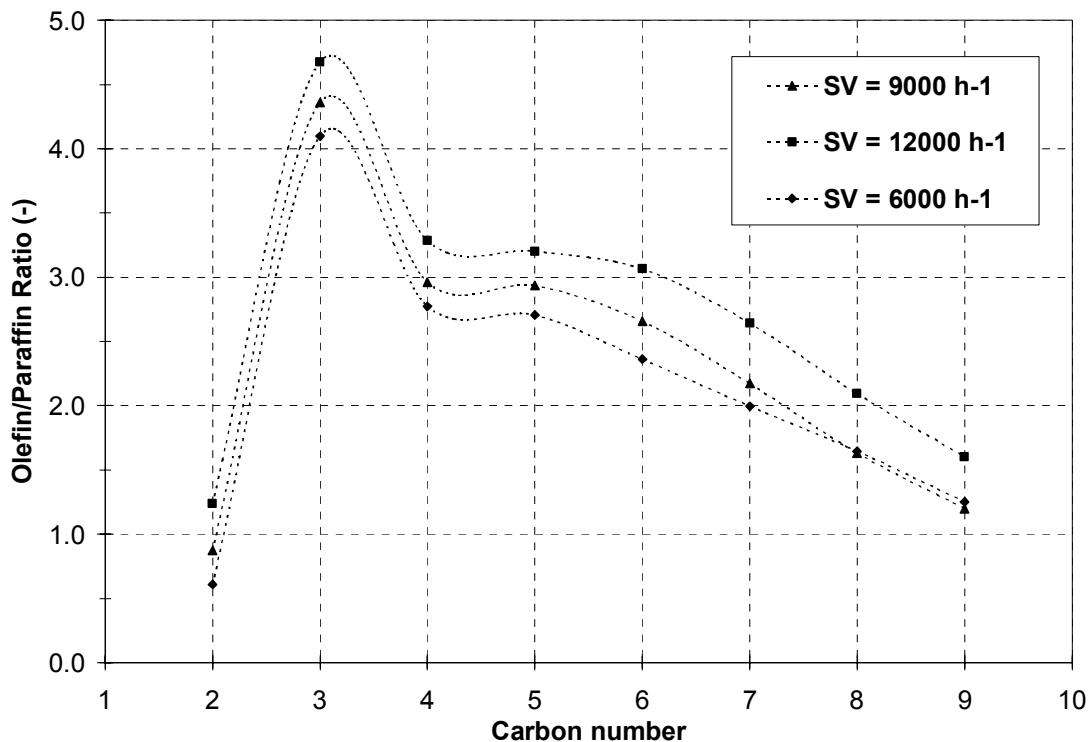
Figure 3.3.4a. Effect of space velocity on the C_2-C_9 olefin/paraffin ratio of Co/Al$_2$O$_3$; T = 204°C; P =300 psig; F =200-400 scc/min
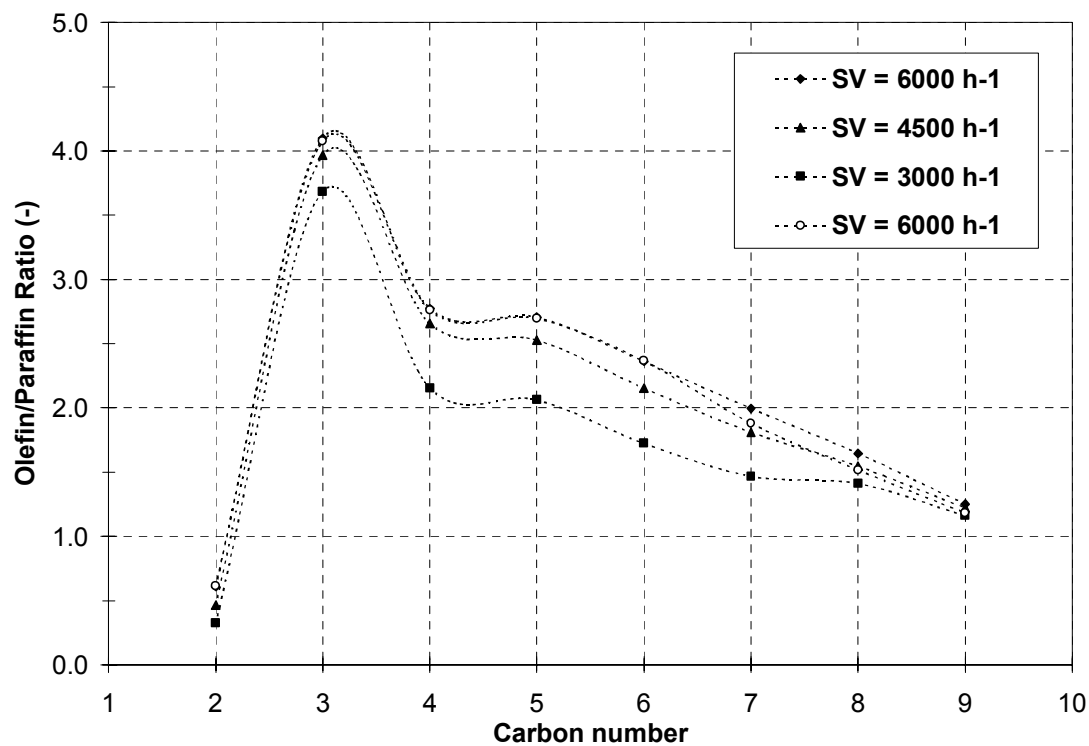
Figure 3.3.4b. Effect of space velocity on the C_2-C_9 olefin/paraffin ratio of Co/Al$_2$O$_3$; T = 204°C; P = 300 psig; F = 200-100 scc/min

Effect of Total Pressure (Under Constant Reactant Molar Fraction)

The effect of varying the total reaction pressure at constant space velocity (6000 h^{-1}) while keeping a constant reactant feed concentration was examined. The range of total reaction pressure variation was from 200 psig to 400 psig. Since the feed composition (i.e., the mole fractions of all the feed species) was kept constant, the reactant partial pressures were kept proportional to the total pressure. Thus since the H$_2$+CO (syngas) feed concentration was always 50%, the syngas partial pressure was varied from 100 psig to 200 psig in these runs.

Figure 3.3.5 shows the effect of total reaction pressure on the CO productivity and the chain growth probability (α). The CO productivity increased with increasing pressure (from 200 to 230 cc CO/cc cat/h) and so did the corresponding CO conversion (20 to 23%, data not shown). The chain growth probability α was also an increasing function of the total pressure within the examined range (the α value increased from 0.920 to 0.928).

Despite the fact that the total reaction pressure was the independent variable in the runs whose data are shown in Fig. 3.3.5, the observed trends are most likely correlated not with the total pressure itself but rather with the reactant (syngas) partial pressure (which was 50% of the total). The results of Fig. 3.3.5 suggest that by increasing the reactant partial pressure (either by increasing the total pressure, as shown, or by decreasing the concentration of inert gases in the feed under a constant total pressure), both CO productivity and α, were enhanced. Since the pulsing concept is based on using a high α catalyst, pulsing experiments on a given FT synthesis catalyst should also be performed at higher syngas partial pressures.
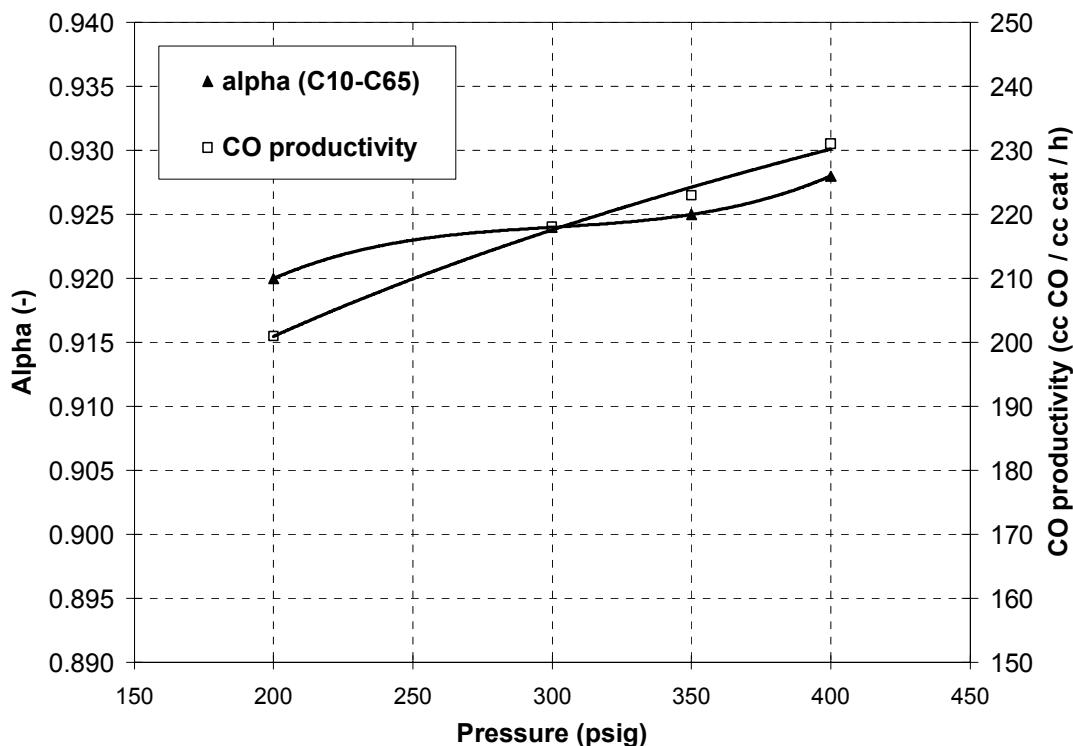
Figure 3.3.5. **Effect of total reaction pressure on the chain growth probability (α) and the CO productivity of Co/Al$_2$O$_3$; T = 203-204°C; SV = 6000 h^{-1}**

Figure 3.3.6 shows the effect of total reaction pressure variation on the olefin/paraffin ratio of the light (C_2-C_9) hydrocarbon products. The order within the legend in this graph corresponds to the order in which the pressure variation runs were performed. Upon decreasing the reaction pressure to 200 psig the temperature of the catalyst bed fell by 1°C (to 203°C). The lower catalyst activity under this reaction condition could obviously decrease the reaction exotherm enough so as to also marginally decrease the bed temperature.

The results of Fig. 3.3.6 clearly show that an increase in the reaction pressure suppressed the olefin/paraffin ratio for every carbon number within the C_3-C_9 range (the C_2 data were essentially identical within the limited accuracy of measuring such small concentrations). Thus an increase in reaction pressure appears to promote the secondary adsorption of the formed olefins leading to longer-chain products, resulting in a lower outlet concentration of olefins.

The extent of reaction pressure variation was limited to within 200-400 psig for the examined set of runs on the Co/Al$_2$O$_3$ catalyst. It is uncertain that the same trends would still be valid under significantly lower or higher reaction pressures. There may be a lower or upper limit of reaction pressure beyond which the observed trends would not be applicable.
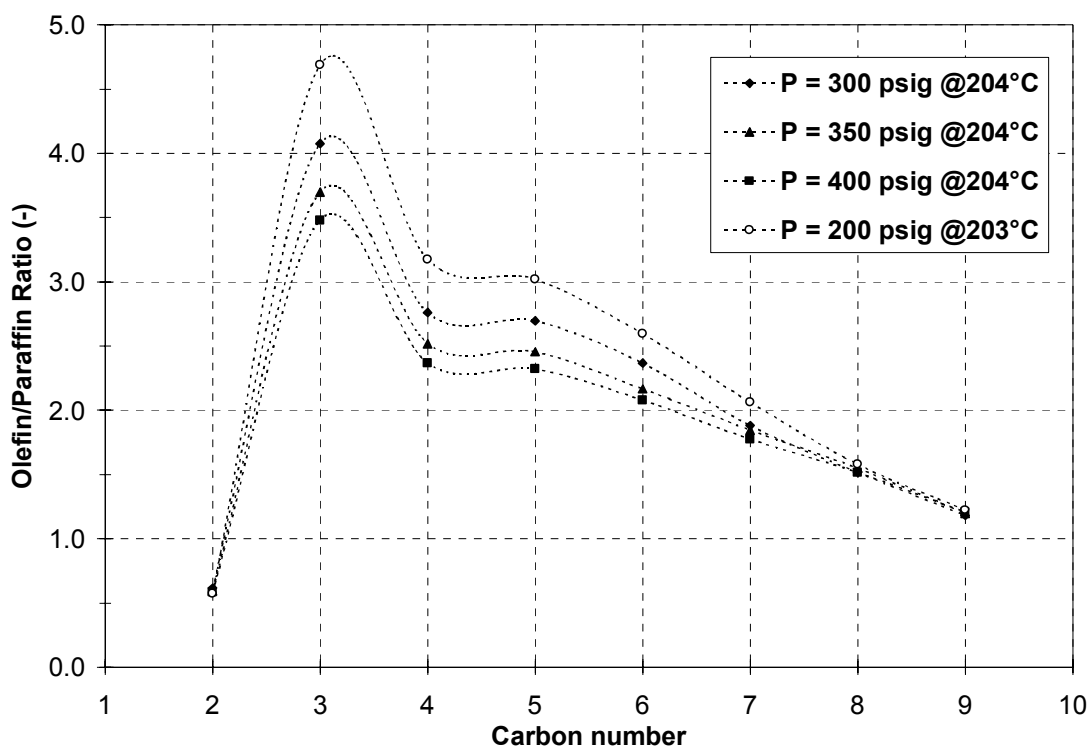
Figure 3.3.6. **Effect of total reaction pressure on C_2-C_9 olefin/paraffin ratio of Co/Al$_2$O$_3$; T = 203-204°C; SV = 6000 h^{-1}**

Effect of Nitrogen Pulse (1 min N$_2$ per 1 h)

After completing the pressure variation runs the reaction pressure was restored to 300 psig and the catalyst reached a new "pseudo steady state" (base run, 24 hours) under these conditions (204°C, 300 psig, 6000 h^{-1}). Then, a 1-min N$_2$ pulse per 1 hour was applied in order to examine the effect of pulsing with an inert gas on the progress of the FT reaction. This pulse run involved substituting the flow of H$_2$+CO+Ar (51.7% of total flow) by an equal flow of N$_2$ for 1 min every hour, thus keeping the total molar flow and reaction pressure constant during the run. Upon completion of the pulse run (24 hours) a post-pulse base run was performed.

The results for the pre-pulse base run, the N$_2$ pulse run, and the post-pulse base run are given in Table 3.3.1. The N$_2$ pulse had essentially no impact on the catalytic activity (CO conversion, X(CO)), product distribution (methane selectivity, S(CH$_4$)), and chain growth probability, **α**) and product yield. These results were consistent with the ones obtained on the Co-ZrO$_2$/SiO$_2$ FT synthesis catalyst, where application of a 1-min N$_2$ pulse also had minimal effect on activity and selectivity (Table 3.2.2).

A more detailed analysis of the product distribution for these runs involving a 1-min N$_2$ pulse per 1 hour, in terms of weight fractions of product groups: C$_1$ (methane), C$_2$-C$_9$ (lights), C$_{10}$-C$_{20}$ (intermediates), and C$_{21+}$ (heavies), also led to the same observation, as shown in Figure 3.3.7. Indeed, the weight fraction values of the N$_2$ pulse run were in good agreement (within the accuracy of the measurements and the % normalization) with those of the pre-pulse and post-pulse base runs.

The olefin/paraffin ratio of the C$_2$-C$_9$ products of the N$_2$ pulse run and the pre-pulse and post-pulse runs were also essentially identical, as shown in Figure 3.2.8. Thus, short (1-min) inert gas pulses do not affect the FT reaction substantially.

Table 3.3.1. Effect of inert (N$_2$) pulse on the activity/selectivity performance of Co/Al$_2$O$_3$; T = 204°C; P = 300 psig; SV = 6000 h^{-1}

Run type	Pulse gas	T (°C)	X(CO) (%)	S(CH$_4$) (mol%)	Alpha (-)	Y(CH$_4$) (cc/cc/h)	Y(C$_{10}$-C$_{20}$) (cc/cc/h)
Base run	-	204	20.8	5.2	0.924	0.010	0.023
Pulse run	N$_2$	204	20.8	5.1	0.923	0.010	0.024
Base run	-	204	20.6	5.2	0.924	0.010	0.027
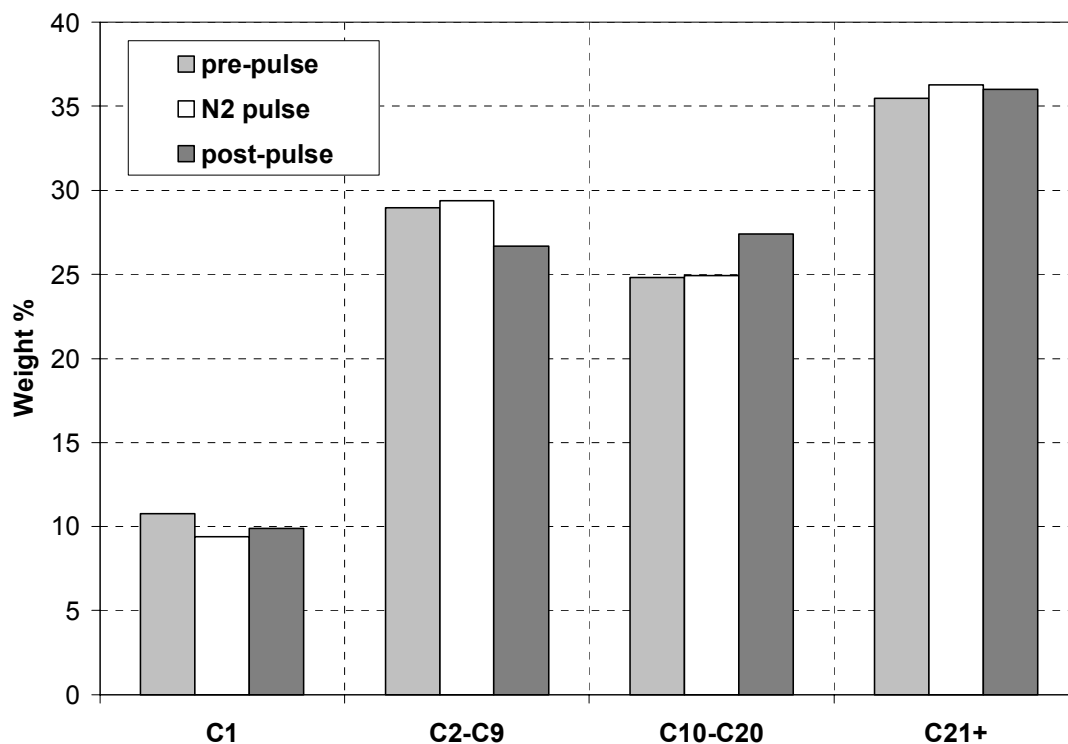
Figure 3.3.7. Effect of N_2 pulse on wt% product fraction of Co/Al_2O_3; T = 204°C; P=300 psig; SV=6000 h^{-1}
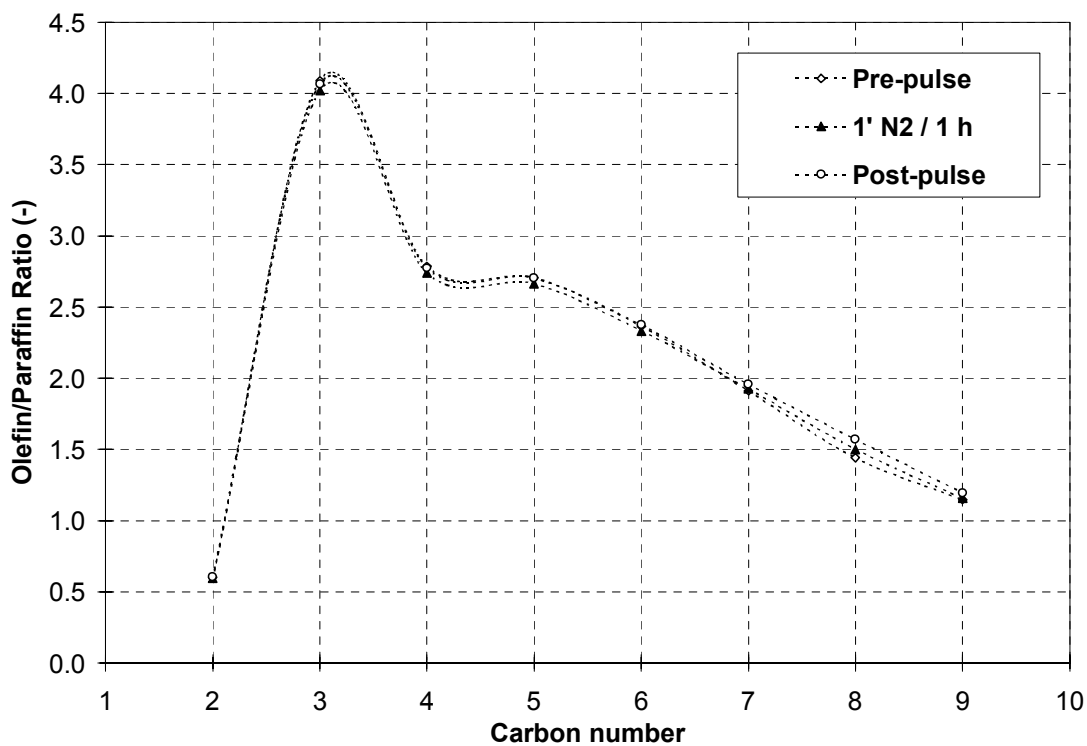
Figure 3.3.8. Effect of N_2 pulse on the C_2-C_9 olefin/paraffin ratio of Co/Al_2O_3; T = 204°C; P = 300 psig; SV = 6000 h^{-1}

Effect of Hydrogen Pulse Frequency (1 min H$_2$ per 1, 2, 4 hours)

The base run after the N$_2$ pulse run was performed under typical reaction conditions (204°C, 300 psig, 6000 h^{-1}). Following that, a series of 1-min H$_2$ pulse runs of variable pulse frequency were applied, so as to examine the effect of H$_2$ pulsing on the activity and selectivity of the FT reaction. These pulse runs involved substituting the flow of H$_2$+CO+Ar (51.7% of total flow) by an equal flow of H$_2$ for 1 min each time, thus keeping the total molar flow and reaction pressure constant during the runs. Upon completion of the pulse runs (each lasting 24 hours) a post-pulse base run was also performed.

The effect of varying the H$_2$ pulse frequency (1 min of H$_2$ per 1, 2, and 4 hours) on the activity (expressed as CO conversion) and C$_1$ (CH$_4$ and CO$_2$) selectivity are shown in the composite plots of Figures 3.3.9 and 3.3.10, respectively. These plots are composed of 10-hour representative segments of a series of sequential runs (typically lasting 24 hours so as to collect sufficient amounts of oil + wax for analysis). These runs are: a (pre-pulse) base run, followed by variable-frequency H$_2$ pulse runs, and ending with another (post-pulse) base run for comparison. The data points correspond to measurements of the reactor effluent every 15 minutes.

Due to this 15-min analysis time of the permanent gases (H$_2$, CO$_2$, Ar, N$_2$, CH$_4$, and CO) only 4 data points can be obtained every 1 hour of each run. In order to better observe the effect of a given pulse, a "delay time" is defined as the time difference between the end of an applied pulse and the following GC analysis (data point). The need for applying a delay time arises from the fact that a step change in the reactant feed cannot be instantaneously detected due to the dead volume of the reaction/analysis system. A delay time of 5 min was used, i.e., the local maxima in Figs. 3.3.9 and 3.3.10 were obtained 5 min after the completion of each 1-min pulse.

The CO conversion during the pre-pulse run (0-10 hour segment in Fig. 3.3.9) was ca. 21%. A 1-min H$_2$ pulse per hour (10-20 hour segment) resulted in a significant increase in CO conversion (from 21% to ca. 37.5%). The temperature of the catalyst also increased by 2°C (to 206°C), which is a clear indication of an enhanced reaction exotherm. However, this increase in temperature cannot be solely responsible for the observed 80% increase in activity.

The CO conversion reached a local maximum after each H$_2$ pulse, and then decreased *gradually* until the next H$_2$ pulse. The lower frequency pulse runs (1-min H$_2$ per 2 hours and 4 hours, 20-30 and 30-40 hour segments in Fig. 3.3.9, respectively) resulted in a less pronounced increase in CO conversion and in the reaction exotherm. The observed decrease in CO conversion after each pulse indicates that the catalytic activity tends to return to its pseudo steady state value. The post-pulse run (40-50 hour segment) gave a CO conversion of ca. 21.5%, verifying the return of the catalyst to its steady state performance. These observations are in good agreement with those obtained for the Co-ZrO$_2$/SiO$_2$ catalyst (Fig. 3.2.1).

The selectivity to CO$_2$ was ca. 0.6% (due to the low water-gas shift activity of the Co catalyst) and showed no measurable variation with H$_2$ pulsing. On the other hand, the selectivity to CH$_4$ (ca. 5% during the pre-pulse run) increased *instantaneously* after each pulse (from 5% up to 15-17%) and quickly returned to its steady state value. The observed decline in the local maxima of the CH$_4$ selectivity was the result of a minor slip in the analysis time of the GC-TCD (it was a few seconds longer than the preset time of 15 min).
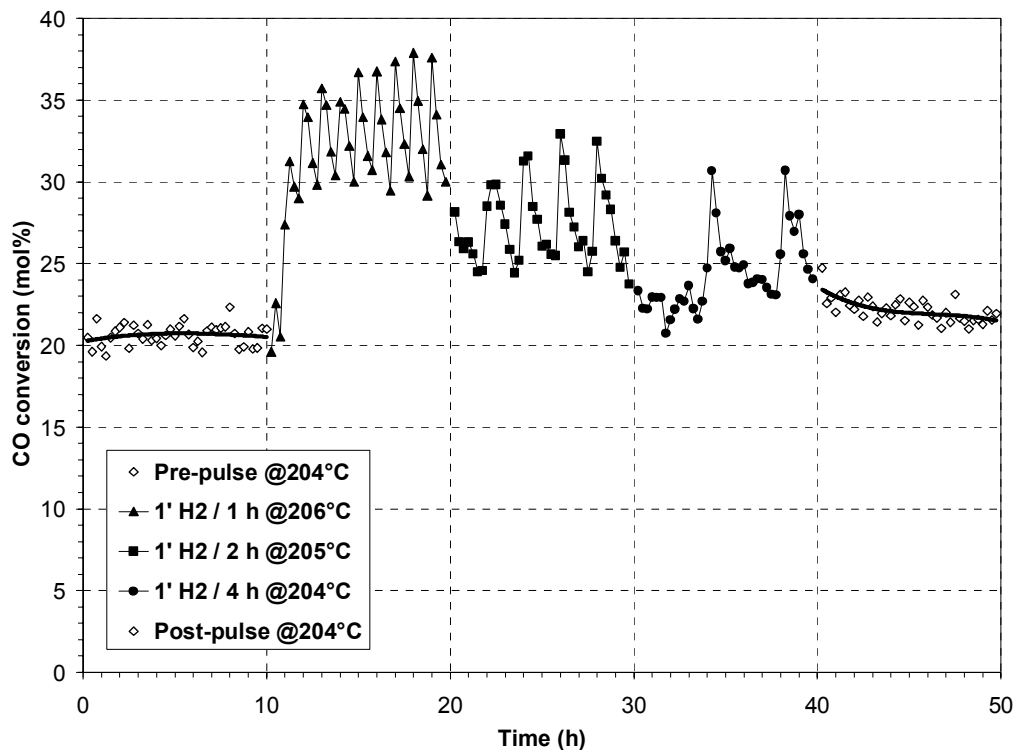
Figure 3.3.9. Effect of H_2 pulse frequency on the CO conversion of Co/Al_2O_3; T = 204-206°C; P = 300 psig; SV = 6000 h^{-1}
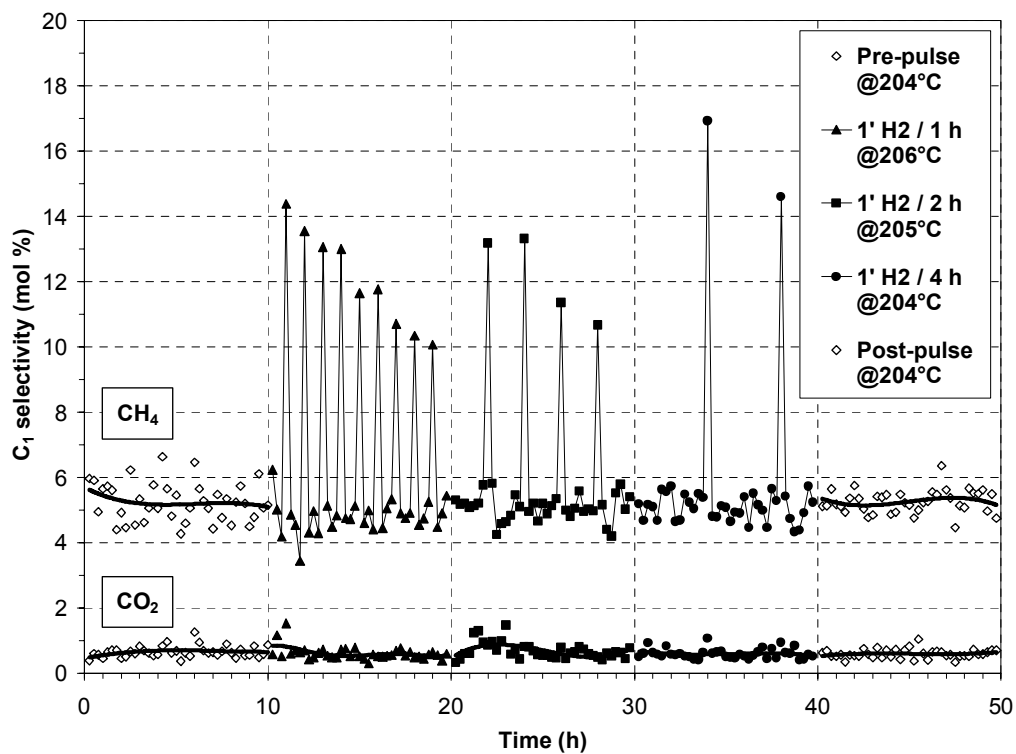
Figure 3.3.10. Effect of H_2 pulse frequency on the C_1 selectivity of Co/Al_2O_3; T = 204-206°C; P = 300 psig; SV = 6000 h^{-1}

Figure 3.3.11 shows a comparison between the molar yield of the desired C_{10}-C_{20} product fraction and the yield of the undesired CH_4 as a function of the H_2 pulse frequency. Pulse frequencies of 1, 0.5, and 0.25-h^{-1} correspond to a 1-min H_2 pulse per 1, 2, and 4 hours, respectively. The zero pulse frequency represents the average of the pre- and post-pulse runs.

The yield of CH_4 increased monotonically with H_2 pulse frequency, whereas the C_{10}-C_{20} yield increased substantially up to the pulse frequency of 0.5 h^{-1} and decreased slightly at 1 h^{-1}. The yield of C_{21+} also increased with the pulse frequency. This increase in product yield is attributed to the enhancement in catalytic activity caused by the H_2 pulsing (Fig. 3.3.9). The *intermediate* pulse frequency of 0.5-h^{-1} (1-min of H_2 per 2 hours) gave the maximum difference in yield between the C_{10}-C_{20} product fraction and the CH_4. This observation is in good agreement with that for the Co-ZrO_2/SiO_2 catalyst (Fig. 3.2.3). Also, it is interesting to note that the increase in H_2 pulse frequency resulted in an observed increase in the chain growth probability α, from a base value of 0.917 to 0.923 for the 1-min H_2 per 1 hour run.

Figure 3.3.12 shows the effect of H_2 pulse frequency on the C_2-C_9 olefin/paraffin ratio. The GC-FID analysis of the light hydrocarbons was performed at 30 min after the last applied pulse for each of the 3 examined variable pulse frequency runs (the importance of this point will be clarified subsequently). The higher pulse frequency of 1 h^{-1} resulted in a clear decrease in the olefin/paraffin ratio throughout the C_2-C_9 range; however, this became less prominent for the C_8 and C_9 species. The olefin/paraffin ratios for the lower pulse frequency runs were rather similar to those of the pre- and post-pulse runs. Thus, a higher H_2 pulse frequency appears to promote hydrogenation of light hydrocarbon products, resulting in suppressing the yield of light olefins.
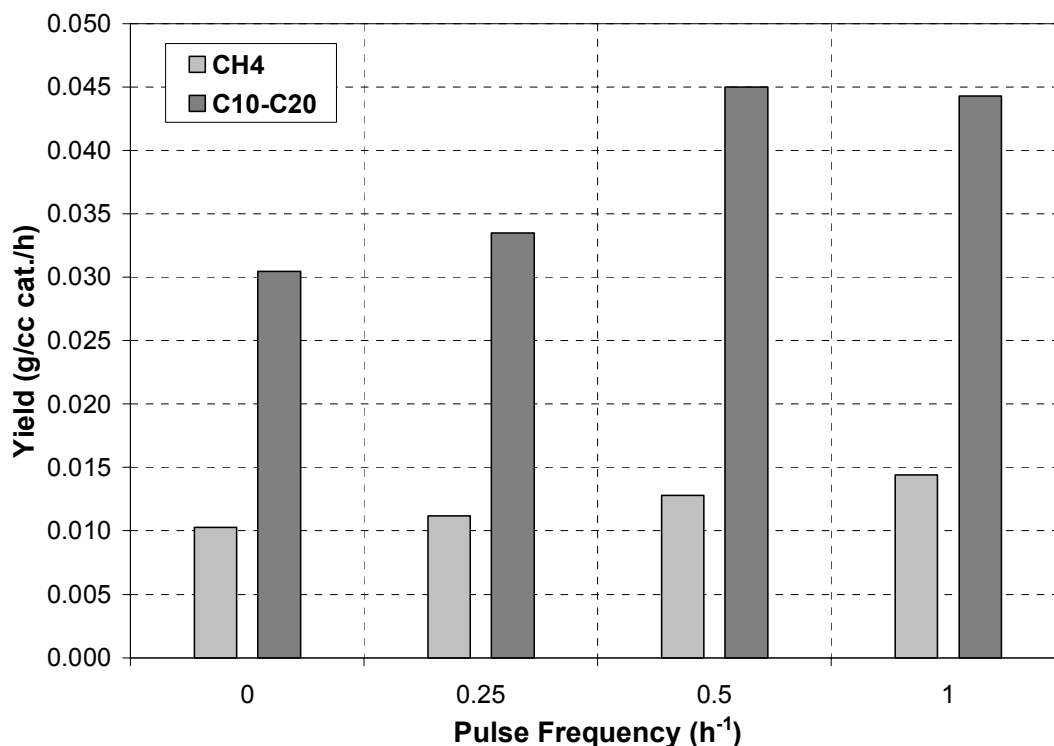
Figure 3.3.11.   Effect of H_2 pulse frequency on the product yield of Co/Al_2O_3; T = 204-206°C; P = 300 psig; SV = 6000 h^{-1}
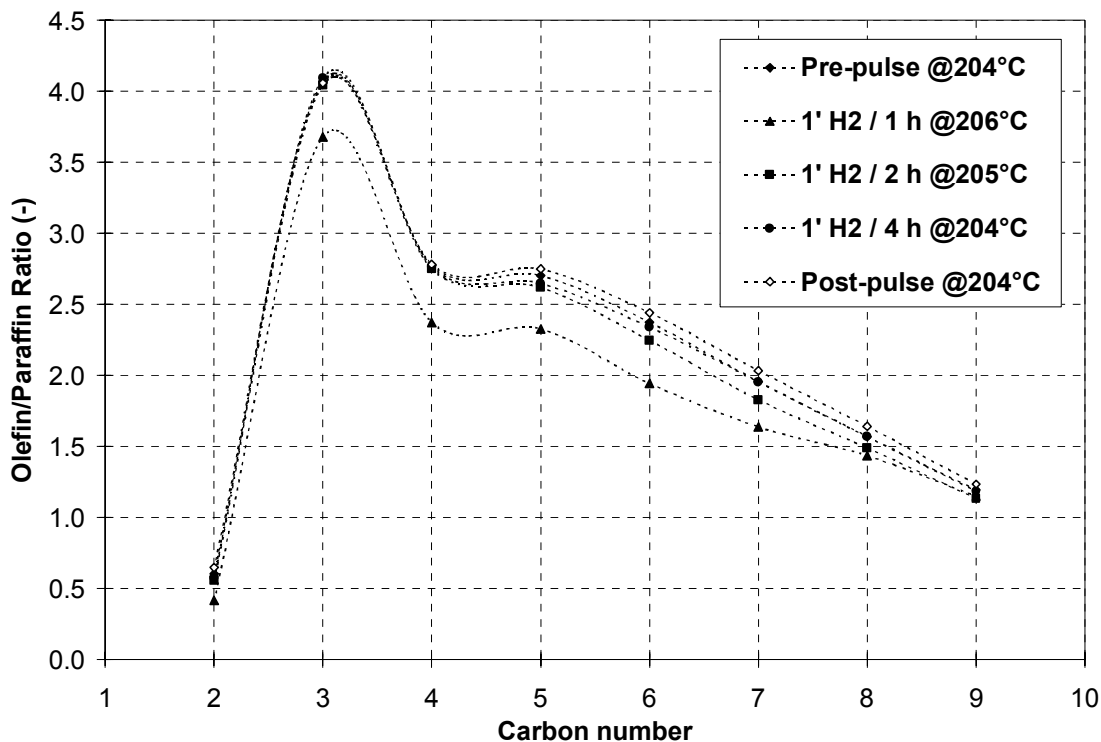
Figure 3.3.12. **Effect of H_2 pulse frequency on the C_2-C_9 olefin/paraffin ratio of Co/Al$_2$O$_3$; T = 204-206°C; P = 300 psig; SV = 6000 h^{-1}**

There are significant limitations in determining the direct effect of an applied pulse on the formation of the various FT products. The frequent GC analysis of the permanent gases (every 15 min) allows for quick monitoring of the CO conversion and C_1 selectivity variation during the time following a pulse (Figs. 3.3.9 and 3.3.10). On the other hand, the analysis of the oil + wax corresponds to a statistical average over the duration of the run. The GC analysis of the light (C_2-C_9) hydrocarbons can be used to monitor the variation in product formation after a pulse more closely.

Figure 3.3.13 gives a comparison of the C_2-C_9 olefin/paraffin ratios measured at different times after the last 1-min H_2 pulse of the 0.5h^{-1}-pulse run. These times ranged from 5 min after the pulse down to 4 hours after the pulse. The results clearly show that beyond 30 min after the pulse there was no significant difference in the olefin/paraffin ratio of the light hydrocarbons, despite the strong (yet declining) enhancement in activity during this time period (Fig. 3.3.9).

The observed decrease in the olefin/paraffin ratio of the C_2-C_4 species was due to enhanced formation of C_2-C_4 paraffins, rather than to a decrease in the formation of C_2-C_4 olefins. This is shown more clearly in Figure 3.3.14, which presents the ratio of the produced amounts at 5 min and at 30 min after the pulse for methane up to nonane (C_9). In agreement with the results of Fig. 3.3.10, the amount of CH$_4$ increased significantly (more than 3 times) immediately after the applied H_2 pulse. Among the other paraffins, ethane, propane and butane also showed enhanced formation, whereas the higher (C_5-C_9) paraffins did not. Interestingly, none of the C_2-C_9 olefins showed any variation with time following the pulse.

41
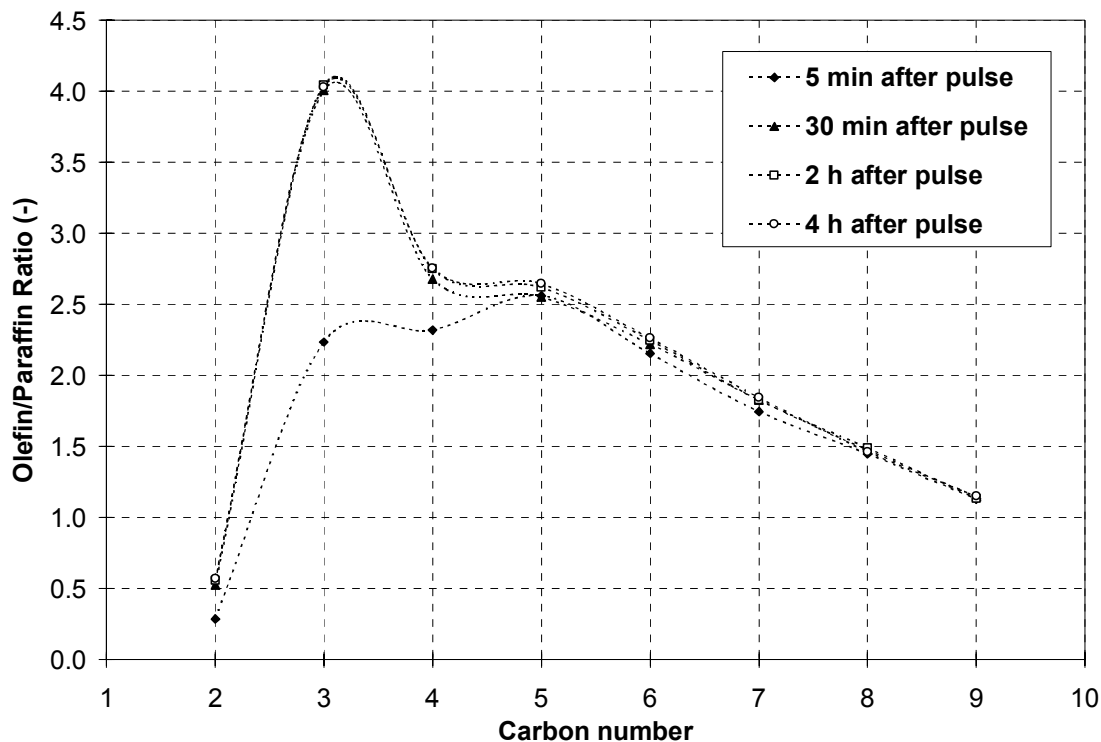
Figure 3.3.13. Effect of time after a 1-min H_2 pulse on the C_2-C_9 olefin/ paraffin ratio of Co/Al$_2$O$_3$; T = 206°C; P = 300 psig; SV = 6000 h^{-1}
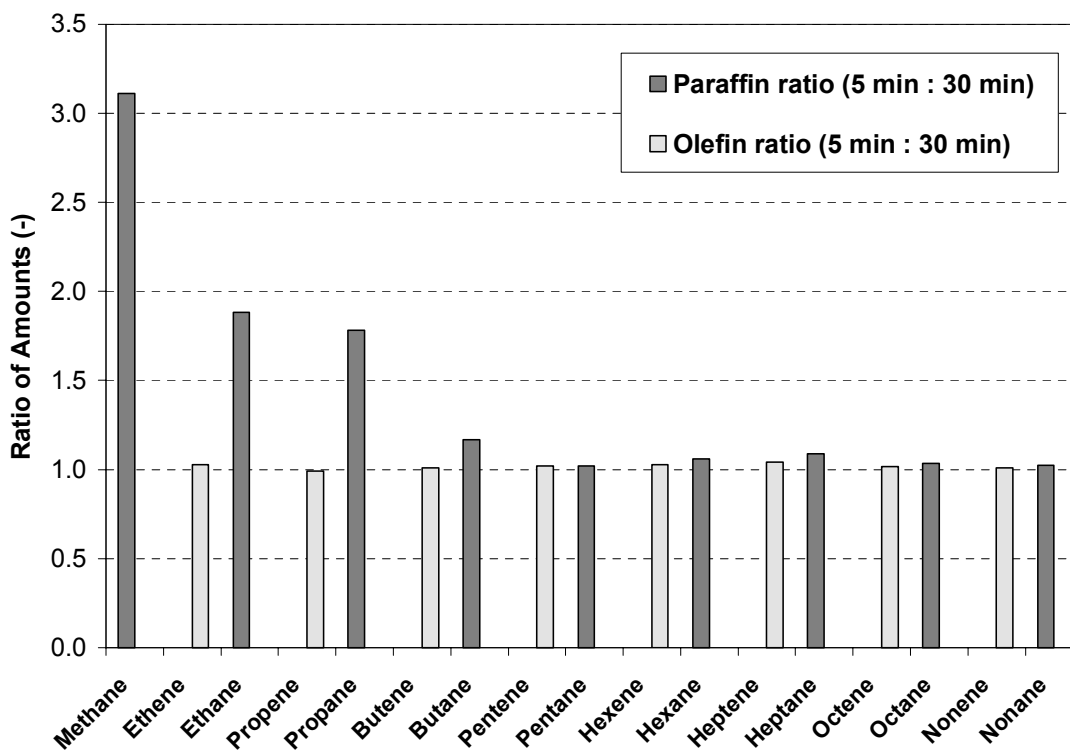
Figure 3.3.14. Effect of 1-min H_2 pulse on the paraffin vs. olefin 5-min : 30-min ratio of Co/Al$_2$O$_3$; T = 206°C; P = 300 psig; SV = 6000 h^{-1}

Effect of Hydrogen Pulse Duration (1, 2, 4 min H₂ per 2 hours)

Following the post-pulse run at 204°C (Figs. 3.3.9 and 3.3.10) H_2 pulse runs of constant frequency but variable pulse duration were applied. The effect of varying the H_2 pulse duration (1, 2, 4 min of H_2 per 2 hours) on CO conversion and C_1 (CH_4 and CO_2) selectivity are given in the composite plots of Figures 3.3.15 and 3.3.16, respectively. These plots are composed of 10-hour representative segments of the base (pre-pulse) run followed by the variable duration H_2 pulse runs (typically lasting 24 hours each so as to collect sufficient amounts of oil + wax for analysis). The GC analysis time was 15 min and a delay time of 5 min between the end of a pulse and the next GC injection was used.

The CO conversion during the pre-pulse run (0-10 hour segment in Fig. 3.3.16) was ca. 21%. A 1-min H_2 pulse (10-20 hour segment) caused an increase in CO conversion up to ca. 29% (a 38% activity increase), followed by a *gradual* decrease in conversion until the next H_2 pulse. The bed temperature remained constant (at 204°C) by decreasing the oven set point by 1°C. Extending the duration of the H_2 pulse to 2 min and 4 min resulted in further increasing the maximum conversion of CO (also at 204°C) to ca. 32% and 35%, respectively.

The selectivity to CH_4 (5.5% in the pre-pulse run, Fig. 3.3.16) increased *instantaneously* after each pulse and then quickly returned to its steady state value. Increasing the duration of the H_2 pulse from 1 min to 2 min to 4 min resulted in an enhancement in the maximum measured CH_4 selectivity from ca. 16% to ca. 22% to ca. 25%, respectively. These observations are in good agreement with those obtained for the Co-ZrO_2/SiO_2 catalyst (Figs. 3.2.5 and 3.2.6).
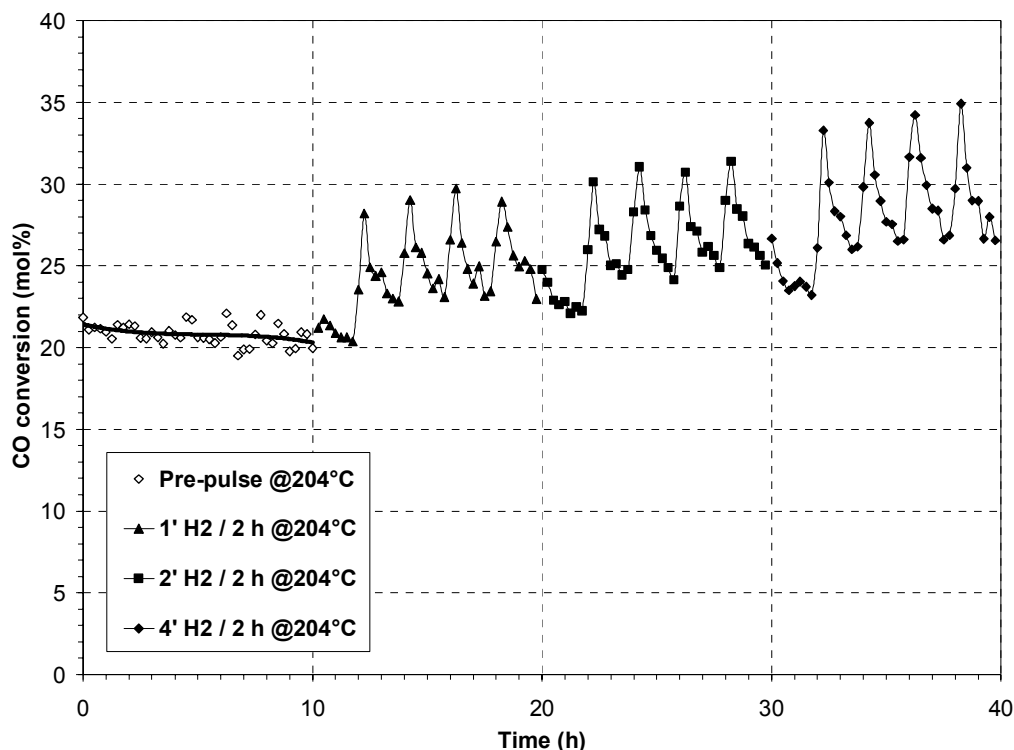
Figure 3.3.15. Effect of H₂ pulse duration on the CO conversion of Co/Al₂O₃; T = 204°C; P = 300 psig; SV = 6000 h⁻¹
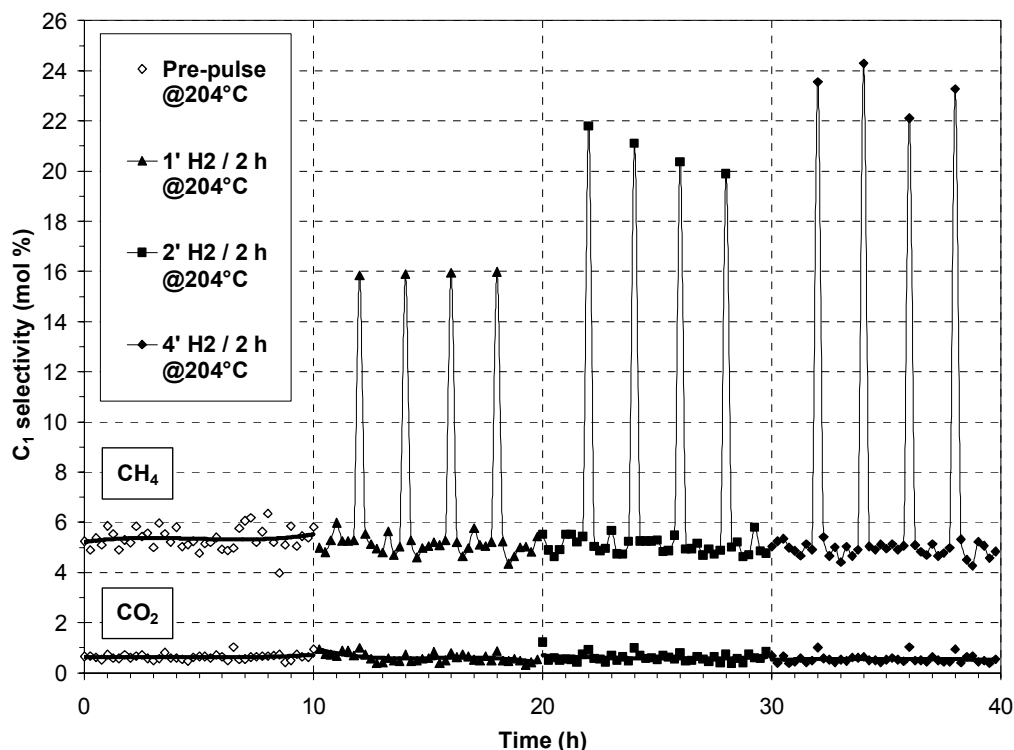
Figure 3.3.16. Effect of H_2 pulse duration on the C_1 selectivity of Co/Al_2O_3; T = 204°C; P = 300 psig; SV = 6000 h^{-1}

At about 16 hours into the last pulse run of this series (i.e., the 4-min H_2 per 2 hours, 30-40 hour segment in Figs. 3.3.15 and 3.3.16) there was a power failure. The reactant feed stopped and the reactor was automatically flushed with N_2. The reactant feed was restored 8 hours later, while the bed temperature had dropped to 201°C. As a result of that, there was no GC measurement of the light hydrocarbons for this run and the calculated weight fractions and molar yields of the products have a rather high degree of uncertainty.

The effect of H_2 pulse duration on the molar yield of C_{10}-C_{20} and CH_4 is shown in Figure 3.3.17. The zero pulse duration represents the pre-pulse run. Both product yields appear to monotonically increase with the duration of the applied H_2 pulse. The percent increase in yield with respect to the pre-pulse run was 25±2% for both products. The observed lesser enhancement in molar yield in comparison to the variable pulse frequency runs (Fig. 3.3.11) may be related to the difference in bed temperature (constant vs. increasing) for these two series of H_2 pulse runs.

Figure 3.3.18 shows the effect of variable H_2 pulse duration on the olefin/paraffin ratio of the light hydrocarbon products. The GC analysis of the light hydrocarbons for the pulse runs was performed at 30 min after the last H_2 pulse. No data for the 4-min H_2 pulse run are reported in Fig. 3.3.18 since, due to the previously mentioned power failure, no GC analysis was performed. The data of Fig. 3.3.18 indicate that an increase in the H_2 pulse duration (from zero min to 1 min to 2 min) resulted in suppressing the olefin/paraffin ratio essentially throughout the C_2-C_9 product range. Therefore, hydrogenation of the light hydrocarbons was apparently enhanced as a result of the higher duration H_2 pulsing.
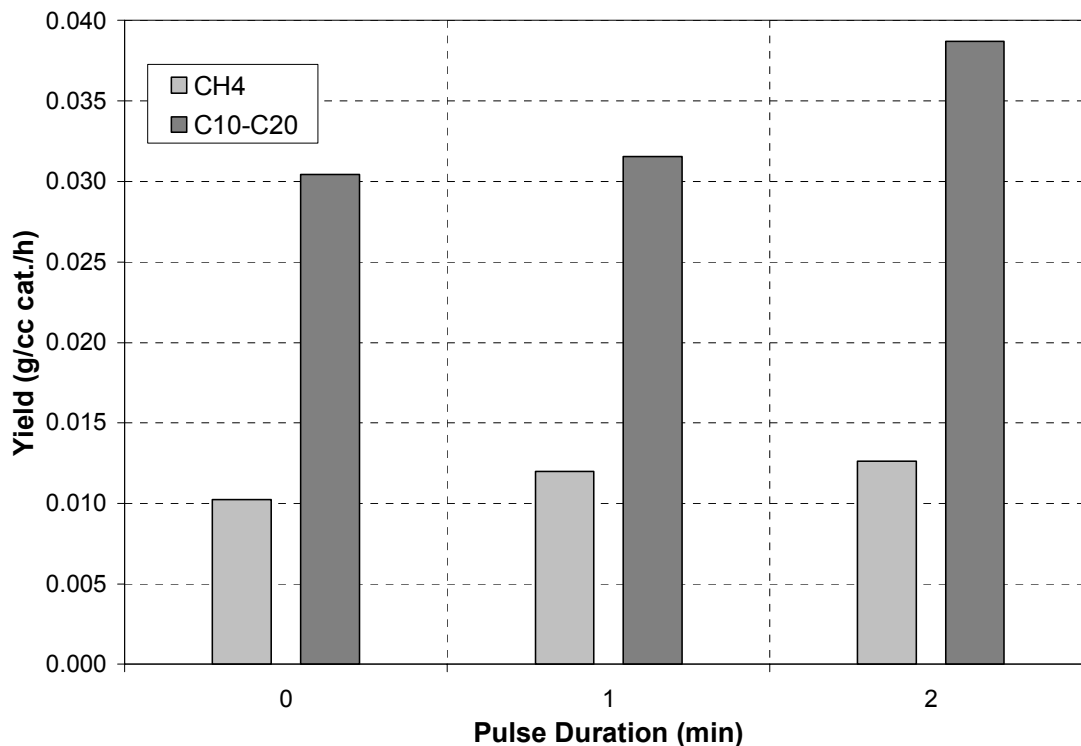
Figure 3.3.17. Effect of H$_2$ pulse duration on the product yield of Co/Al$_2$O$_3$; T = 204°C; P = 300 psig; SV = 6000 h^{-1}
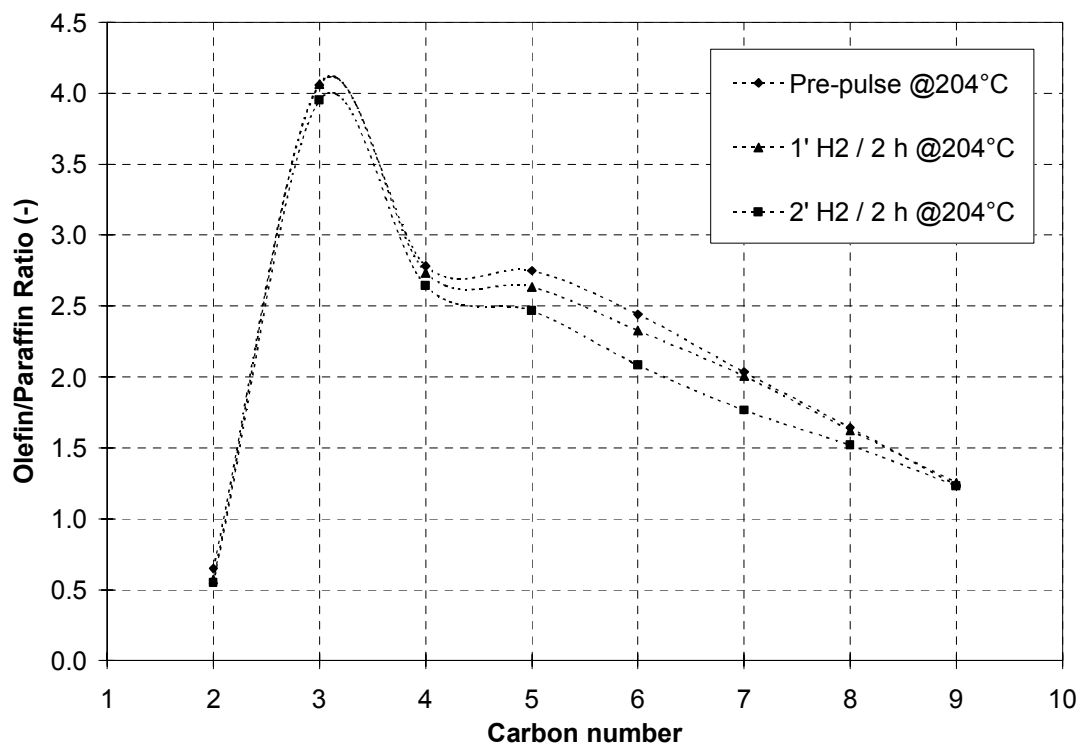
Figure 3.3.18. Effect of H$_2$ pulse duration on the C$_2$-C$_9$ olefin/paraffin ratio of Co/Al$_2$O$_3$; T = 204°C; P = 300 psig; SV = 6000 h^{-1}

Effect of Low Reactant Partial Pressure and Steam Addition

After restoring the reactant feed the reaction was carried out for 24 hours at 203°C so as to establish a new pseudo steady state. Then, the reactant partial pressure was decreased from 50% syngas to 17% syngas under constant feed flow (200 scc/min) and total reaction pressure (300 psig). After running for a period of 24 hours under these low partial pressure conditions, 10% steam was added to the feed while maintaining constant feed flow and pressure. The purpose of this set of runs was to simulate in a fixed-bed reactor the higher conversion in the presence of high concentration of steam typically encountered when running FT synthesis in a slurry reactor.

The measured CO conversion under 50% syngas at 203°C was ca. 17.5% (CO productivity of ca. 175 cc CO per cc catalyst per hour), and the CH_4 and CO_2 selectivity was ca. 6.0% and 0.7%, respectively. Upon lowering the reactant partial pressure to 17% the CO conversion increased to ca. 35% (CO productivity of ca. 120 cc CO / cc cat / h); thus, the CO productivity decreased by ca. 30%. The selectivity to CH_4 and CO_2 was ca. 5.5% and 1.0%, respectively, indicating a mild suppression of the methane formation and an enhancement in the water-gas shift reaction.

Figure 3.3.19 presents the C_2-C_9 olefin/paraffin ratio for the 2 concentrations of syngas (high and low). The lower syngas concentration increased the olefin/paraffin ratio for the C_3-C_5 range, but decreased it for the rest of the examined species in Fig. 3.3.19.
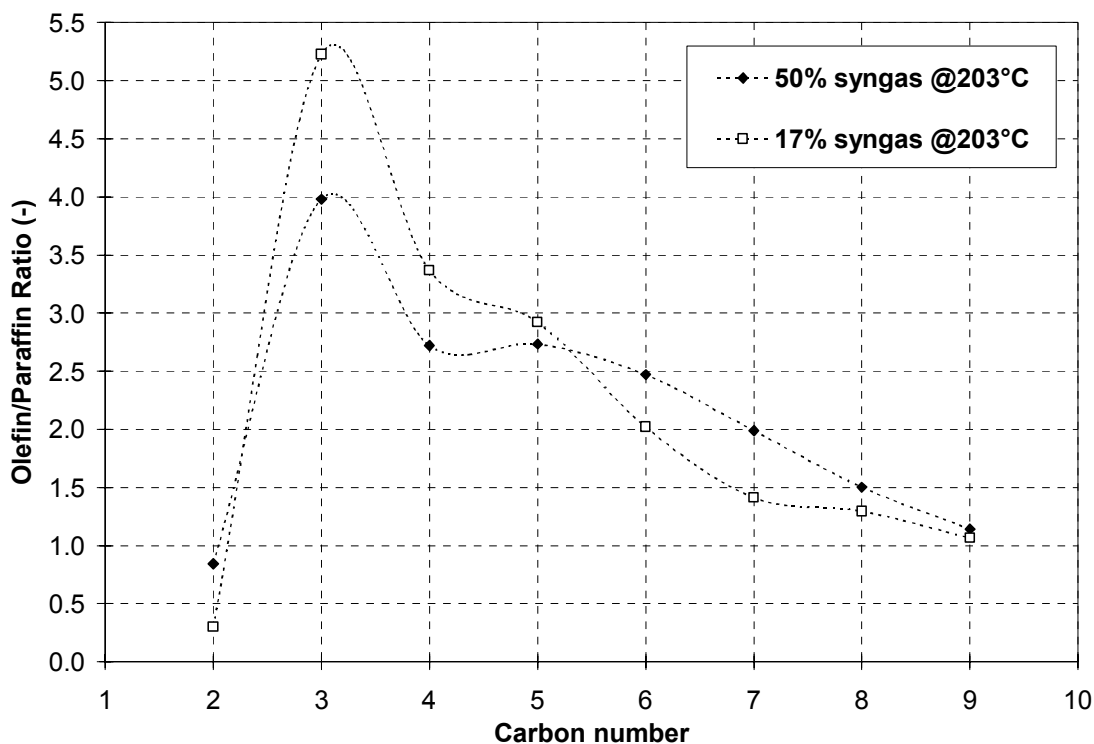
Figure 3.3.19. **Effect of reactant partial pressure on the C_2-C_9 olefin/paraffin ratio of Co/Al$_2$O$_3$; T = 203°C; P = 300 psig; SV = 6000 h^{-1}**

Upon adding 10% steam to the feed, the CO conversion decreased to ca. 31% (CO productivity of ca. 100 cc CO / cc cat / h) within a period of 24 hours, due to enhanced catalyst deactivation in the presence of excess steam. The effect of the addition of 10% steam on the selectivity to CH_4 and CO_2 is shown in Figure 3.3.20. The selectivity to CH_4 decreased from 5.5% to 3.5%, which apparently is correlated to the overall decrease in activity as a result of the addition of steam. The selectivity to CO_2 was found to increase from 1.0% to almost 3.0%, suggesting the enhancement of the water-gas shift activity of the catalyst due to the presence of steam (a reactant for this reaction).

A 1-min H_2 pulse per 1 hour run was performed under the conditions of low (17%) reactant concentration and in the presence of 10% steam in the feed. Despite some instability on the data acquired during this 24-hour run, the CO conversion was found to increase in a pattern similar to those described previously (i.e., an increase after the pulse followed by a gradual decrease until the next pulse) and reached a maximum value of ca. 41% after each applied H_2 pulse. This activity enhancement due to pulsing clearly overcame the activity loss due to the presence of steam.

The selectivity to CH_4 increased up to 12% and that to CO_2 also increased up to ca. 4.0% after each pulse; they both quickly returned to their steady state value of ca. 2.0% (lower than before the pulse run). The observed increase in the selectivity to CO_2 with the H_2 pulse was rather unexpected, since the presence of excess H_2 should favor the reverse water-gas shift reaction, i.e., lowering the outlet concentration of CO_2 (co-reactant with H_2 in that reaction).
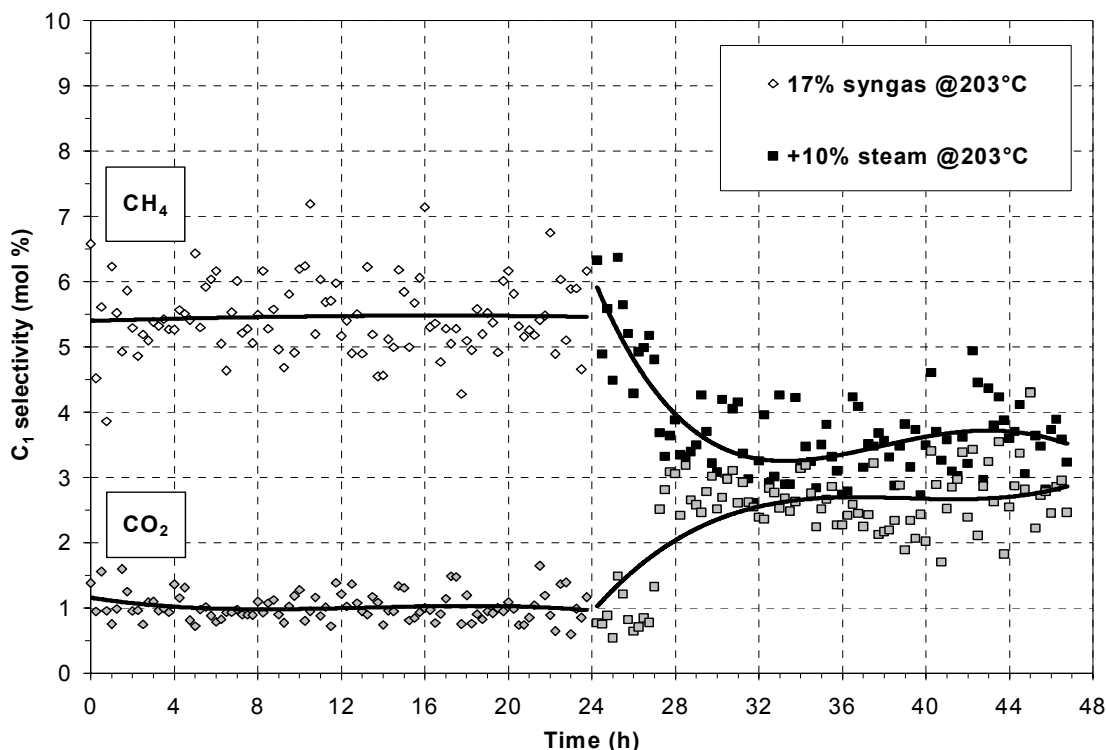
Figure 3.3.20. Effect of steam addition on the C_1 selectivity of Co/Al_2O_3; T = 203°C; P = 300 psig; SV = 6000 h^{-1}

3.4. FT Reaction on 0.5% Ru/Al$_2$O$_3$ in a Fixed-Bed Reactor (FBR)

A 0.5wt%Ru/Al$_2$O$_3$ catalyst was synthesized (at North Carolina State University, in sub-contract to RTI) using the incipient wetness impregnation method on a high-purity CATAPAL alumina. After drying, the catalyst was reduced (*without prior calcination*) in 7%H$_2$/Ar at 300°C and was then passivated in air at room temperature. The actual Ru loading (determined by elemental analysis) was 0.5wt%. A physical mixture of 2 cc (1.77 g) of the reduced Ru/Al$_2$O$_3$ catalyst and 10 cc (16.02 g) of a low-surface-area (0.2 m^2/g) α-alumina (SA5397, Norton) was loaded into the reactor. The catalyst was reduced *in-situ* under H$_2$ at 300°C for 8 h, and was cooled and pressurized to ca. 400 psig (28.2 atm). The FT reaction started by feeding a 3.3%Ar/33.3%CO/63.4%H$_2$ gas mixture, under the following reaction conditions:

Reactants: H$_2$ = 63.4%, CO = 33.3% (H$_2$:CO = 1.9), Inert (Ar) = 3.3% (Ar:CO = 0.1)
F = 100 scc/min, SV = 3000 h^{-1}, P = 28 atm (typical operating pressure: 100-1000 atm)

The reaction temperature was increased slowly to 245°C (typical operating T: 160°C). However, the reaction did not actually reach a "pseudo-steady state"; the CO conversion was found to increase at a very slow rate (from ca. 12% to ca. 18% in a period of 66 hours) and the measured bed temperature was 243°C (bottom) and 252°C (top). Despite not attaining steady state, this isothermal run was followed by a pulse run, involving substitution of the reactant feed flow (H$_2$/CO/Ar) with an equal molar flow of a pulse gas (H$_2$). The total molar flow and the reaction pressure were kept constant between base and pulse runs. A pulse sequence of 1 min per 1 hour was applied. The time-on-stream data on the outlet H$_2$:CO ratio, the CO conversion, and selectivity to CH$_4$/CO$_2$ are shown in Figures 3.4.1, 3.4.2, and 3.4.3, respectively.
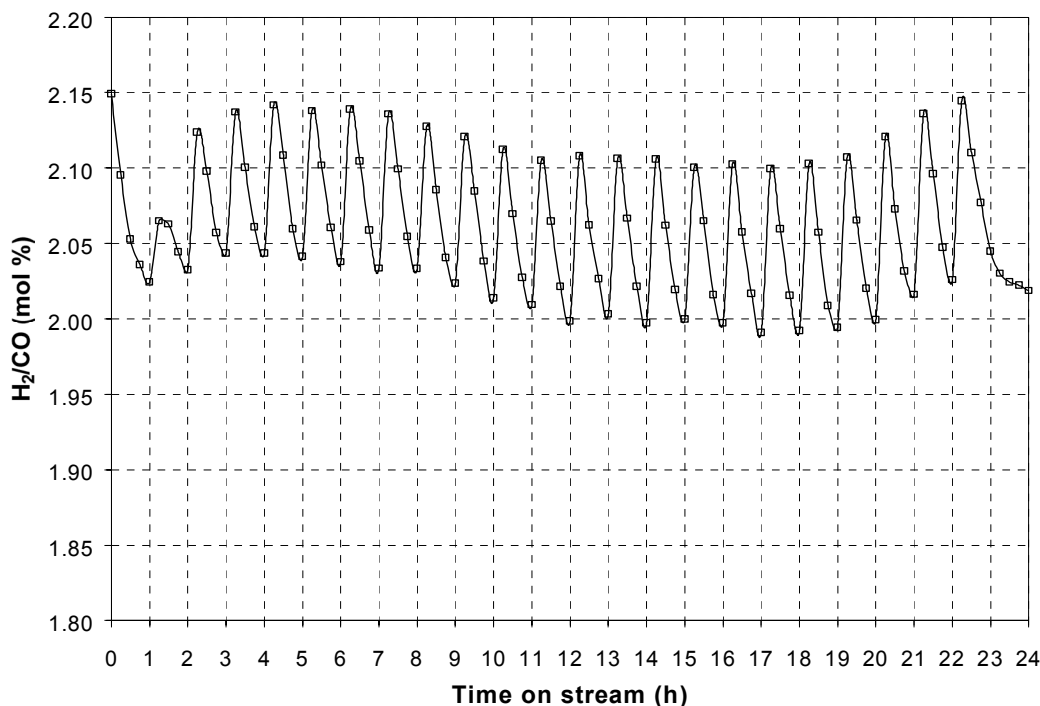
Figure 3.4.1. Effect of H$_2$ pulse on the outlet H$_2$:CO ratio of Ru/Al$_2$O$_3$; P = 400 psig; SV = 3000 h^{-1}
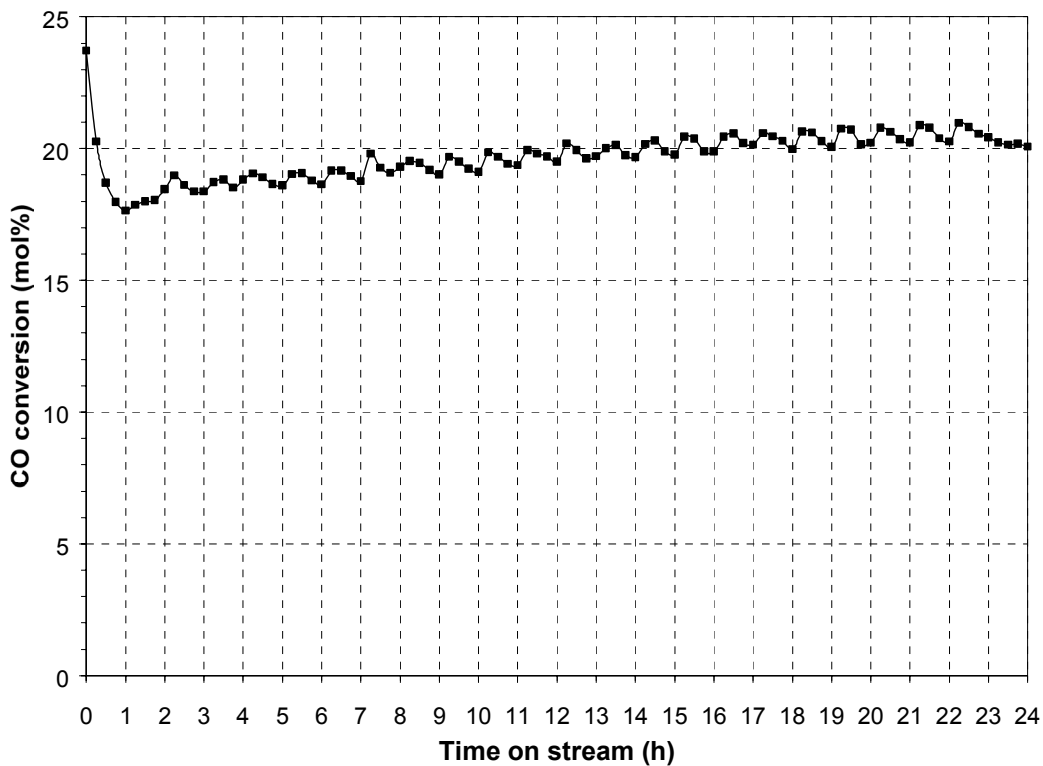
Figure 3.4.2. **Effect of H_2 pulse on the CO conversion of Ru/Al$_2$O$_3$; P = 400 psig; SV = 3000 h^{-1}**
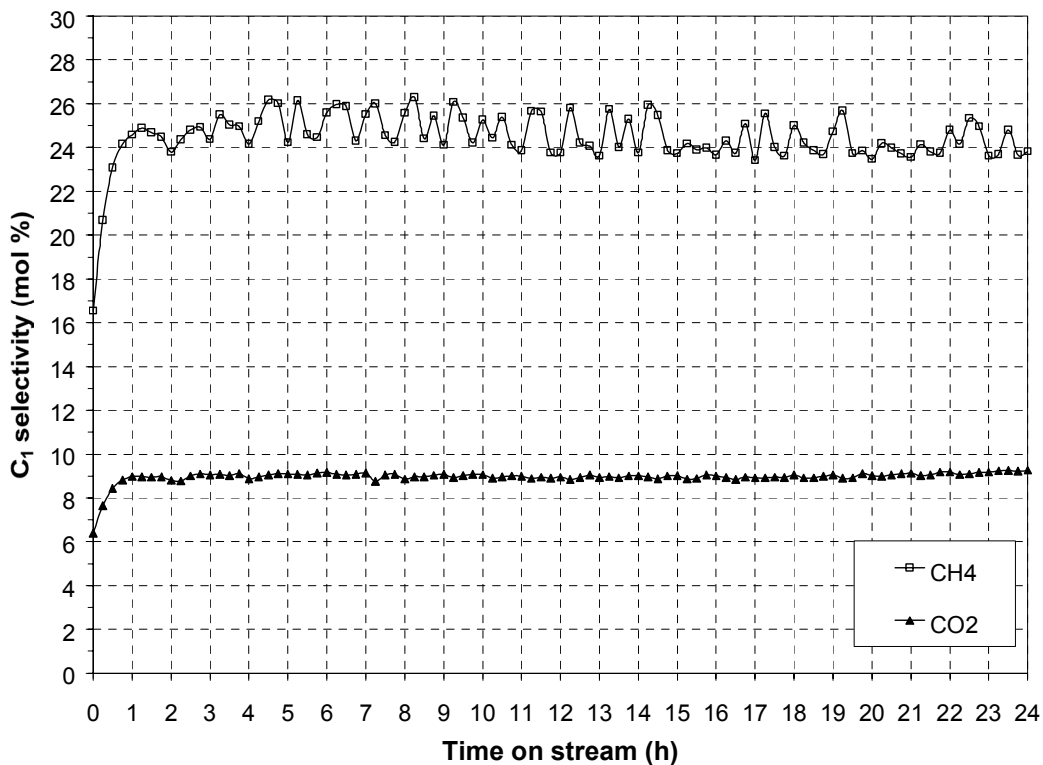
Figure 3.4.3. **Effect of H_2 pulse on the C$_1$ selectivity of Ru/Al$_2$O$_3$; P = 400 psig; SV = 3000 h^{-1}**

The applied H_2 pulse increased the outlet H_2:CO ratio only moderately (from ca. 2.0 to ca. 2.1), in a time-pattern similar to that observed for the other examined catalysts (Fig. 3.4.1). The CO conversion increased from ca. 18% to ca. 20% during the 24-hour run; however, this increase in activity was apparently not associated with the application of the H_2 pulse, since it matched with that observed for the isothermal run (increase by ca. 6% in almost 3 days). Indeed, each applied H_2 pulse had only minimal positive effect on CO conversion (increase of only 1%, Fig. 3.4.2). The selectivity to CH_4 and CO_2 was very high (ca. 24% and ca. 9%, respectively), with small fluctuations (mainly for CH_4) due to the applied pulse sequence. Therefore, the H_2 pulse had only minimal effect on the activity and C_1 selectivity of the Ru/alumina catalyst, which showed high methanation (product CH_4) and water-gas-shift (product CO_2) activity.

The poor FT synthesis performance of Ru/alumina could be due to insufficient reduction of Ru at 300°C. In order to examine this hypothesis, after the pulse run the reactor was depressurized gradually, the catalyst was reduced again *in-situ* under H_2 at 350°C for 8 hours, it was cooled to 115°C and pressurized back to 400 psig under the H_2/CO/Ar reactant mixture. The catalyst was then heated from 115°C to 215°C by 15°C/h. Due to an error in the controller program, after reaching the target temperature of 215°C the bed was cooled back to the initial temperature of 115°C. The heating process was repeated and the bed temperature was stabilized at 214°C (bottom) and 219°C (top). The variation in CO conversion with time-on-stream is shown in the composite plot of Figure 3.4.4, composed of two 14-hour segments of the two heat-up processes. The CO conversion curves for the two activation runs were essentially identical (Fig. 3.4.4), suggesting that there was no effect of applying these procedures on catalyst activity. The effect of temperature on the rate of CO disappearance (calculated from the measured CO conversion assuming differential plug-flow reactor conditions) is shown in Figure 3.4.5.
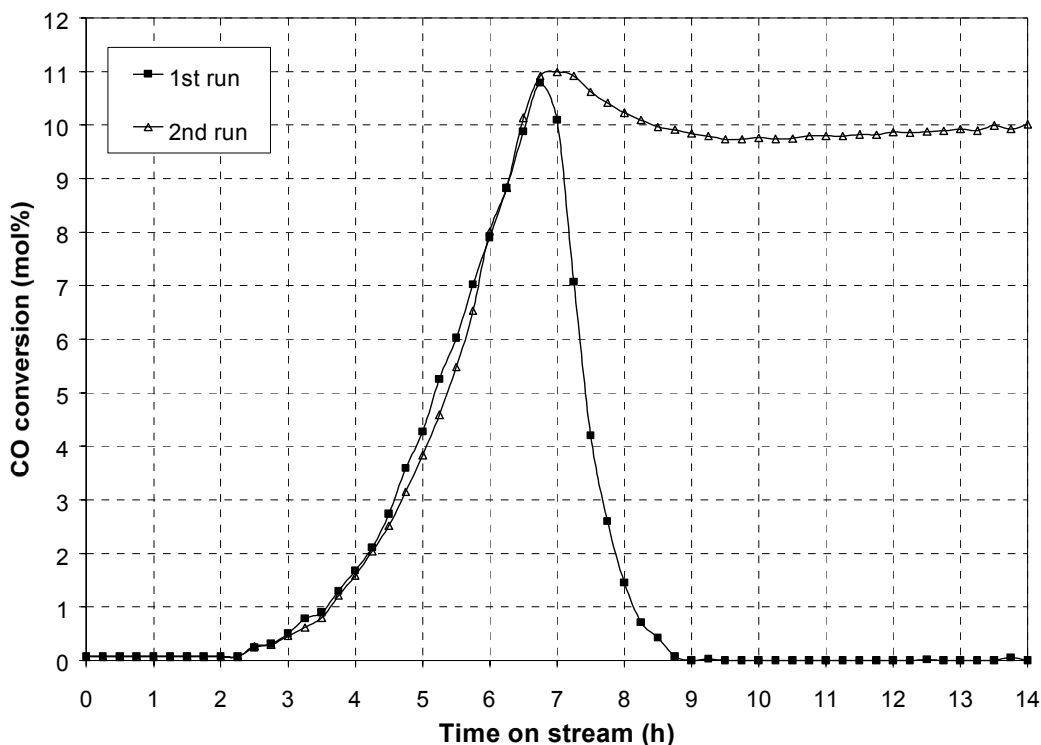
Figure 3.4.4. **Effect of the activation process on the CO conversion of Ru/Al$_2$O$_3$; P = 400 psig; SV = 3000 h^{-1}**

50
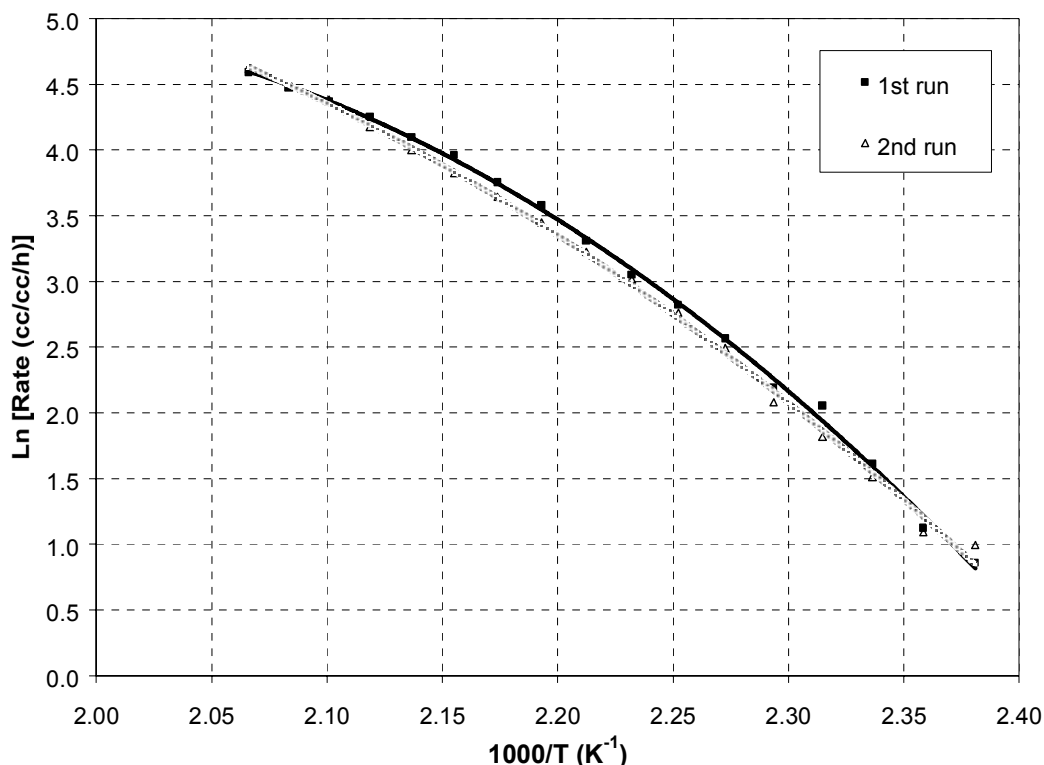
Figure 3.4.5. **Effect of temperature on the rate of CO consumption of Ru/Al$_2$O$_3$; P = 400 psig; SV = 3000 h^{-1}**

The Arrhenius-type plots of Fig. 3.4.5 present the dependence of the experimentally determined rate of reaction (rate of CO consumption) on the reciprocal temperature of reaction (the "bottom" bed temperature was used). The slope of these curves provides a measurement for the apparent energy of activation for the overall reaction on the Ru/alumina catalyst, under the examined reaction conditions. The curvature of the plots in Fig. 3.4.5 implies a shift between two regimes with a different reaction-controlling (rate-determining) step. Based on the low-T data (7 last points) of these curves the obtained apparent energy of activation is:

$$E_{a\,(low-T)} = 125\pm5 \text{ kJ/mol}.$$

On the other hand, the high-T data (first 5 points) give the apparent activation energy of:

$$E_{a\,(high-T)} = 65\pm7 \text{ kJ/mol}.$$

The decrease in the apparent activation energy with increasing reaction temperature is a clear indication of a transition from a kinetics-controlled reaction (at low-T) to a diffusion-controlled reaction (at high-T) under the examined conditions. More specifically, for a 1st order reaction (1st order dependence of the reaction rate on the concentration of CO) the apparent activation energy under diffusion-control is close to one half of that under kinetics-control. The numerical values of the two apparent activation energies in this experiment appear to be in good agreement with this prediction. Therefore, the obtained data imply a pseudo-1st order dependence of the overall FT reaction on the concentration of CO.

After the second activation procedure, the bed temperature was stabilized at 214/219°C, thus allowing the reaction to reach a new "pseudo-steady state". The measured conversion was ca. 11% (in comparison to 12%-18% at 243/252°C), indicating a clear activation of the catalyst, with still a tendency for minor increase in activity with time on stream. The outlet H_2:CO ratio dropped to ca. 1.9 (compared to ca. 2.0 prior to the activation). The most important difference, however, in the measured parameters before and after the activation, was the strong suppression of the selectivity to CH_4 (ca. 14% instead of ca. 24%) and CO_2 (ca. 4% instead of ca. 9%). This shift in selectivity from the undesired C_1 compounds to the desired FT reaction hydrocarbon products was apparently related to the lower reaction temperature while maintaining a reasonable conversion of CO (which in turn suggests a better activation of the catalyst).

Following this "base" run a 1-min H_2 pulse per 1 hour was applied, so as to compare the effect of H_2 pulsing between the runs prior to and after the activation. The time-on-stream response of the CO conversion and the CH_4/CO_2 selectivity are given in Figures 3.4.6 and 3.4.7, respectively. The CO conversion increased from 11% to 12% in the 24-hour duration of the run. Again, this minor increase in activity was due to the continuous activation of the catalyst by the strong reaction exotherm, rather than by the applied H_2 pulse sequence. Each H_2 pulse had only minimal positive effect on the measured CO conversion (Fig. 3.4.6). The selectivity to CH_4 showed a minor increase with each H_2 pulse (ranging between 12% and 14%), and the selectivity to CO_2 remained essentially constant at 4% (Fig. 3.4.7).
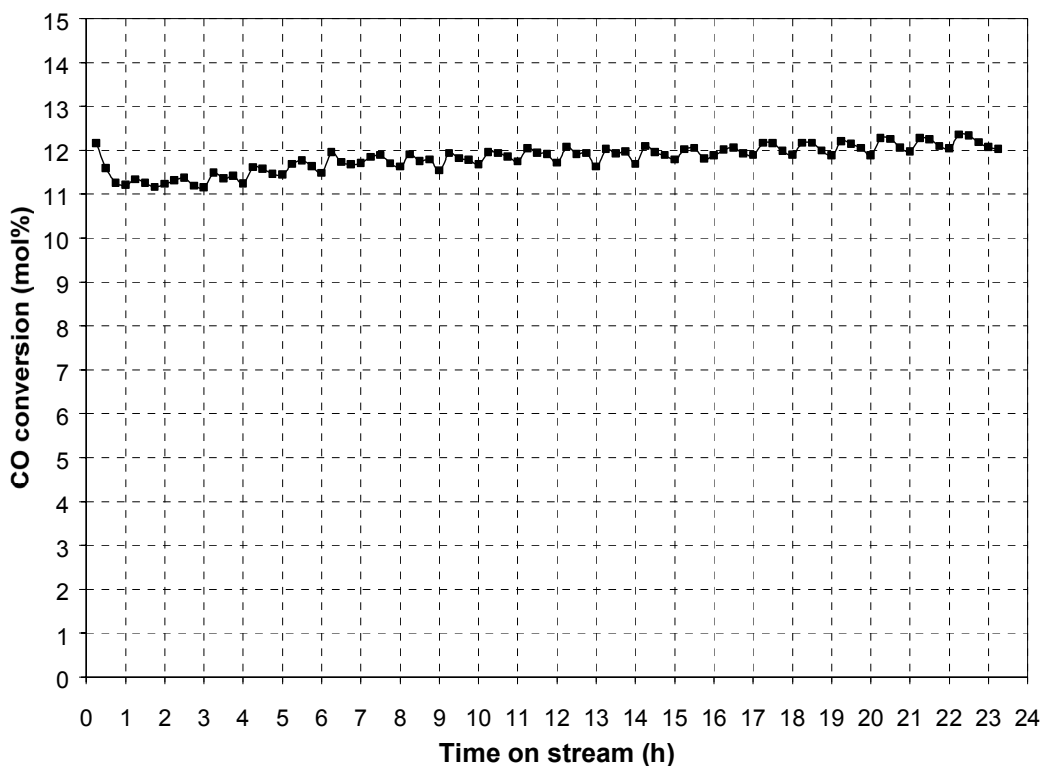
Figure 3.4.6. **Effect of H_2 pulse on the CO conversion of Ru/Al$_2$O$_3$; P = 400 psig; SV = 3000 h^{-1}**
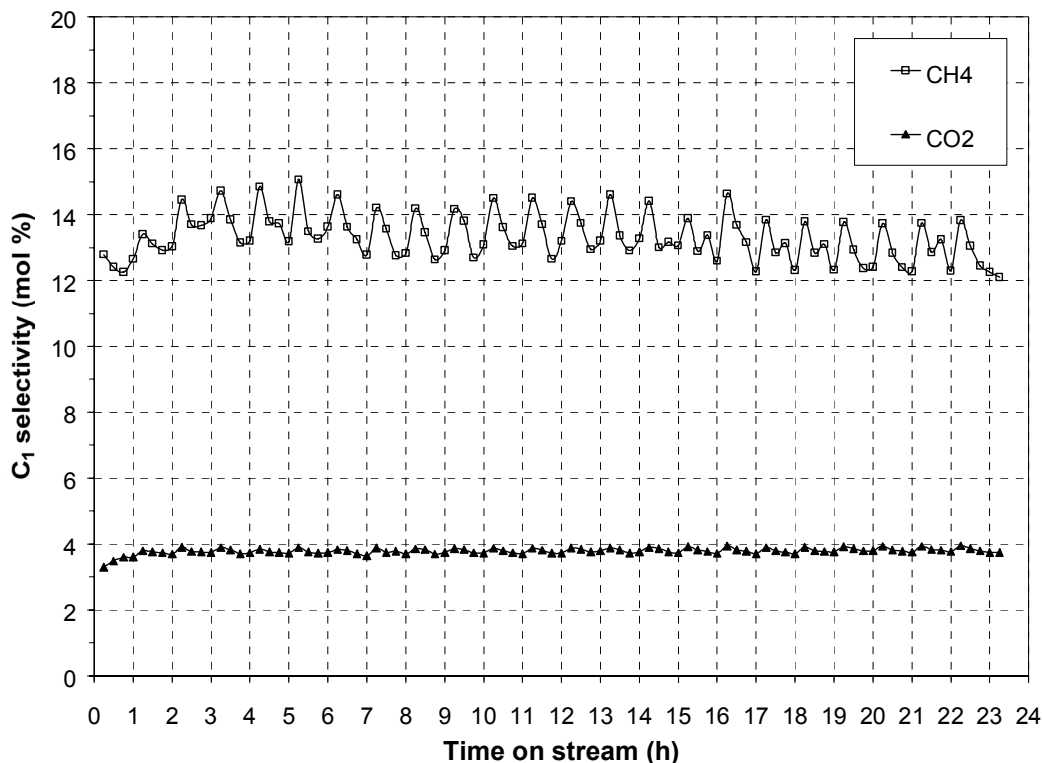
Figure 3.4.7. Effect of H_2 pulse on the C_1 selectivity of Ru/Al$_2$O$_3$; P = 400 psig; SV = 3000 h^{-1}

Therefore, the H_2 pulsing appeared to have only minimal impact on the activity and selectivity of the Ru/alumina catalyst even after the second reduction. The catalyst was significantly better activated after applying the second reduction procedure, resulting in exhibiting the same activity at lower reaction temperatures, which in turn suppressed the selectivity to undesired compounds CH_4 and CO_2.

The analysis of the wax for the base run at 214/219°C resulted in obtaining a hydrocarbon product distribution with a chain growth factor α of ca. 0.74, which is clearly a very low value for the given type of catalyst. The molar selectivity to the C_{10}-C_{20} compound range was ca. 24%. Due to difficulties in the collection of the wax sample for the H_2 pulse run the corresponding product analysis involved a large degree of uncertainty. Based on the C_{10}-C_{30} product fraction the obtained α value was ca. 0.80, while the selectivity to C_{10}-C_{20} was ca. 19%. The observed increase in the α value for the H_2 pulse run could not be positively attributed to the pulsing itself, since a follow-up base run at the same temperature (214/219°C) also gave a higher α value (ca. 0.79). Despite the significant uncertainty associated with these values, the observed chain growth is overall much lower than that expected for the Ru/alumina catalyst based on literature references. It is quite possible that the reaction pressure for this experiment (400 psig) is not high enough for this catalyst to show significant FT reaction activity.

3.5. FT Reaction on Fe/K/Cu/SiO$_2$ catalyst (HPR-43) in a Fixed-Bed Reactor (FBR)

The effect of pulsing on the FT synthesis activity and product distribution of a very-high-α (~0.95) Fe/K/Cu/SiO$_2$ catalyst, synthesized by the Hampton University, RTI, University of Pittsburgh team under another DOE contract (DE-FG22-96PC96217), was examined. A series of runs were performed after establishing a "pseudo-steady state" at appropriate reaction conditions, including H$_2$, 24%CO$_2$/N$_2$, and CO pulses. The objective of this series of runs was to examine the effect of various pulsing types on the FT reaction activity and the C$_{10}$-C$_{20}$ yield of the Fe/K/Cu/SiO$_2$ catalyst (denoted as HPR-43).

A physical mixture of 3 cc (3.04 g) of catalyst HPR-43 and 9 cc (14.41 g) of a low-surface-area (0.2 m^2/g) α-alumina (SA5397, Norton) was loaded into the 3/8 in o.d. stainless steel reactor, between two beds of the α-alumina. The catalyst was reduced *in-situ* under a reactant (H$_2$+CO/Ar) gas mixture (H$_2$:CO=0.67, CO:Ar=9) at 280°C for 8 hours, it was cooled to 112°C and was then gradually pressurized to ca. 300 psig (21.4 atm), establishing the following base reaction conditions:

Reactants (41.25%): CO = 24.75%, H$_2$ = 16.5% (H$_2$:CO = 0.67)
Inerts (58.75%): N$_2$ = 56%, Ar = 2.75% (CO:Ar = 9)
P = 300 psig (21.4 atm), F = 300 scc/min, SV = 6000 h^{-1}

The reaction temperature was increased so as to start the FT reaction, and was stabilized at 231°C, allowing the reaction to reach a "pseudo-steady state". Pulse runs involved substituting the reactant (H$_2$+CO/Ar) feed flow (44% of total molar flow) with an equal molar flow of a pulse gas, namely H$_2$, 24% CO$_2$/N$_2$, or CO. The total molar flow and reaction pressure was maintained constant between base and pulse runs. A single pulse sequence of 1 min per 1 hour was applied in all cases.

Effect of H$_2$ pulse at 231°C

After establishing a "pseudo-steady state" at 231°C and 298±2 psig, a 1-min H$_2$ pulse per 1 hour was applied. One 8-hour run was performed under these conditions. The reactant feed was then returned to its standard composition (base run) and a new "pseudo-steady state" was attained at 230°C. The effect of the H$_2$ pulse on the outlet H$_2$:CO ratio, CO conversion, and C$_1$ (CH$_4$/CO$_2$) selectivity vs. time-on-stream is shown respectively in Figures 3.5.1, 3.5.2, and 3.5.3. The last 8 hours of the initial base run are shown as the first 8 hours (0-8 h) in these figures. The 8-hour H$_2$-pulse run is shown next (8-16 h), followed by the first 8 hours of the new base run (16-24 h). The data points are measurements of the reactor effluent gas every 15 min.

Due to the 15-min analysis time of the permanent gases (H$_2$, CO$_2$, Ar, N$_2$, CH$_4$, CO), only 4 data points can be obtained for every 1-hour pulse cycle. In order to better observe the effect of a given pulse, a "delay time" is defined as the time difference between the end of a pulse and the following GC data point. The need for applying a delay time arises from the fact that a step change in reactant feed cannot be instantaneously detected due to the dead volume of the reaction/analysis system. A delay time of 5 min was used, i.e., the first 1-min H$_2$ pulse was applied at 8 hours and 55 min (55 min after starting the pulse run), and the next data point was obtained at 9 hours on stream (Figs 3.5.1, 3.5.2, and 3.5.3).
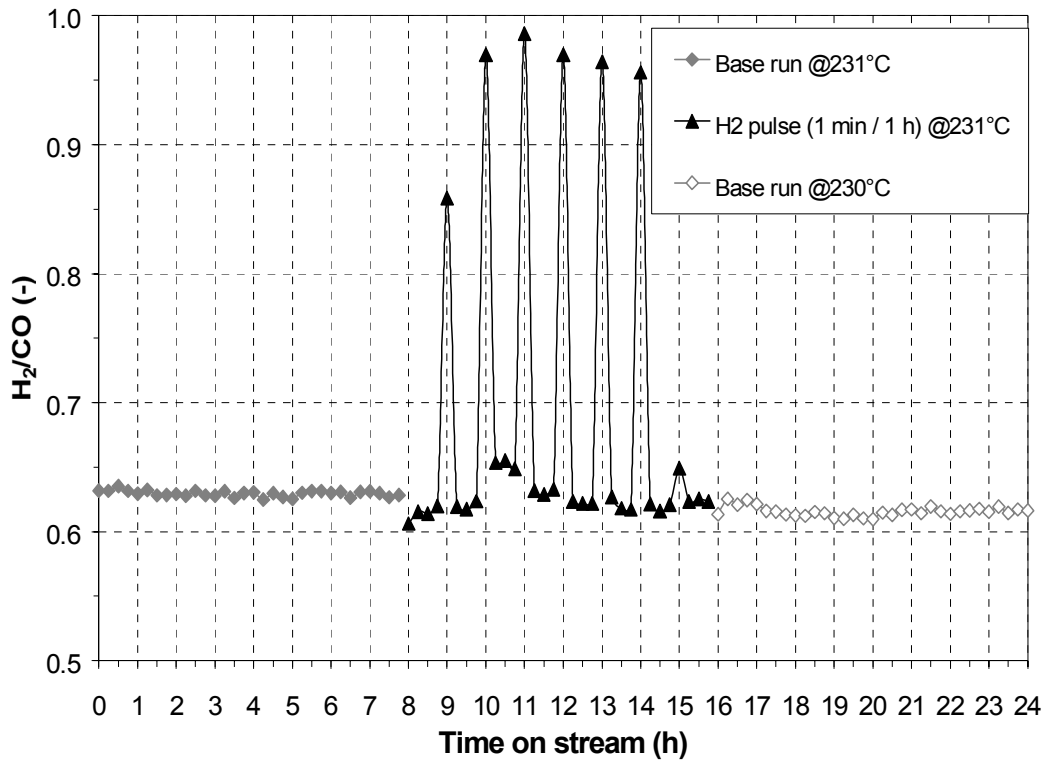
Figure 3.5.1. Effect of H_2 pulse on the outlet H_2:CO ratio of HPR-43; P = 300 psig; SV = 6000 h^{-1}
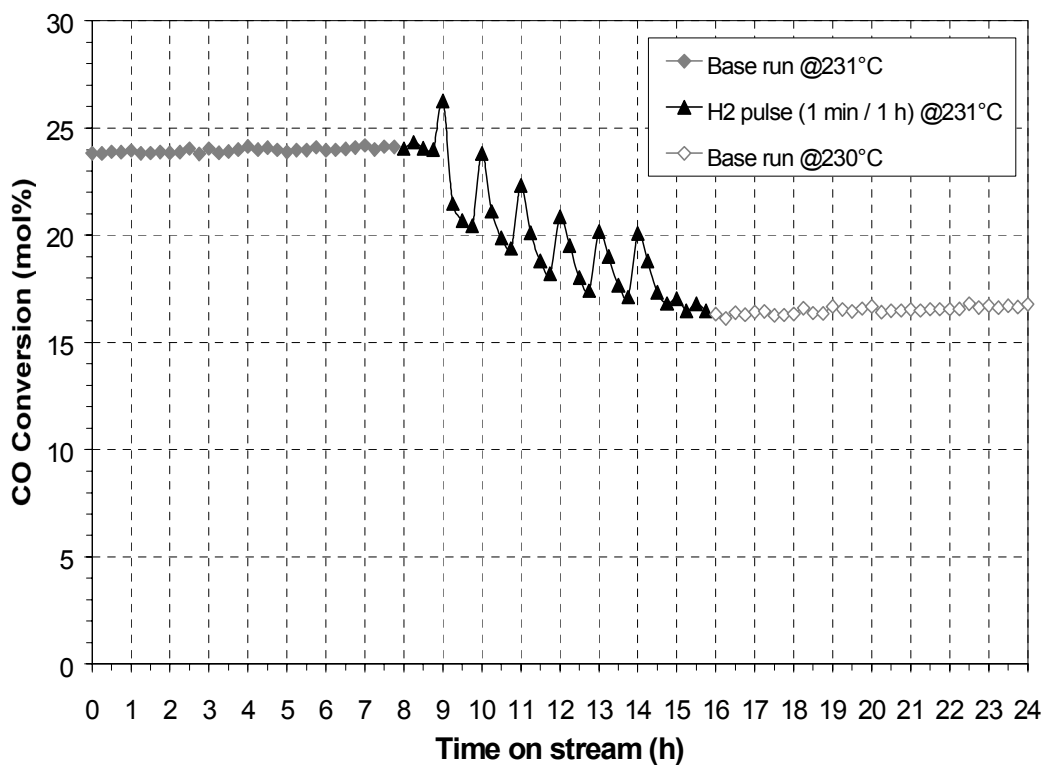
Figure 3.5.2. Effect of H_2 pulse on the CO conversion of HPR-43; P = 300 psig; SV = 6000 h^{-1}
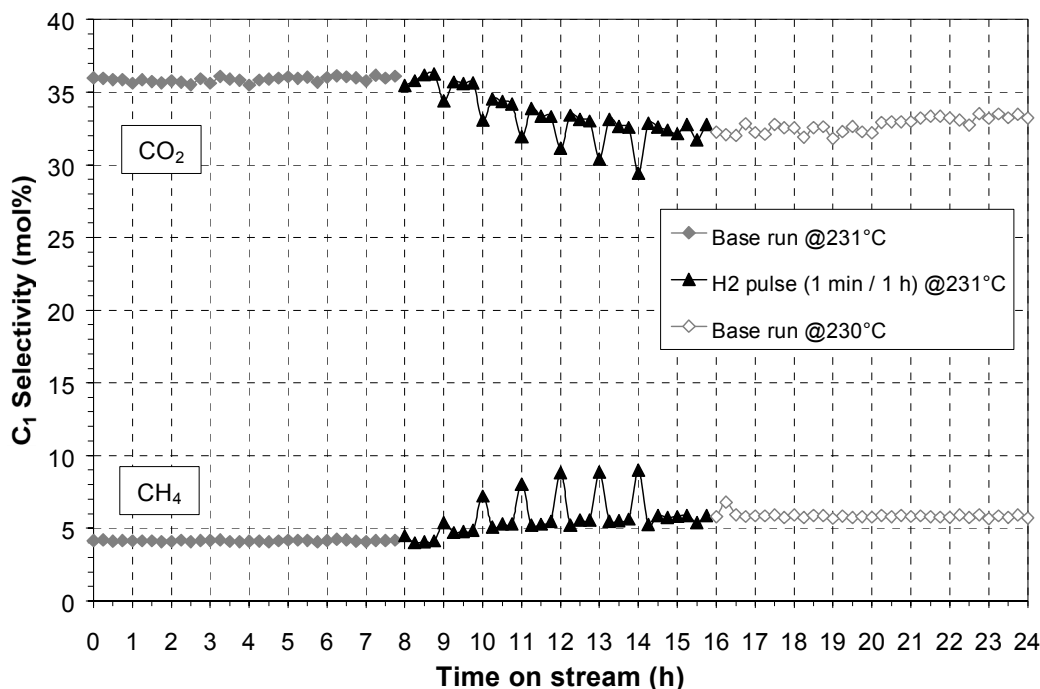
Figure 3.5.3. Effect of H_2 pulse on the C_1 selectivity of HPR-43; P = 300 psig; SV = 6000 h^{-1}

The 1-min H_2 pulse per 1 hour increased the outlet H_2:CO ratio from 0.63 (base run) to ca. 0.95±0.05 (at 5 min after the pulse), but this ratio was quickly restored (after 20 min) to its original value (Fig. 3.5.1). As seen in Fig. 3.5.2, the H_2 pulse caused a significant decrease in CO conversion, from ca. 24% (initial base run) to ca. 17% (final base run). The corresponding decrease in CO productivity was from ca. 350 cc/cc cat./h to ca. 250 cc/cc cat./h. The H_2 pulse also decreased the selectivity towards CO_2 (from ca. 36% down to ca. 33%) and increased the selectivity towards CH_4 (from ca. 4% to ca. 6%, Fig. 3.5.3).

The effect of H_2 pulse on the product distribution of HPR-43 at 231°C is presented in the form of the logarithm of the molar fraction of the products vs. the corresponding carbon number (α-plot) in Figure 3.5.4. The product distribution curves for the base run before and after the H_2 pulse run are also shown for comparison. The H_2 pulse was found to slightly decrease the α-value (from 0.95 to 0.94) while increasing the C_{10}-C_{20} weight fraction (from 13.6/15.2% up to 19.8%) and the corresponding yield of this product fraction (from 0.016 g/cc cat./h up to 0.022 g/cc cat./h). Therefore, the H_2 pulse had a positive effect on the C_{10}-C_{20} yield but also caused a decrease in catalyst activity and an undesirable increase in the selectivity towards CH_4.

Effect of 24%CO_2/N_2 pulse at 230°C

After the base run at 230°C (the results of which were shown in Figs. 3.5.1 to 3.5.4) a 1-min 24%CO_2/N_2 pulse was applied. With respect to the base runs before and after this pulse, there was essentially no effect on CO conversion (18%) and selectivity to CH_4 (5%) or CO_2 (35%). The effect of the CO_2 pulse on product distribution (compared to that of the base runs before and after the pulse) is shown in Figure 3.5.5. There was no measurable effect of the CO_2 pulse on the product distribution as well (α=0.94) or the C_{10}-C_{20} yield.
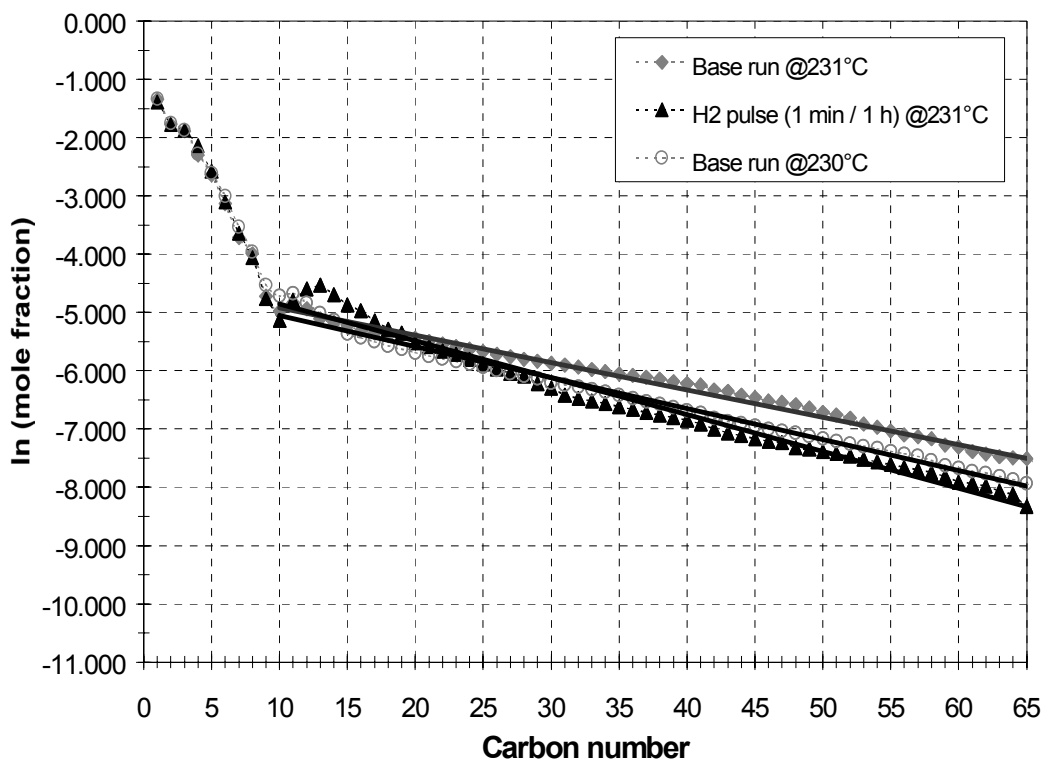
Figure 3.5.4. Effect of H_2 pulse on the product distribution of HPR-43; P = 300 psig; SV = 6000 h^{-1}
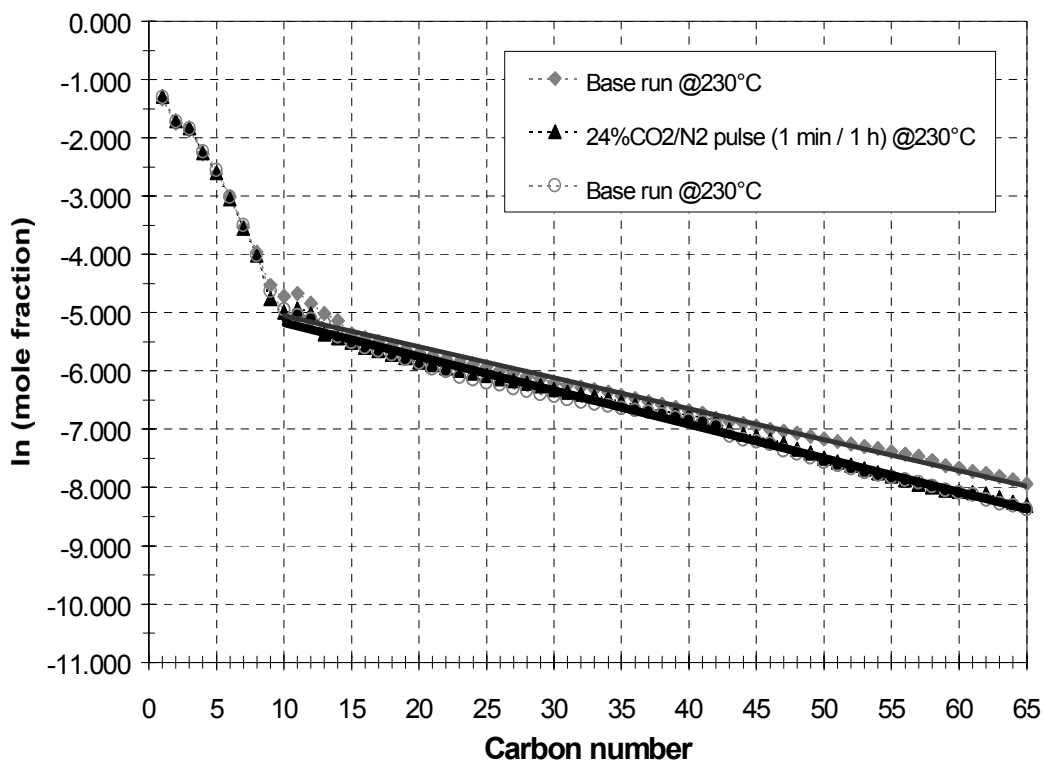
Figure 3.5.5. Effect of a 24%CO_2/N_2 pulse on the product distribution of HPR-43; P = 300 psig; SV = 6000 h^{-1}

Effect of CO pulse at 246/253°C

At the reaction temperature of 230°C the temperature distribution within the catalyst bed appeared to be essentially uniform (difference of ca. 1°C or less between the top and bottom of catalyst bed). However, upon heating up the bed to higher temperatures, an increase in this deviation between top and bottom bed T was observed. After a slow heating process, a new "pseudo-steady state" was established at 246°C (bottom bed T) / 253°C (top bed T). At these reaction conditions, the effect of a 1-min CO pulse per 1 hour on the outlet H_2:CO ratio, the CO conversion, and the CH_4/CO_2 selectivity vs. time-on-stream is shown in Figures 3.5.6, 3.5.7, and 3.5.8, respectively. The last 12 hours of the base run before the CO pulse are shown as the first 12 hours (0-12 h) in these figures. The 24-hour CO-pulse run is shown next (12-36 h), followed by the first 12 hours of the new base run (36-44 h).

The outlet H_2:CO ratio decreased from ca. 0.7% to ca. 0.5% as a result of the CO pulse (Fig. 3.5.6). As seen in Fig. 3.5.7, the applied CO pulse caused a decrease in CO conversion (from ca. 45% prior to the pulse run down to ca. 41% after the pulse run) and in CO productivity (from ca. 670 scc/cc cat./h to ca. 610 scc/cc cat./h). On the other hand, no measurable effect of the CO pulse on CH_4 or CO_2 selectivity prior to and after the pulse run was observed (Fig. 3.5.8).

The effect of CO pulse on the product distribution of HPR-43 at 246/253°C is shown in the α-plot of Figure 3.5.9. The CO pulse had only minimal effect on the measured α-value (from 0.94 to 0.93), while increasing the C_{10}-C_{20} weight fraction (from 17.1/16.7% up to 21.7%) and the corresponding yield of this fraction (from 0.045/0.041 g/cc cat./h up to 0.053 g/cc cat./h). Therefore, the CO pulse benefits the C_{10}-C_{20} yield without increasing the CH_4 or CO_2 selectivity.
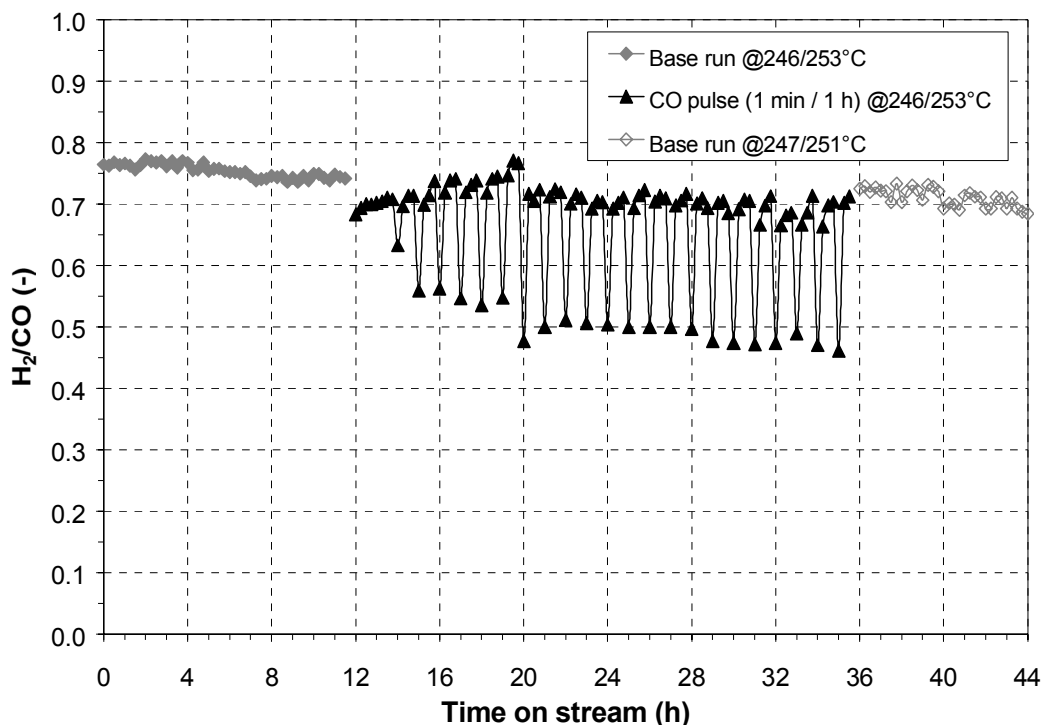
Figure 3.5.6. **Effect of CO pulse on the outlet H_2:CO ratio of HPR-43; P = 300 psig; SV = 6000 h^{-1}**
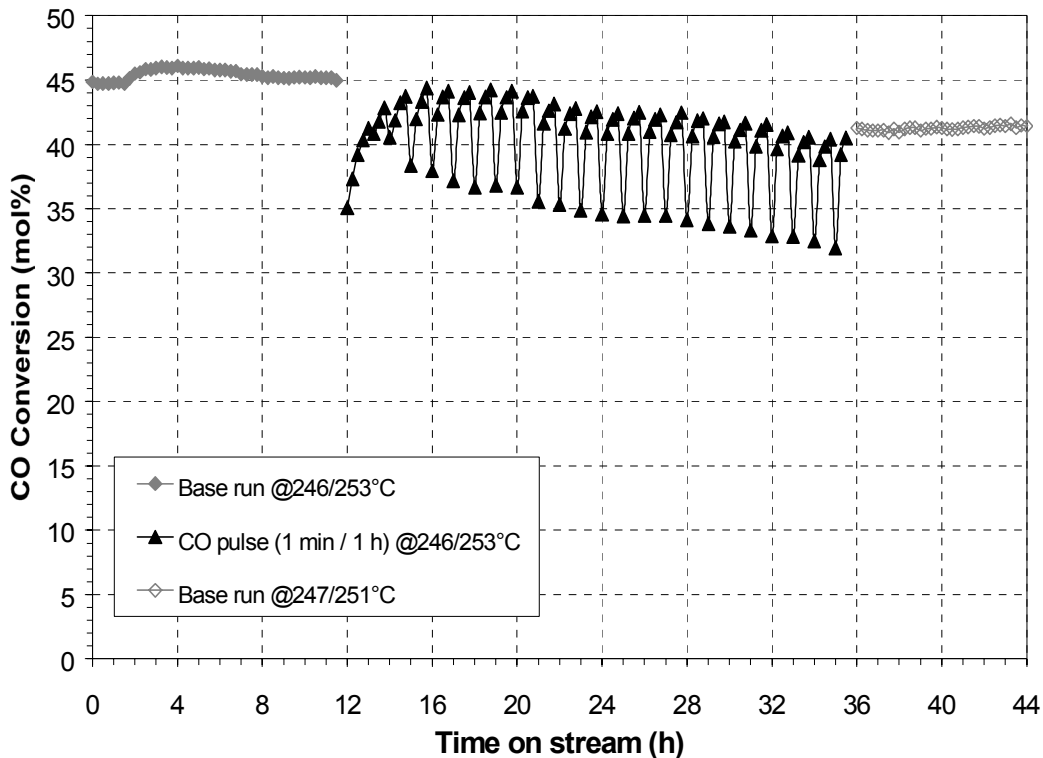
Figure 3.5.7. Effect of CO pulse on the CO conversion of HPR-43; P = 300 psig; SV = 6000 h^{-1}
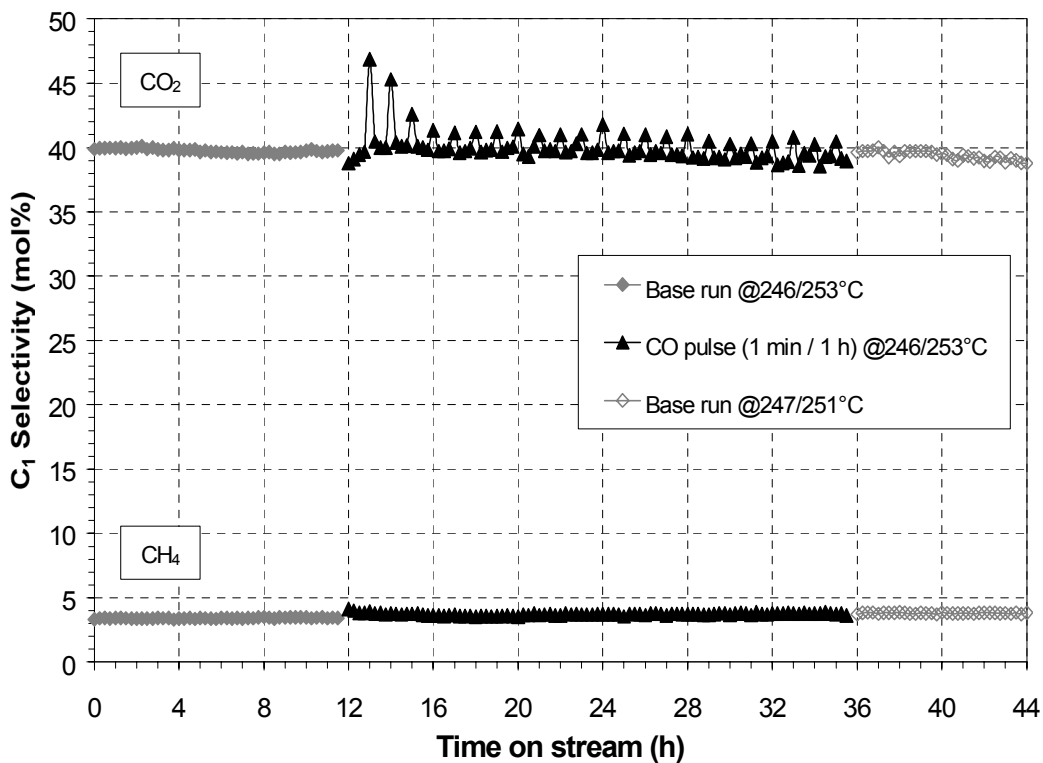
Figure 3.5.8. Effect of CO pulse on the C$_1$ selectivity of HPR-43; P = 300 psig; SV = 6000 h^{-1}
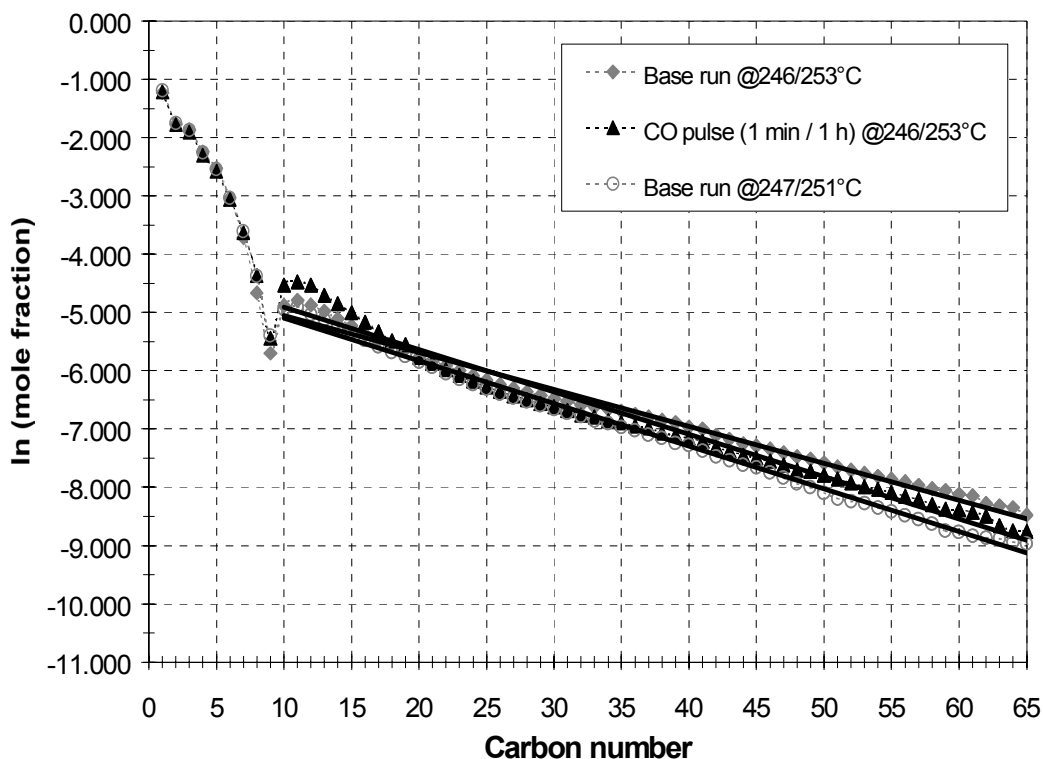
Figure 3.5.9. **Effect of CO pulse on the product distribution of HPR-43; P = 300 psig; SV = 6000 h^{-1}**

Effect of H$_2$ and CO pulse at elevated temperatures

A 1-min H$_2$ pulse per 1 hour was applied for a period of 24 hours after the reaction system had reached a new "pseudo-steady state" at 262/272°C. The measured CO conversion decreased from ca. 51% prior to the pulse run to ca. 40% after the pulse run (the corresponding CO productivity was ca. 750 and ca. 600 scc/cc cat/h, respectively). Also, an increase in the selectivity to CH$_4$ was observed (from ca. 4.5% to ca. 5.5%), whereas there was no measurable variation in the CO$_2$ selectivity.

A 1-min CO pulse per 1 hour was then applied for 24 hours after reaching a new "pseudo-steady state" at 261/271°C. In good qualitative agreement with previous observations, the CO conversion decreased moderately (from ca. 42% to ca 38.5%) as a result of the CO pulse, whereas the CH$_4$ and CO$_2$ selectivity remained constant (ca. 5% and 42%, respectively). Consequently, the observed effect of the H$_2$ and the CO pulse appears to be applicable throughout the examined reaction temperature range (i.e., from ca. 230°C to ca. 270°C).

3.6. Fixed-bed (RTI) and CSTR data (Syntroleum Corp.) of catalyst HPR-43

Syntroleum Corp. performed a CSTR run of the FT reaction on catalyst HPR-43. All tests were run at GHSV=2300 h^{-1}, 300 psig, and a H$_2$:CO feed ratio of 0.67, using 10 cc of catalyst in paraffin wax. Because of equipment limitations, the tests were run at 232°C for the first 310 hours; then the temperature was increased to 260°C for an additional 218 hours. The percent CO conversion and the rate of CO conversion (in cc CO / cc cat / h) with time on stream are given in Figure 3.6.1. The CO productivity at 232°C was ca. 350 cc CO / cc cat / h (corresponding to 25% CO conversion) and remained steady after the first 24 hours. When the temperature was increased to 260°C the conversion initially increased and then decreased to the previous level. This may have been be due to loss of catalyst from the reactor – possibly due to buildup of wax.

A comparison between the fixed bed data (obtained by RTI) and the CSTR data (obtained by Syntroleum) on catalyst HPR-43 is presented in Table 3.6.1. Despite differences in the reactant feed concentration (CO+H$_2$ was 41.25% in the FBR runs vs. 95.1% in the CSTR runs) and space velocity (6000 h^{-1} and 2300 h^{-1}, respectively) some interesting observations could be made. The CO productivity and chain-growth probability α were found to be quite comparable at corresponding reaction conditions. The molar selectivity to CH$_4$ was higher in the FBR runs than in the CSTR runs (4% vs. ca. 2%, respectively). This was apparently related to the superior heat dissipation in the CSTR, which prohibited the formation of hot spots within the catalyst particles that favor the methane formation reaction.
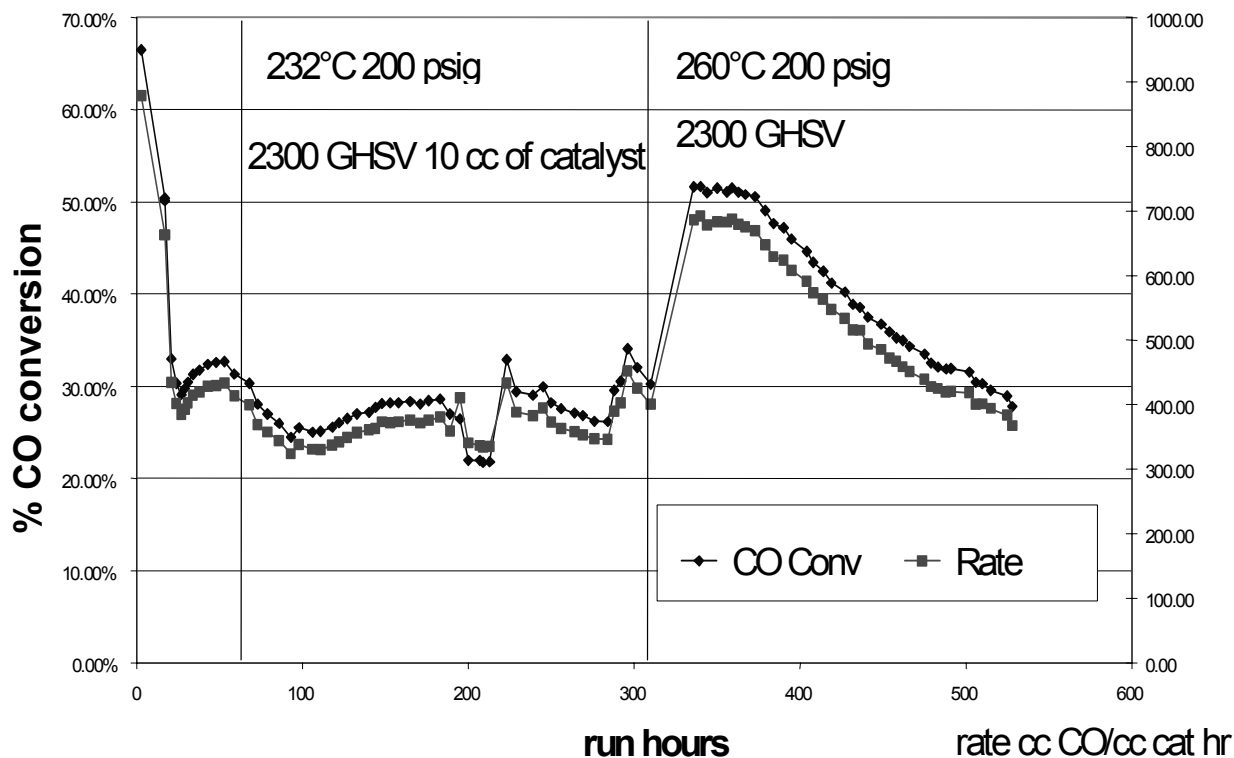
Figure 3.6.1. **Percent CO conversion and rate (cc CO / cc cat / h) from CSTR run of HPR-43; T = 232/260°C; P = 200/300 psig; SV = 2300 h^{-1}**

Table 3.6.1. Performance of fixed-bed reactor (FBR) vs. CSTR for FT reaction on HPR-43

	Fixed bed		CSTR	
CO (%)	24.8		56.7	
H_2 (%)	16.5		38.4	
N_2 + Ar (%)	58.7		4.9	
SV (h^{-1})	6000		2300	
T (°C)	231	258	232	260
P (psig)	300	300	200	300
CO productivity (cc/cc/h)	350	650	350	800
Alpha (-)	0.95	0.92	0.94	-
Water (g/cc/h)	0.05	0.036	0.022	0.008
Oil + Wax (g/cc/h)	0.07	0.1	0.1	0.13
CH_4 selectivity (mol%)	4.0	4.0	2.2	2.1
C_{10}-C_{20} yield (g/cc/h)	0.016	0.051	-	-

3.7. FT Reaction on Fe/K/Cu/SiO$_2$ catalyst (HPR-43) in a CSTR (RTI)

Prior to loading the catalyst, a "blank reactor" experiment was performed, so as to check the reaction system under actual reaction conditions, and to establish the potential contribution of the reactor walls to the activity for FT synthesis. The reactor was heated to 250°C and pressurized to 300 psig under N$_2$ flow of 530 sccm. The reactant gases were fed into the reactor establishing the following reaction conditions:

Reactants (94.3%): H$_2$ = 37.7%, CO = 56.6% (H$_2$:CO = 0.67)
Inerts: Ar = 5.7% (Ar:CO = 0.1)
P = 300 psig (21.4 atm), F = 530 sccm

Analysis of the effluent gases was performed for three configurations: a) bypassing the reactor at 300 psig and 25°C, b) flow through the reactor at 300 psig and 250°C, and c) flow through the reactor at 300 psig and 36°C. In all cases there was no measurable activity for FT synthesis, and no formation of methane or other light hydrocarbons or CO$_2$. Thus, the baseline ("blank reactor") activity of the CSTR was verified to be essentially zero.

Following the "blank reactor" experiment, the reaction system was cooled to room temperature and depressurized. Then, the stainless-steel liner was filled with 225 cc (186.75 g, density of 0.83 g/cc) of Oronite Synfluid PAO 8 cSt (CAS 68037014), a clear, colorless, odorless liquid, which is a hydrogenated 1-decene-based homo-polymer with vapor pressure of 0.1 mm Hg at 232°C. Then, 15 cc (15 g) of the HPR-43 catalyst were added, and the liner containing the catalyst and the synfluid was positioned inside the reactor vessel. The reaction system was pressurized under N$_2$ (467 sccm) to 140 psig and the stirrer was set to 800 RPM. The catalyst was activated under syngas flow (467 sccm, H$_2$:CO = 0.67) from 30°C to 280°C at 140 psig using a heating rate of 1°C/min, and remained at the steady-state temperature of 270°C for ca. 8 hours. GC analysis of the effluent gases indicated that after 8 hours at 270°C, the reaction reached steady state; the measured CO conversion was ca. 30%, and the selectivity to CO$_2$ was stabilized at ca. 48%, thus indicating that the activation of the catalyst was completed.

The reactor was then pressurized gradually from 140 psig up to 350 psig (24.8 atm) at 270°C, under a feed flow of 467 sccm, and a H$_2$:CO inlet ratio of 0.67. The effect of increasing reaction pressure from 150 psig to 275 psig to 350 psig on the activity of the catalyst (expressed as CO conversion, in mol%, and CO productivity, in cc CO / cc cat / h) is shown in Figure 3.7.1. As expected, the CO conversion increased with increasing pressure (from ca. 30% at 150 psig to ca. 56% at 350 psig). Naturally, the same trend was observed for the CO productivity.

The yield of the reaction products (expressed in mg carbon per gram of catalyst per hour) as a function of the reaction pressure at 270°C is given in Figure 3.7.2. The reaction products were categorized as CO$_2$, CH$_4$ (methane), C$_2$-C$_4$ light gases, all these being the undesirable products, and C$_{5+}$ hydrocarbons, these being the desirable products. All product yields were found to increase with increasing reaction pressure. However, due to enhanced activity towards CO$_2$, the C$_{5+}$ product as fraction of the total converted carbon decreased with increasing pressure (from ca. 41% at 150 psig down to ca. 35% at 350 psig). The yield of methane was quite low at every examined pressure (corresponding to a molar selectivity of ca. 2.5%).
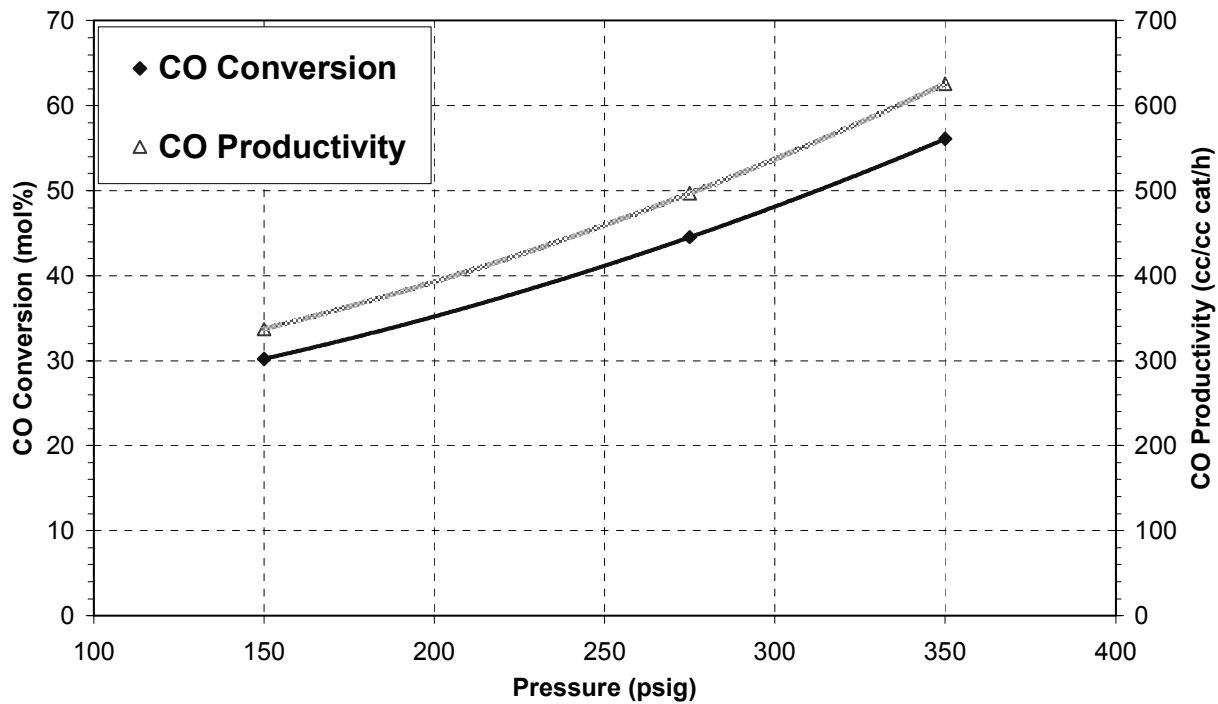
Figure 3.7.1. Effect of reaction pressure on the CO conversion and CO productivity of HPR-43; T = 270°C; SV = 1868 h⁻¹
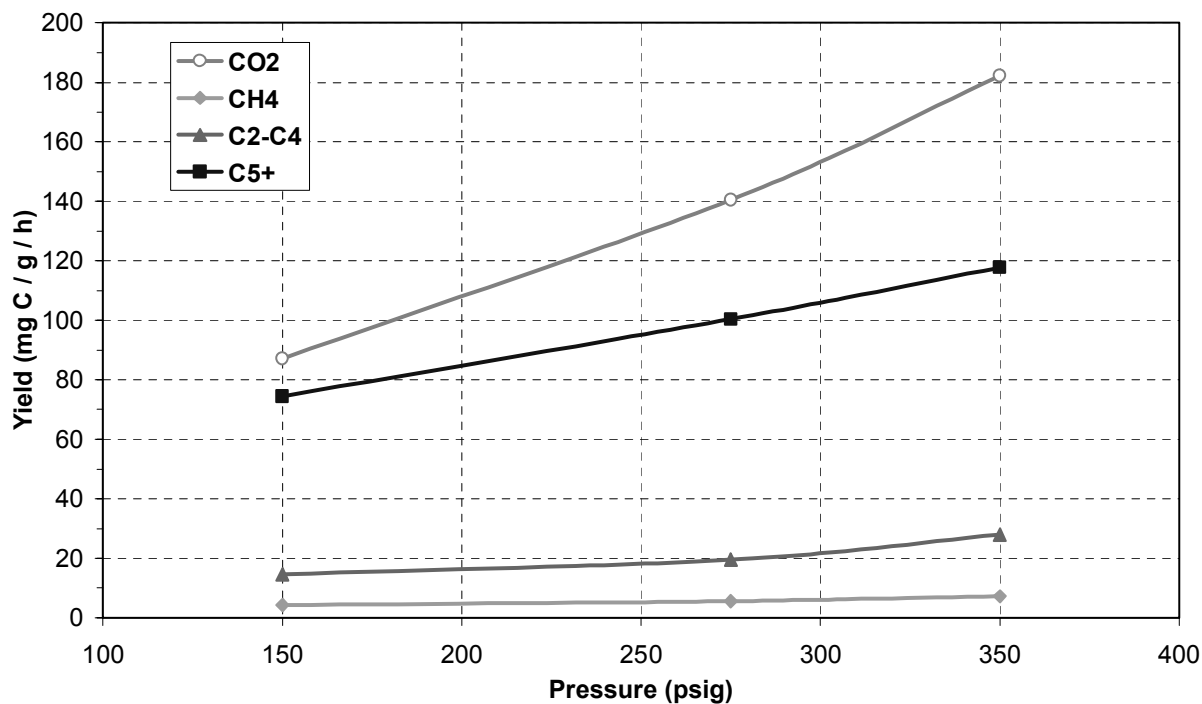
Figure 3.7.2. Effect of reaction pressure on the product yield of HPR-43; T = 270°C; SV = 1868 h⁻¹

The effect of increasing reaction pressure on the olefin/paraffin ratio of the C_2-C_8 hydrocarbon products is shown in Figure 3.7.3. The olefin/paraffin ratio in the C_2-C_8 product range decreased with increasing the reaction pressure from 150 psig to 350 psig. This increase in reaction pressure appears to promote the secondary adsorption of the formed olefins, possibly leading to longer-chain products, and resulting in a lower outlet concentration of olefins. This observation is in good agreement with pervious ones using the Co/Al_2O_3 catalyst (Fig. 3.3.6).

Upon completing the pressure variation experiment, the reaction pressure was maintained at 350 psig, and the reaction temperature was decreased from 270°C down to 250°C and 230°C, and then was increased to 240°C, all other reaction parameters (feed flow, H_2:CO feed ratio) being the same. The effect of varying the reaction temperature on the CO conversion and CO productivity of HPR-43 is shown in Figure 3.7.4. As expected, by decreasing the reaction temperature from 270°C down to 230°C, the CO conversion decreased from ca. 56% down to ca. 13% (naturally, the same trend was observed for the CO productivity).

The effect of varying the reaction temperature on the yield of the reaction products, shown in Figure 3.7.5, was found to be more interesting. Again, by decreasing the reaction temperature the carbon-based yield of all products (CO_2, CH_4, C_2-C_4, and C_{5+}) decreased, as expected. However, due mainly to a lower selectivity towards CO_2, the C_{5+} product as fraction of the total converted carbon increased with decreasing temperature (from ca. 35% at 270°C to ca. 54% at 230°C). Thus, lower temperatures (230-240°C) appear to favor the selectivity to the desirable C_{5+} product fraction. The molar selectivity to methane decreased to less than 2% with decreasing reaction temperature.
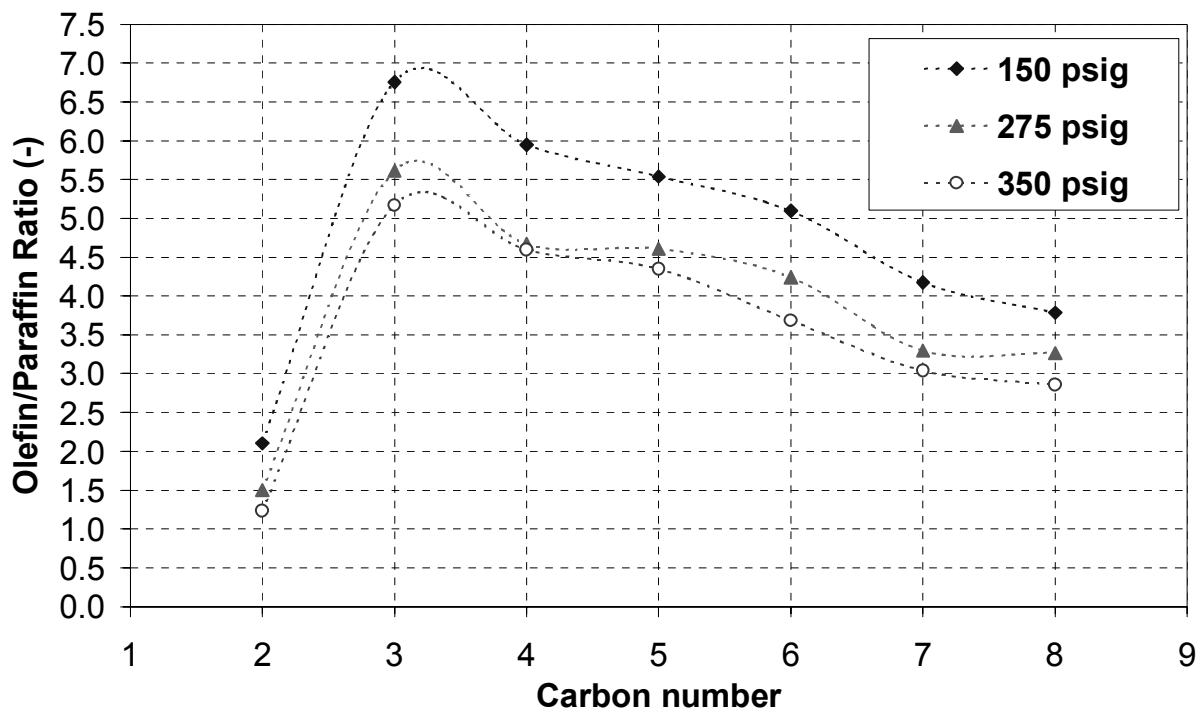
Figure 3.7.3. **Effect of reaction pressure on the C_2-C_8 olefin/paraffin ratio of HPR-43; T = 270°C; SV = 1868 h^{-1}**
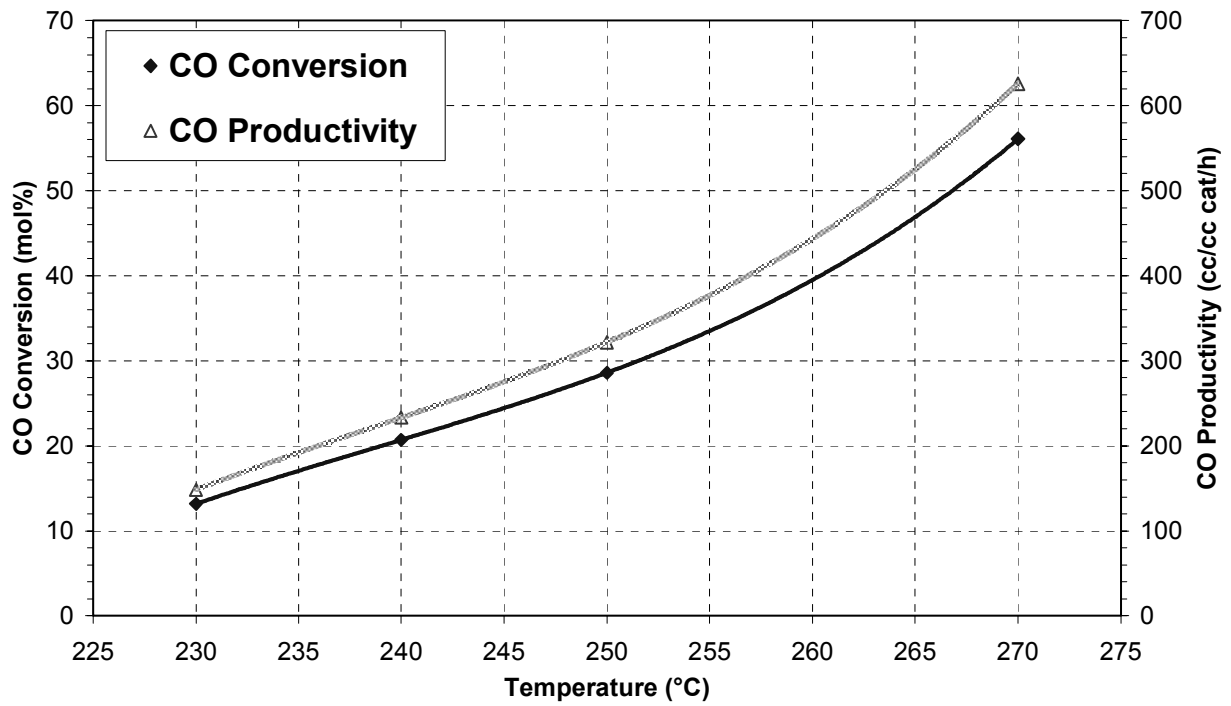
Figure 3.7.4. Effect of reaction temperature on the CO conversion and CO productivity of HPR-43; P = 350 psig; SV = 1868 h^{-1}
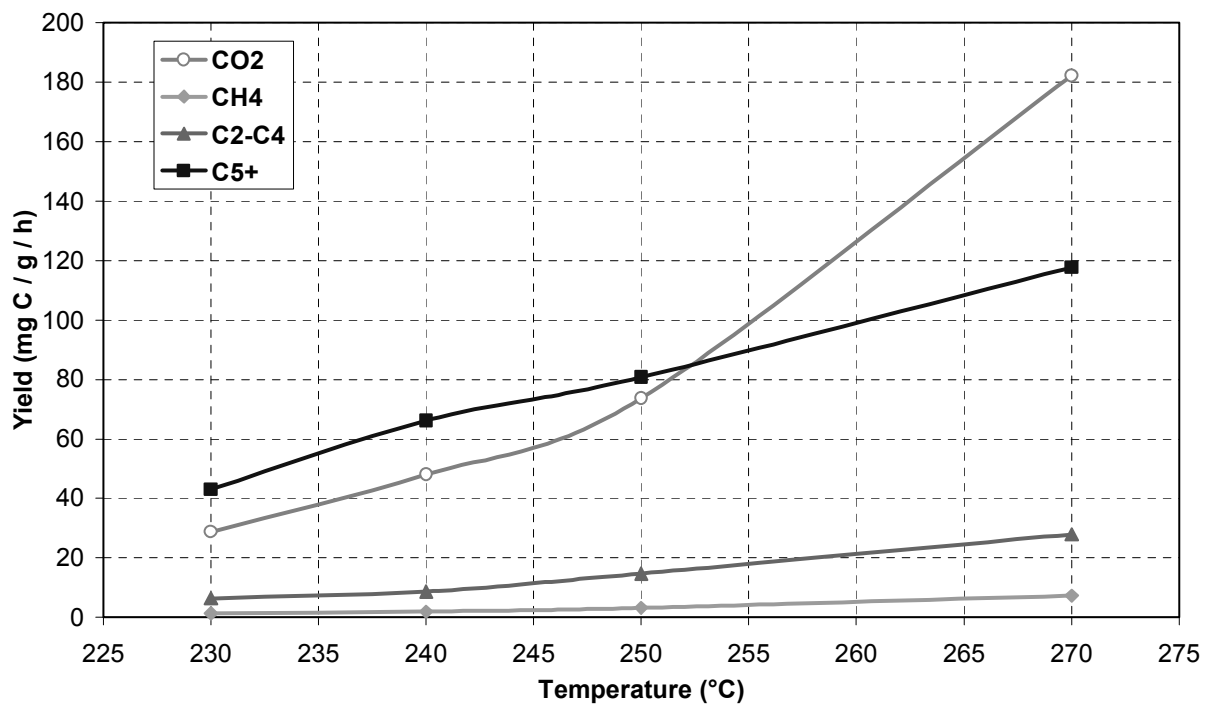
Figure 3.7.5. Effect of reaction temperature on the product yield of HPR-43; P = 350 psig; SV = 1868 h^{-1}

The effect of varying the reaction temperature on the olefin/paraffin ratio of the C_2-C_8 hydrocarbon products is shown in Figure 3.7.6. Based on the results of Fig. 3.7.6, three divisions within the C_2-C_8 product range could be identified. The C_2 (ethylene/ethane) ratio was found to increase monotonically with decreasing temperature (from ca. 1.25 at 270°C to ca. 4.2 at 230°C). The olefin/paraffin ratio for the C_3-C_5 product fraction showed the opposite trend, i.e., decreased with decreasing reaction temperature. The olefin/paraffin ratio for the C_6-C_8 product fraction showed a less clear trend with temperature, thus not allowing for a clear conclusion. This rather complex behavior of the olefin/paraffin ratio of the C_2-C_8 hydrocarbon products appears to indicate that more than one parameter (for instance, rates of propagation, olefin readsorption, and termination) can be influenced by the reaction temperature.

Upon completing the temperature variation experiment, the reaction temperature was maintained at 240°C, and the feed H_2:CO ratio was varied from 0.67 up to 1.6, and then down to 1.1 and back to 0.67, all other reaction parameters (feed flow, pressure) being the same. The effect of varying the feed H_2:CO ratio on the CO conversion and CO productivity of HPR-43 is shown in Figure 3.7.7. By increasing the feed H_2:CO ratio from 0.67 to 1.6 the CO conversion increased from ca. 20% to ca. 43%. The CO productivity remained essentially constant at ca. 230 scc CO / cc cat / h for a H_2:CO ratio of 0.67 and 1.1, but increased to ca. 320 scc CO / cc cat / h at the H_2:CO ratio of 1.6.

Upon returning to the original feed H_2:CO ratio of 0.67, the catalyst activity returned to its original value (19.5±1%). Thus, the catalyst activity was only reversibly affected by the applied variation in the feed H_2:CO ratio.
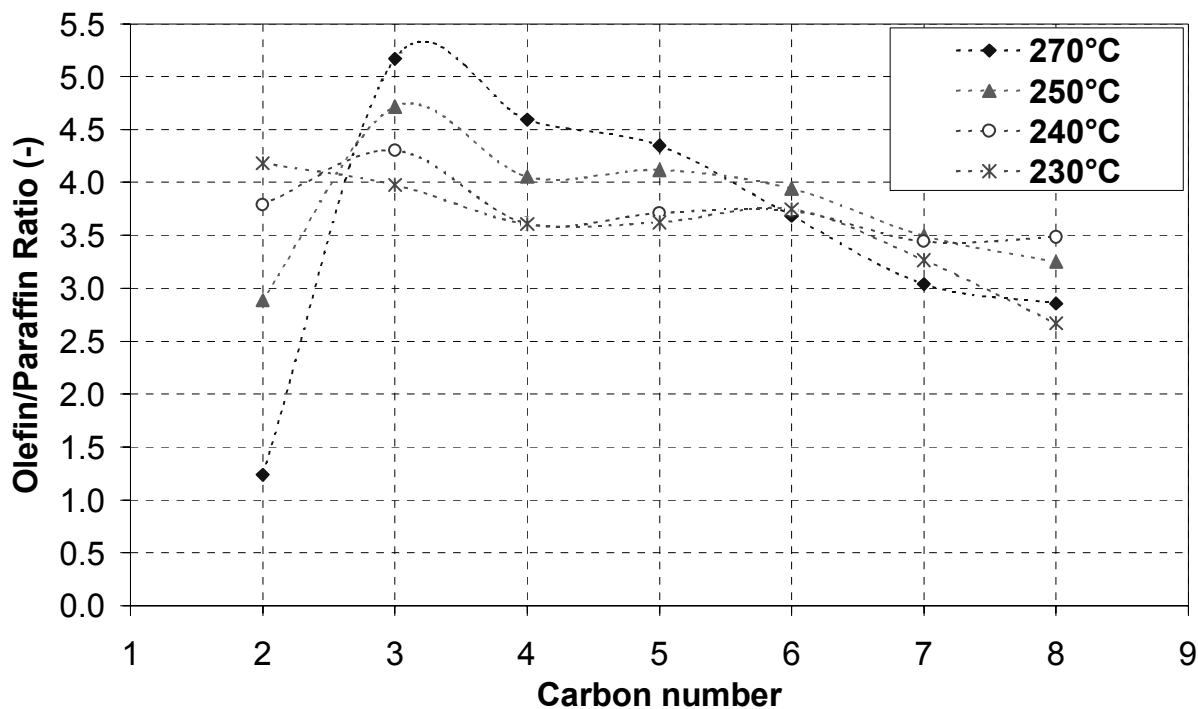
Figure 3.7.6. **Effect of reaction temperature on the C_2-C_8 olefin/paraffin ratio of HPR-43; P = 350 psig; SV = 1868 h^{-1}**
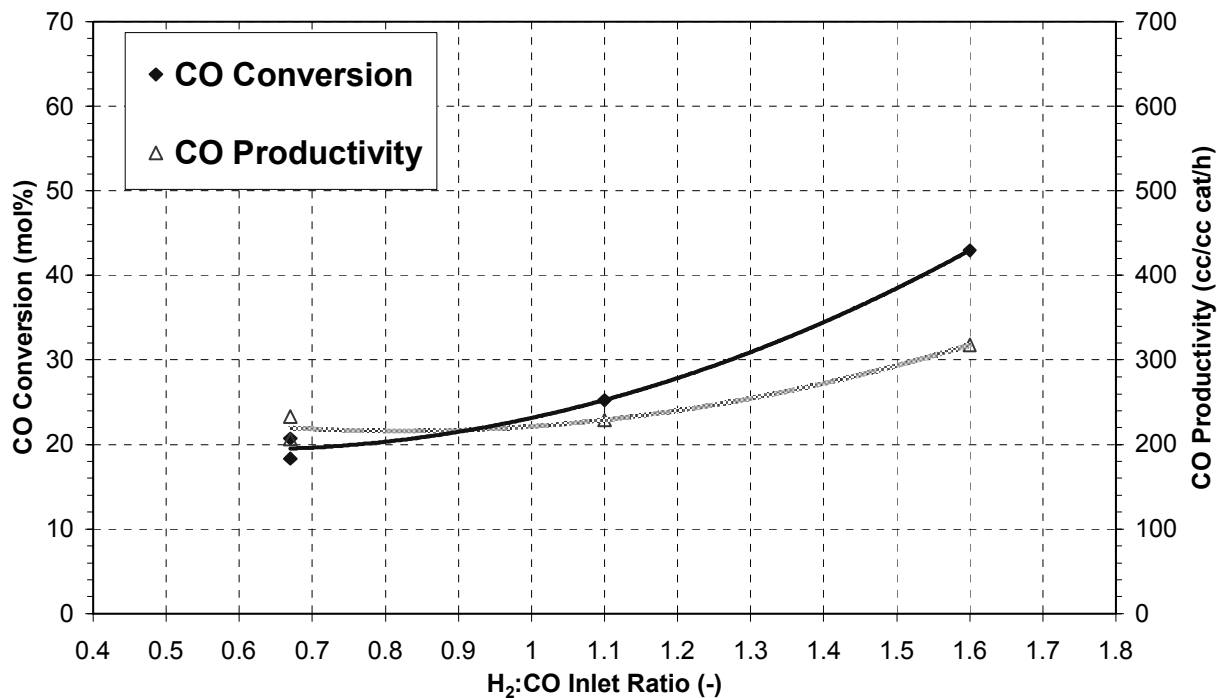
Figure 3.7.7. **Effect of feed H$_2$:CO ratio on the CO conversion and CO productivity of HPR-43; T = 240°C; P = 350 psig; SV = 1868 h^{-1}**

The effect of varying the feed H$_2$:CO ratio on the yield of the reaction products is shown in Figure 3.7.8. The carbon-based yield of all products increased by increasing the H$_2$:CO ratio to 1.6. However, the C$_{5+}$ product as fraction of the total converted carbon decreased with increasing the H$_2$:CO ratio (from ca. 53% at 0.67 to ca. 50% at 1.6). Thus, a high H$_2$:CO ratio (about 1.6) appears to be less favorable towards the selectivity to the desirable C$_{5+}$ product fraction.

The effect of varying the H$_2$:CO feed ratio on the olefin/paraffin ratio of the C$_2$-C$_8$ hydrocarbon products is given in Figure 3.7.9. Increasing the H$_2$:CO ratio from 0.67 to 1.6 resulted in a decrease in the olefin/paraffin ratio throughout the C$_2$-C$_8$ product range. Clearly, higher concentrations of inlet H$_2$ would tend to enhance the rate of hydrogenation of olefins, thus suppressing their outlet concentration while enhancing the outlet paraffin concentration, and consequently, decreasing the measured olefin/paraffin ratio.

Upon returning to the original H$_2$:CO ratio of 0.67, the olefin/paraffin ratio of the C$_2$-C$_4$ product fraction was restored to their original values, but the olefin/paraffin ratio of the C$_5$-C$_8$ product fraction remained at lower values than the original ones, values that were very similar to those for the higher H$_2$:CO ratios of 1.1 and 1.6. It is unclear whether this inconsistency was an actual phenomenon, possibly related to some hysteresis effect in the outlet concentration of the higher-carbon products, or perhaps an artifact of a biased hydrocarbon analysis (possibly due to contamination from previous samples).
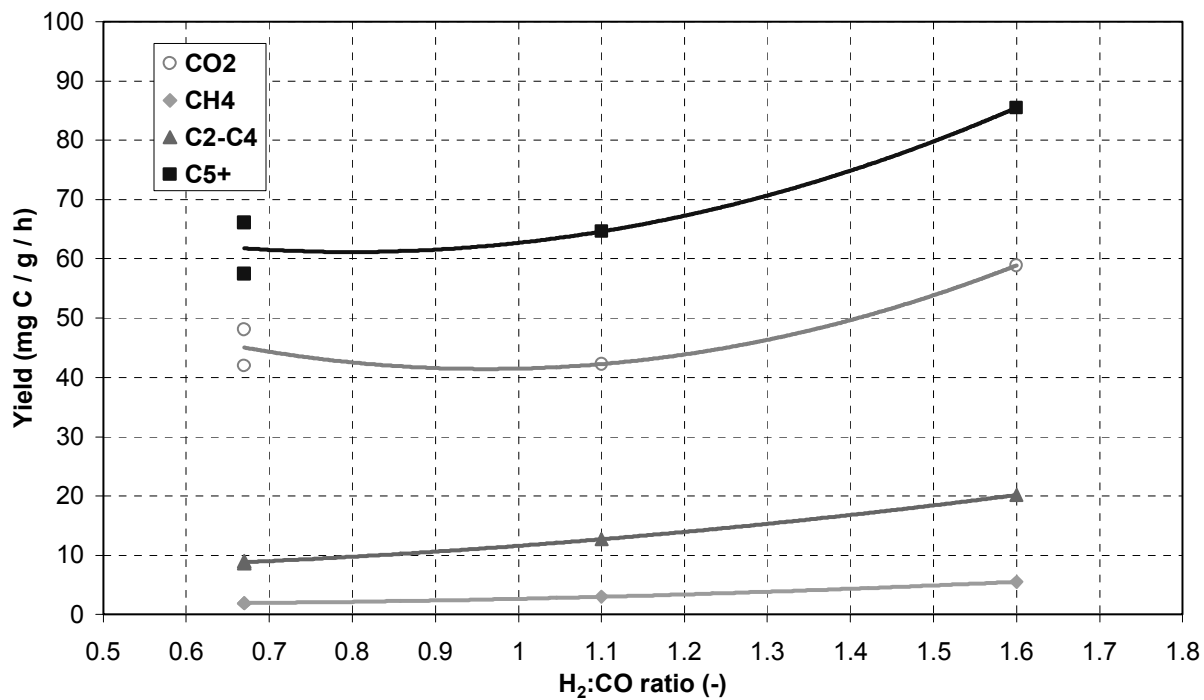
Figure 3.7.8. Effect of feed H_2:CO ratio on the product yield of HPR-43; T = 240°C; P = 350 psig; SV = 1868 h^{-1}
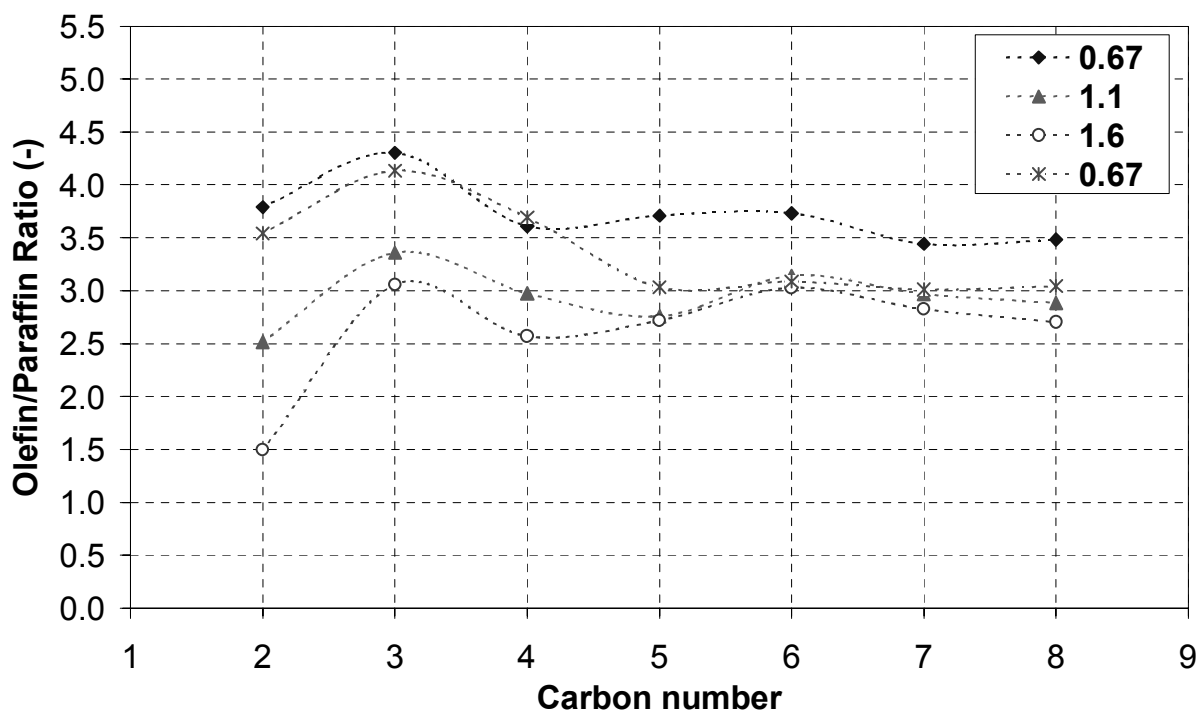
Figure 3.7.9. Effect of feed H_2:CO ratio on the C_2-C_8 olefin/paraffin ratio of HPR-43; T = 240°C; P = 350 psig; SV = 1868 h^{-1}

After completing the study of the effect of the feed H_2:CO ratio at 240°C, the reactor was depressurized to 140 psig, and the catalyst was reactivated by heating with a heating rate of 1°C/min from 240°C to 290°C (instead of 280°C). The catalyst was maintained at 290°C for 12 hours, at which time the concentration of the exiting gases achieved a pseudo steady state. Then, the reactor was cooled to 270°C at 140 psig.

In a manner similar to the previous study, the reaction pressure was gradually increased up to 350 psig. The effect of this increase in reaction pressure on the CO conversion, the yield of the reaction products (CO_2, CH_4, C_2-C_4, and C_{5+}), as well as the olefin/paraffin ratio of the C_2-C_8 hydrocarbon products was qualitatively very similar to that of the previously described set of runs (as shown in Figs. 3.7.1, 3.7.2, and 3.7.3, respectively). In fact, the CO conversion at 350 psig was again found to be ca. 56%, same as before (see Fig. 3.7.1).

Afterwards, again in a manner similar to the previous study, the reaction temperature was varied from 270°C to 250°C to 230°C and then to 240°C at 350 psig. Again, the effect of this variation in reaction temperature on the CO conversion, product yield, and olefin/paraffin ratio was found to be qualitatively very similar to that of the previously described set of runs (as shown in Figs. 3.7.4, 3.7.5, and 3.7.6). Therefore, the trends described in these runs and shown in the above figures were verified as accurate and reproducible.

4. CONCLUSIONS

Based on the presented results the following conclusions can be drawn:

The α-alumina used for diluting the examined catalysts in the fixed-bed reactor shows no measurable activity for FT synthesis at temperatures up to 270°C, thus its presence does not affect the activity of the examined catalysts.

"Blank" pulse runs (i.e., runs involving no variations in feed composition) have no effect on measurements of the progress of the FT reaction (conversion, selectivity). "Inert" (N_2) pulsing shows only minimal variations in activity (CO conversion) or in product selectivity (α-value, CH_4 yield, and C_{10}-C_{20} yield) for FT synthesis.

H_2 pulsing causes significant increase in the activity (CO conversion and productivity) of both the 14wt% Co/Al_2O_3 and the 14.5wt% Co-Zr/SiO_2 FT synthesis catalyst. The activity then decreases gradually until the next pulse, indicating a tendency to return to its pseudo steady state. The selectivity to undesirable CH_4 increases instantaneously after each H_2 pulse and is then quickly restored to its pseudo steady state value. Thus, H_2 pulsing increases catalytic activity while only temporarily increasing the formation of CH_4.

An increase in the H_2 pulse frequency has a positive effect on the selectivity to C_{10}-C_{20} and C_{21+} compounds (while maintaining or slightly decreasing the selectivity to CH_4) for both the Co-Zr/SiO_2 and Co/Al_2O_3 catalysts, but the chain-growth probability α remains essentially unaffected. An increase in the H_2 pulse duration increases the maximum obtained CO conversion and the instantaneous selectivity to CH_4.

The extent of the CH_4 formation reaction appears to be correlated to the increase in H_2 concentration as caused by pulsing. The FT reaction, however, appears to have a different dependence on H_2 concentration, since it progresses within a different time frame. Optimization of the pulse characteristics (i.e., pulse frequency and duration) is required in order to maximize the selectivity towards the desirable C_{10}-C_{20} diesel fraction.

The effect of H_2 pulsing on light hydrocarbon formation is like a *rippling* phenomenon. The formation of paraffinic (and apparently olefinic also) hydrocarbons exhibits a local maximum with respect to the time after the pulse, whereas this maximum shifts to longer times with increasing carbon number. Furthermore, the magnitude of the observed increase in formation is greater for paraffins than for the corresponding olefins, and appears to decline with increasing carbon number.

Addition of 10% steam in the feed causes a decrease in catalytic activity and suppresses the formation of CH_4 while enhancing the formation of CO_2 by enhancing the extent of the water gas shift reaction. It increases the olefin/paraffin ratio of the light hydrocarbons. Application of a H_2 pulse in the presence of added steam decreases this olefin/paraffin ratio. Thus, H_2 pulsing is a simple method to overcome the loss of activity and shift in paraffin vs. olefin selectivity caused by the presence of excess steam.

A decrease in syngas concentration has a strong suppressing effect in the olefin/paraffin ratio of the light (C_2-C_9) hydrocarbons. Higher syngas concentration (and lower space velocity, to a lesser extent) can increase the chain growth probability α and thus serve as a more favorable reaction condition for investigating the effect of pulsing.

Hydrogen pulsing has only minimal effect on the activity and C_1 selectivity of the Ru/alumina FT synthesis catalyst, which appears to show enhanced methanation and water-gas-shift activity. A second reduction procedure produces a better-activated catalyst, showing the same activity at lower temperatures, along with lower selectivity to undesirable compounds CH_4 and CO_2. Still there is only minimal impact of H_2 pulsing on the catalyst performance even after the second reduction.

Hydrogen pulsing has a positive effect on the C_{10}-C_{20} yield of the high-α Fe/K/Cu/SiO_2 FT catalyst. However, it also causes a significant decrease in catalyst activity (CO conversion) and an undesirable increase in the selectivity to CH_4. Pulsing with CO also has a positive effect on the C_{10}-C_{20} yield and no measurable effect on the selectivity to CH_4 and CO_2, and causes only a moderate decrease in CO conversion. Pulsing with a 24%CO_2/N_2 gas mixture has essentially no effect on catalytic activity or product distribution (α-value, C_{10}-C_{20} yield).

An increase in reaction pressure enhances the activity of the HPR-43 (Fe/K/Cu/SiO_2) FT catalyst studied in a CSTR. The yield of all the products of the reaction (CO_2, CH_4, C_2-C_4 light gases, and desirable C_{5+} hydrocarbons) increases with increasing reaction pressure. However, due to enhanced activity of the catalyst towards CO_2 at the high temperature of the experiment, the C_{5+} product as fraction of the total converted carbon decreased with increasing pressure.

An increase in reaction pressure also decreases the olefin/paraffin ratio of the C_2-C_8 product range. The increase in reaction pressure appears to promote the secondary adsorption of the formed olefins, possibly leading to longer-chain products, and resulting in a lower outlet concentration of olefins.

A decrease in reaction temperature decreases the activity as well as the yield of all reaction products of HPR-43. However, due mainly to a lower selectivity towards CO_2, the C_{5+} product as fraction of the total converted carbon increases with decreasing temperature. Lower temperatures appear to favor the selectivity to the desirable C_{5+} product fraction.

An increase in the feed H_2:CO ratio increases the activity as well as the yield of all reaction products of HPR-43. However, it decreases the C_{5+} product as fraction of the total converted carbon. High H_2:CO ratios appear to be less favorable towards the selectivity to the desirable C_{5+} product fraction.

An increase in the feed H_2:CO ratio also decreases the olefin/paraffin ratio of the C_2-C_8 product range. Higher concentrations of inlet H_2 tend to enhance the rate of hydrogenation of olefins, suppressing their outlet concentration while enhancing the outlet paraffin concentration, thus decreasing the measured olefin/paraffin ratio.

5. RECOMMENDATIONS

From the results and conclusions of this work the following recommendations should be considered:

Pulsing experiments on any given FT synthesis catalyst (whether cobalt-based or iron-based) should be performed under conditions that maximize the yield of the heavy hydrocarbon products (high chain-growth probability **α**). These conditions are a high synthesis gas partial pressure (high total reaction pressure, minimal or no presence of inerts), and (to a lesser degree) a low space velocity. High temperatures favor the formation of excess light gases, so moderate temperatures are more preferable for pulse-type runs.

More aggressive pulsing conditions (specifically, pulse frequency) need to be examined, in order to establish the long-term impact of pulsing on product formation beyond experimental uncertainty. An increase in the catalyst bed temperature of the fixed-bed reactor, resulting from the application of high-frequency, high-duration pulsing, inhibits evaluation of the true intrinsic effect of pulsing on catalyst performance. High pulse frequencies (two or more pulses per hour) would have to be coupled with lower pulse durations (lower than the 1 min used in this work).

Equal emphasis to pulsing experiments using the fixed-bed reactor should be given to pulsing using the CSTR. The superior control of the catalyst temperature in the CSTR compared to the FBR would allow the evaluation of a more extensive range of pulsing parameters (pulse frequency and duration) and their true intrinsic impact on the performance of the catalyst for FT synthesis.

6. BIBLIOGRAPHY

1. R.B. Anderson, The Fischer-Tropsch Synthesis, Acad. Press, New York, 1984.
2. M.E. Dry, Appl. Catal. A, 138 (1996) 319.
3. A.A. Adesina, Appl. Catal. A, 138 (1996) 345.
4. M.E. Dry, The Fischer-Tropsch Synthesis, in Catalysis - Science and Technology 1 (J.R. Ander and M. Boudart, eds.), Springer-Verlag, New York, 1981.
5. G. Parkinson, Chem. Eng., 4 (1997) 39.
6. C.D. Chang, W.H. Lang, and A.J. Silvestri, J. Catal., 56 (1979) 268.
7. R.J. Gormley, V.U.S. Rao, R.R. Anderson, R.R. Schehl, and R.D.H. Chi, J. Catal., 113 (1988) 195.
8. S. Bessell, Appl. Catal. A, 126 (1995) 235.
9. K. Jothimurugesan and S.K. Gangwal, Ind. Eng. Chem. Res., 37(4) (1998) 1181.
10. D.L. King, J.A. Cusamano, and R.L. Garten, Catal. Rev. Sci. Eng., 23(1-2) (1981) 233.
11. A.A. Adesina, R.R. Hudgins, and P.L. Silveston, Can. J. Chem. Eng., 25 (1995) 127.
12. J.W. Dun, and E. Gulari, Can. J. Chem. Eng., 64(2) (1986) 260.
13. G. Beer, Gas Conversion Process Using a Chain-Limiting Reactor, WO Patent No. 98/ 19979 (1997).
14. E. Peacock-Lopez and K. Lindenberg, J. Phys. Chem., 88 (1984) 2270.
15. E. Peacock-Lopez and K. Lindenberg, J. Phys. Chem., 90 (1986) 1725.
16. A.A. Khodadadi, R.R. Hudgins, and P.L. Silverston, Canadian J. Chem. Eng., 74 (1996) 695.
17. F.M. Dautzenberg, J.M. Heller, R.A. van Santen, and H. Berbeek, J. Catal., 50 (1977) 8.
18. A. Hoek, M.F.M. Post, J.K. Minderhoud, and P.W. Lednor, Process for the Preparation of a Fischer-Tropsch Catalyst and Preparation of Hydrocarbons from Syngas, US Patent No. 4,499,209 (1985).
19. E. Iglesia, S.C. Reyes, and R.J. Madon, J. Catal., 129 (1991) 238.

APPENDICES

Appendix I.

Two-page abstract entitled "*Fischer-Tropsch Synthesis on a Co-ZrO$_2$/SiO$_2$ Catalyst: Effect of H$_2$ Pulsing*", presented in the 17th North American Catalysis Society Meeting, Toronto, Canada, June 3-8, 2001.

Appendix II.

Six-page camera-ready manuscript entitled "*Effect of Periodic Pulsed Operation on Product Selectivity in Fischer-Tropsch Synthesis on Co-ZrO$_2$/SiO$_2$*", presented and published in the Proceedings of the 6th Natural Gas Conversion Symposium, Girdwood, Alaska, June 17-21, 2001.

APPENDIX I   Fischer-Tropsch Synthesis on a Co-ZrO$_2$/SiO$_2$ Catalyst: Effect of H$_2$ Pulsing

Fischer-Tropsch Synthesis on a Co-ZrO$_2$/SiO$_2$ Catalyst: Effect of H$_2$ Pulsing

A.A. Nikolopoulos and S.K. Gangwal
Research Triangle Institute, P.O. Box 12194, RTP, NC 27709-2194, U.S.A.

Introduction

Currently there is significant commercial interest in producing diesel-fuel-range middle distillates (C$_{10}$-C$_{20}$ paraffins) from natural-gas-derived syngas by Fischer-Tropsch (FT) synthesis. Increasing the selectivity of the FT reaction to diesel (C$_{10}$-C$_{20}$) or gasoline (C$_5$-C$_{11}$) products by altering the Shultz-Flory-Anderson (SFA) distribution is economically attractive. Use of bifunctional (FT-active metal on zeolite) catalysts to produce gasoline-range hydrocarbons has been economically unsuccessful [1-2]; the enhanced cracking activity of the zeolite lowers the chain-growth probability **α**, thus producing increased amounts of undesirable C$_1$-C$_4$ gases.

The present emphasis has shifted towards maximizing the yield of zero-sulfur high-cetane C$_{10}$-C$_{20}$ products from FT synthesis. Among various approaches, periodic pulsing of H$_2$ or other gases has been examined so as to limit chain growth on a high-**α** FT catalyst by removing the growing chain from the catalyst surface [3-5], thus maximizing the C$_{10}$-C$_{20}$ yield (Figure 1). Experimental studies have shown the potential to alter the SFA distribution [6,7]; however, they were conducted under conditions of limited industrial interest. The scope of this study is to investigate the effect of H$_2$ pulsing on the activity and product distribution of a high-**α** (~0.9) Co/ZrO$_2$/SiO$_2$ FT synthesis catalyst, in an attempt to maximize the C$_{10}$-C$_{20}$ product yield.
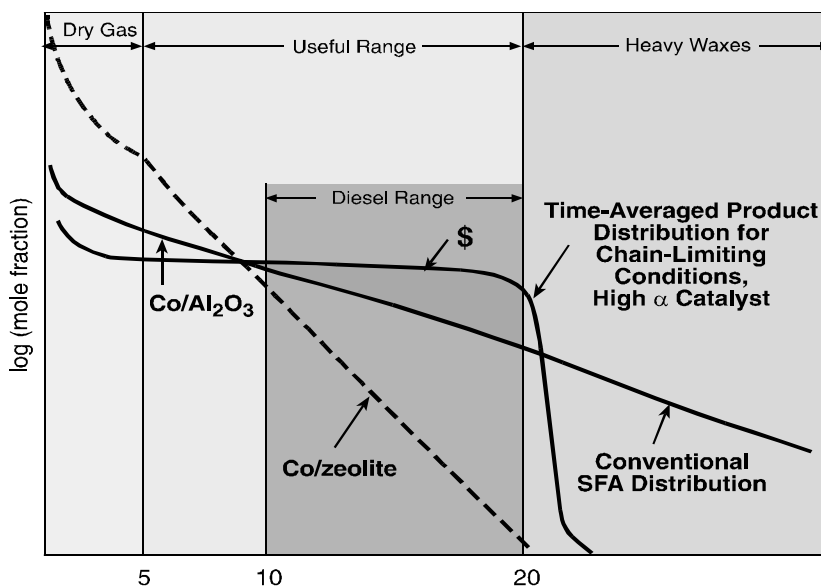
Figure 2. Product distribution (**α**-plot) for FT synthesis

Experimental

A 25%Co-18%Zr/SiO$_2$ catalyst was synthesized by sequential incipient wetness impregnation of a high-purity, high-surface-area silica (XS16080, Norton) with Zr tetrapropoxide and Co nitrate [8]. A mixture of 2 cc of the calcined Co-Zr/SiO$_2$ catalyst and 10 cc of a low-surface-area α-alumina (SA5397, Norton) was loaded into a 0.305-in stainless steel down-flow reactor. The catalyst was reduced *in-situ* in H$_2$ at 350°C and was cooled and pressurized to approximately 300 psig. The feed was 33.3% H$_2$, 16.7% CO (H$_2$:CO=2:1), 1.7% Ar (internal standard), balance N$_2$, at 6000 h^{-1} space velocity. Pulse runs involved substituting the reactant feed flow with an equal molar flow of a pulse gas, thus maintaining the total molar flow and pressure between base and pulse runs.

Results

Runs with a "blank" pulse (i.e., switching between two equal flows of H$_2$+CO/ Ar) indicated no effect on CO conversion or product distribution (α-value, C$_{10}$-C$_{20}$ yield). A 1-min N$_2$ pulse per 1 hour gave only minimal variation in activity (CO conversion) and product selectivity. On the other hand, a 1-min H$_2$ pulse per 1 hour resulted in a significant increase in CO conversion at 225°C. The measured CO conversion after the pulse was observed to gradually decrease before the next pulse. The CH$_4$ selectivity also increased substantially (due to the excess of H$_2$) but was quickly restored to its base value. Thus H$_2$ pulsing increased the desired CO productivity while only instantaneously increasing the undesired CH$_4$ selectivity.

The effect of varying H$_2$ pulse frequency (1-min H$_2$ per 1, 2, and 4 hours) on the activity and product yield of the Co-ZrO$_2$/SiO$_2$ catalyst is given in Table 1. Both CH$_4$ yield and C$_{10}$-C$_{20}$ yield increase with H$_2$-pulse frequency. An optimum set of pulse parameters (pulse frequency, pulse duration) appears to be required for maximizing the C$_{10}$-C$_{20}$ yield.

Table 1. Effect of H$_2$ pulse frequency on product yield @225°C, P=300 psig

Frequency (h^{-1})	Alpha (-)	CH$_4$ (wt%)	CH$_4$ yield (g/cc cat/h)	C$_{10}$-C$_{20}$ (wt%)	C$_{10}$C$_{20}$ yield (g/cc cat/h)
0 (no pulse)	0.887	17.0	0.0189	28.2	0.0312
0.25	0.892	15.8	0.0228	26.4	0.0380
0.5	0.885	14.3	0.0223	31.0	0.0484
1	0.890	15.4	0.0253	29.7	0.0490

References

C.D. Chang, W.H. Lang, and A.J. Silvestri, J. Catal., 56 (1979) 268.

K. Jothimurugesan and S.K. Gangwal, Ind. Eng. Chem. Res., 37(4) (1998) 1187.

G. Beer, WO Patent No. 98/ 19979 (1997).

E. Peacock-Lopez and K. Lindenberg, J. Phys. Chem., 88 (1984) 2270.

E. Peacock-Lopez and K. Lindenberg, J. Phys. Chem., 90 (1986) 1725.

A.A. Khodadadi, R.R. Hudgins, and P.L. Silverston, Canadian J. Chem. Eng., 74 (1996) 695.

F.M. Dautzenberg, J.M. Heller, R.A. van Santen, and H. Berbeek, J. Catal., 50 (1977) 8.

A. Hoek, M.F.M. Post, J.K. Minderhoud, and P.W. Lednor, US Patent No. 4,499,209 (1985).

APPENDIX II   Effect of periodic pulsed operation on product selectivity in Fischer-Tropsch synthesis on Co-ZrO$_2$/SiO$_2$

Effect of periodic pulsed operation on product selectivity in Fischer-Tropsch synthesis on Co-ZrO$_2$/SiO$_2$

A.A. Nikolopoulos, S.K. Gangwal, and J.J. Spivey[*]

Research Triangle Institute, P.O. Box 12194, RTP, NC 27709-2194, U.S.A.

The effect of H$_2$ pulsing on the activity and product distribution of a high-**α** (~0.9) Co/ZrO$_2$/SiO$_2$ Fischer-Tropsch (FT) synthesis catalyst was investigated in an attempt to maximize the diesel-range product yield. H$_2$ pulsing increases CO conversion significantly but only temporarily; catalyst activity decreases gradually towards its steady state. Increasing H$_2$-pulse frequency has a positive effect on the yield of both CH$_4$ (undesirable) and C$_{10}$-C$_{20}$ (desirable) products. An optimum H$_2$-pulse frequency is apparently required in order to maximize the yield of diesel-range FT products without substantially increasing the CH$_4$ yield.

1. INTRODUCTION

The Fischer-Tropsch synthesis (FTS) can convert solid fuel- or natural gas-derived syngas (CO+H$_2$) to liquid fuels and high-value products. The extensively reviewed Fischer-Tropsch (FT) reaction [1-3] produces a non-selective distribution of hydrocarbons (C$_1$-C$_{100+}$) from syngas. FT catalysts are typically based on Group-VIII metals (Fe, Co, Ni, and Ru), with Fe and Co most frequently used. The product distribution over these catalysts is generally governed by the Schultz-Flory-Anderson (SFA) polymerization kinetics [4].

Currently there is significant commercial interest in producing diesel-fuel range middle distillates (C$_{10}$-C$_{20}$ paraffins) from natural gas-derived syngas [5]. Increasing the selectivity of FTS to desired products such as diesel (C$_{10}$-C$_{20}$) or gasoline (C$_5$-C$_{11}$) by altering the SFA distribution is economically attractive. Use of bifunctional catalysts (FT-active metals on zeolite, e.g. ZSM-5) to produce high-octane gasoline-range hydrocarbons (explored in the past 2 decades), has been economically unsuccessful [6-9]. The zeolite cracking activity lowers the chain-growth probability (**α**), producing gasoline-range products in excess of 48 wt% of the total hydrocarbon product; however, it also produces a significant amount of undesirable C$_1$-C$_4$ gases (Figure 1).

The present emphasis has shifted towards maximizing the yield of high-cetane C$_{10}$-C$_{20}$ products from FTS. Increased worldwide demand for low-sulfur diesel has further stressed the importance of development of zero-sulfur FT-diesel products. An alternative approach to the use of bifunctional catalysts to alter selectivity is periodic FT reactor operation (pulsing) [3]. It entails alternatively switching between two predetermined input compositions over the FT catalyst to promote time-average rate, selectivity, and catalyst life [10-12]. Periodic pulsing of H$_2$ has been examined so as to limit chain growth by removing the growing

---

[*] Present address: Chemical Engineering Dept., North Carolina State University, Raleigh, NC 27695
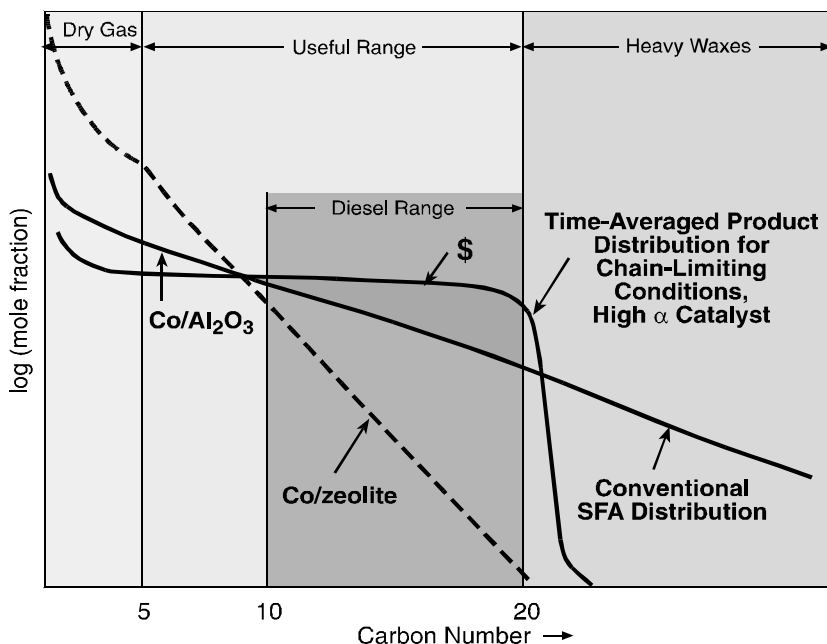
Figure 3. Product distribution (**α**-plot) for FT synthesis

hydrocarbon chain from the catalyst surface [13-15]. Experimental studies have shown the potential to alter the SFA distribution [16,17]; they were performed, however, at conditions of limited industrial interest.

The chain-limiting concept using pulsing to maximize diesel yield is shown in a plot of carbon number vs. mole fraction (Fig. 1). The slope of the curve is determined by the chain-growth probability, **α**. Periodic operation on a high-**α** catalyst may result in removal of the growing chain from the surface at

the desired C_{10}-C_{20} length, thereby maximizing diesel yield without increasing the dry gas. Thus, the objective of this study is to investigate the effect of H_2 pulsing on the activity and product distribution of a high-**α** (~0.9) $Co/ZrO_2/SiO_2$ FT synthesis catalyst, in an attempt to maximize the C_{10}-C_{20} product yield.

2. EXPERIMENTAL

2.1. Catalyst synthesis and characterization

A 25%Co-18%Zr/SiO$_2$ catalyst was synthesized by sequential incipient wetness impregnation of a high-purity, high-surface-area (144-m^2/g) silica support (XS 16080, Norton) [18]. The support (crushed and sieved to a particle size of 100-150 μm) was degassed in vacuum and heated to 80°C. A zirconium tetrapropoxide ($Zr(OCH_2CH_2CH_3)_4$) solution in 1-propanol (Aldrich) was used for the incipient wetness impregnation, performed in two steps. After each impregnation step, the product was dried (120°C, 2 h) and calcined in air (500°C, 1 hour). The produced material had a nominal loading of 18%Zr/silica.

Cobalt was impregnated on the zirconia/silica support using a cobalt nitrate hexahydrate precursor ($Co(NO_3)_2.6H_2O$, Aldrich). The hexahydrate was dissolved in water and the formed solution was added in a controlled manner to the zirconia/silica support, forming the catalyst with a nominal composition of 25%Co-18%Zr/SiO$_2$. Finally, the catalyst was calcined in air at 350°C for 1 hour.

The surface area of the $Co-ZrO_2/SiO_2$ catalyst was measured (by BET method) to be 102±3 m^2/g. Its pore volume was estimated at 0.40±0.01 cc/g (by mercury porosimetry). Its crystalline structure was examined by X-ray diffraction (XRD). The predominant phase was Co_3O_4, with no other Co-O or Zr-O crystalline phases or cobalt silicate present in the diffraction pattern.

2.2. Reaction set-up

The reaction system consisted of the gas-feed, a fixed-bed reactor, and a sampling/ analysis system for the liquid and gaseous products. The feed system blended CO/Ar, H_2, N_2, or other premixed gases in desired concentrations. A time-programmable interface system (Carolina Instrumentation Co.) was used to control a series of actuated valves, so that a (reactant or inert) flow opened / closed automatically and independently of the others. Appropriate periodic switch of these valves offered the capability to perform various pulsing-type experiments with this configuration.

A stainless-steel 3/8-in o.d. (0.305-in i.d.) downflow reactor was enclosed in a three-zone programmable furnace. The liquid products were collected and separated into a wax trap (waxes) maintained at 140°C and a water trap (oil + water) maintained at 25°C. Two sets of these traps, positioned in parallel, enabled continuous operation. A Kammer back-pressure-control valve, located downstream of the traps, controlled the reactor and trap pressure.

An on-line GC-Carle (TCD) analyzed the permanent gases (H_2, CO_2, Ar, N_2, CH_4, CO). Argon was used as internal standard. An on-line GC-FID (100-m Petrocol column, ramped from –25 to 300°C) analyzed the light hydrocarbons (C_1-C_{15}). A third off-line GC-FID (15-m SPB-1 capillary column, 0.1-μm, ramped from 50 to 350°C) analyzed the composite wax and oil collected from the wax and water traps, respectively.

2.3. Reaction procedure

A physical mixture of 2 cc (1.55 g) of the calcined Co-ZrO_2/SiO_2 catalyst and 10 cc (15.91 g) of a low-surface-area (0.2 m^2/g) α-alumina (SA5397, Norton) was loaded into the reactor. The catalyst was reduced *in-situ* under H_2 at 350°C for 14 h, and was cooled and pressurized to ca. 300 psig (19.4 atm). The FT reaction was started by feeding a 10%Ar/CO gas mix, thus establishing the following base reaction conditions:

      Syngas (H_2 + CO)=50%, H_2:CO=2:1 (i.e., 33.3% H_2 and 16.7% CO)

      Inerts (N_2 + Ar)=50% (1.7% Ar, 48.3% N_2)

      P=300 psig, F=200 scc/min, SV=6000 h^{-1}.

The reaction temperature was increased (by 0.5°C/h or less) to 224°C and was stabilized at this value, thus allowing the reaction to reach a "pseudo-steady state". Pulse runs involved substituting the reactant feed flow (H_2+CO/Ar) with an equal molar flow of a pulse gas. The total molar flow and the reaction pressure were kept constant between base and pulse runs.

3. RESULTS AND DISCUSSION

A "blank" pulse run (i.e., switching between two equal flows of H_2/CO/Ar reactant mix) was performed in order to identify the possible effect of the periodic pressure disturbance (directly related to the applied pulse) due to non-ideal switching of the actuated valves. This run produced no measurable variation on CO conversion, H_2:CO ratio, or product distribution (**α**-value, C_{10}-C_{20} yield). Therefore, pulse runs involving no variations in feed composition have no effect on measurements of the progress of the FT reaction.

A 1-min N_2 (inert) pulse per 1 hour (i.e., substituting the H_2/CO/Ar flow, which is 51.7% of the total, with an equal flow of N_2 for 1 min every hour) was applied so as to examine the effect of inert pulsing on the reaction progress. The N_2 pulse gave only minimal variations in activity (CO conversion) or product selectivity (**α**-value, CH_4 yield, C_{10}-C_{20} yield), implying that short (1-min) disruptions in reactant flow do not substantially affect the FT reaction.

In contrast to the inert pulse, a 1-min H_2 (reactant) pulse caused significant variations in CO conversion and CH_4 selectivity. Effects of varying the H_2 pulse frequency (1-min H_2 per 1, 2, and 4 hours) on the CO conversion and the C_1 (CH_4 and CO_2) selectivity are shown in the composite plots of Figures 2a and 2b, respectively. These plots are composed of 10-hour segments of a series of sequential runs (typically lasting 48 hours, so as to collect sufficient amounts of oil + wax for the analysis), starting and ending with a base (no pulse) run. The data points correspond to measurements of the reactor effluent gas every 15 minutes.

A 1-min H_2 pulse per 1-hour (10-20-hour segment in Figs. 2a and 2b) caused a significant increase in CO conversion (from 16% to ca. 30%). The measured temperature of the catalyst bed also increased to 226°C, indicating a strong reaction exotherm. The conversion of CO decreased *gradually* until the next H_2 pulse. A less-pronounced increase in CO conversion was also observed for the 1-min H_2 pulse per 2-h and 4-h runs. The observed decrease in CO conversion after the pulse indicates that the activity tends to return to its steady state (comparing also the base runs before and after the 3 pulse runs). The measured changes in CO conversion cannot be attributed to variations in the inlet CO concentration since the conversion was based on comparing the inlet and outlet *ratios* of CO to the inert Ar (fed at a fixed ratio from a single gas cylinder).

The selectivity to CH_4 was observed to increase *instantaneously* after each H_2 pulse (from 13-14% to ca. 20% for all examined pulse runs). It was then quickly restored to its base value (Fig. 2b). Thus, H_2 pulsing increases catalytic activity while only briefly increasing the undesirable formation of CH_4.
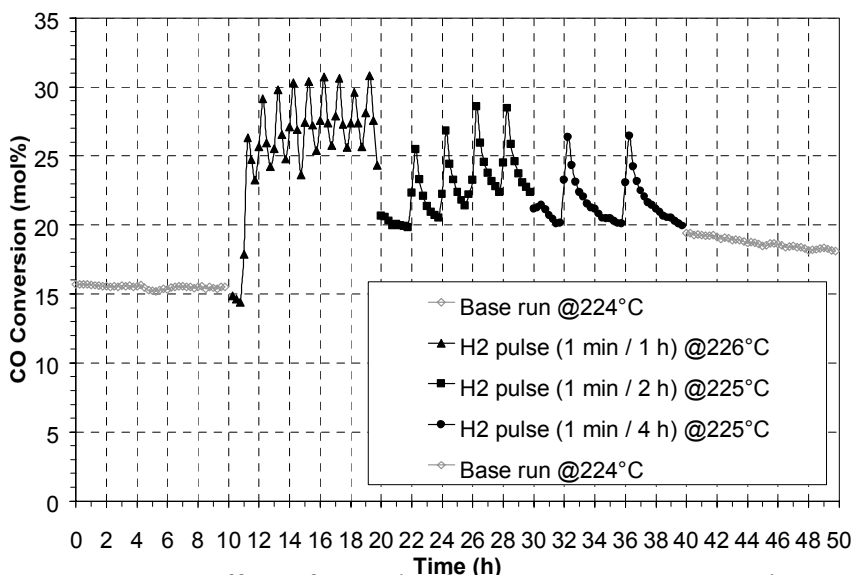
Figure 2a. Effect of H_2 pulse frequency on CO conversion
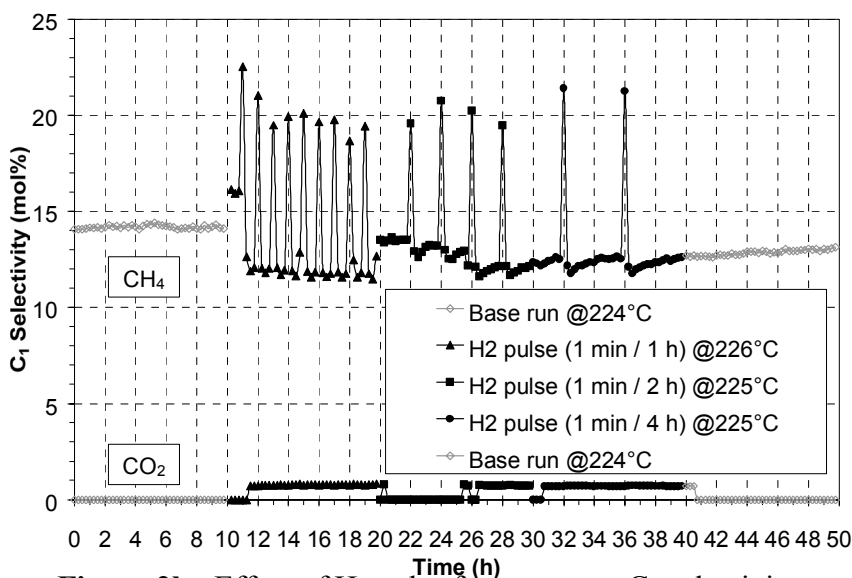
Figure 2b. Effect of H_2 pulse frequency on C_1 selectivity

81
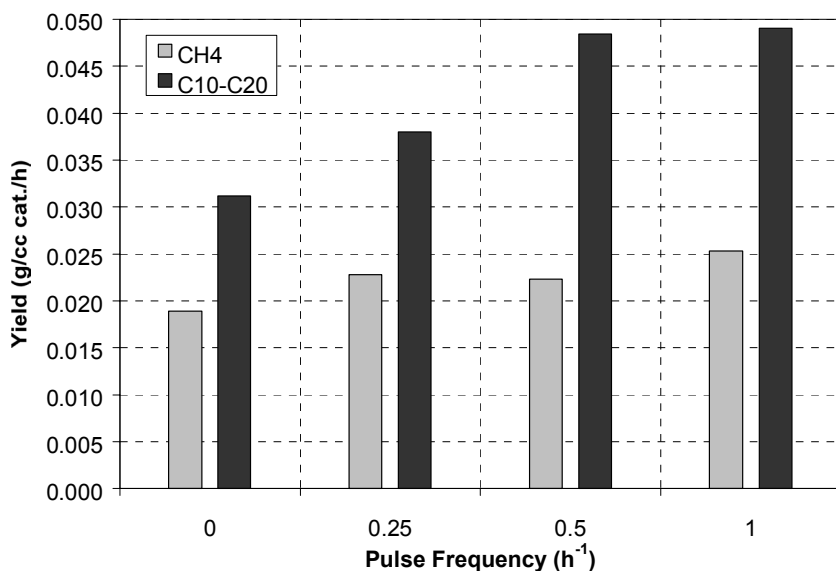
Figure 3. Effect of H_2 pulse frequency on product yield

The effect of varying H_2 pulse frequency on the desired C_{10}-C_{20} yield vs. the undesired CH_4 yield is shown in Figure 3. Pulse frequencies of 1, 0.5, and 0.25, h^{-1} correspond to a 1-min H_2 pulse per 1, 2, and 4 hours, respectively. The zero pulse frequency corresponds to the average of the two no-pulse (base) runs before and after the 3 pulse runs.

Both C_{10}-C_{20} and CH_4 yields increase with H_2-pulse frequency (and so does the yield of C_{21+}), obviously due to the enhancement in catalytic activity caused by the pulsing (Fig. 2a). As seen in Fig. 3, the effect of the 1-min H_2 pulse per 1 hour compared to the (average) base run was to increase the C_{10}-C_{20} yield by ca. 57%, while the CH_4 yield only increased by ca. 34%. Although this comparison entails a temperature change (from 224°C to 226°C), the increase in the C_{10}-C_{20} yield is more than what could be accounted for solely by a 2°C increase in reaction temperature. The CH_4 selectivity in the pulse runs (13-14% on molar basis) is lower than that of the base runs (15.5%), whereas the selectivity to C_{10}-C_{20} and C_{21+} compounds is higher (28-32% vs. 27%, and 23-24% vs. 20%, respectively). The α-values of the pulse runs (based on the molar fractions of C_{10}-C_{65} products) are found to be essentially identical to that of the base runs (0.890±0.005). Thus, the applied H_2 pulsing apparently does not alter the SFA distribution.

Within the examined pulse frequency range, the greater difference between the yields of the desirable C_{10}-C_{20} and the undesirable CH_4 is obtained at the *intermediate* pulse frequency of 0.5 h^{-1} (1-min H_2 per 2 hours). Also, upon extrapolating to higher H_2-pulse frequencies, we could expect a stronger reaction exotherm and thus an increase in reaction temperature, which is known to cause a shift in FTS product distribution to lower molecular weight compounds and to enhance the methanation reaction [4]. Higher pulse frequencies would thus tend to increase the CH_4 yield much more than the C_{10}-C_{20} yield. An optimum H_2-pulse frequency (depending on catalyst and reaction conditions) would therefore be required for maximizing the C_{10}-C_{20} yield without substantially increasing the CH_4 yield.

Another series of H_2-pulse runs on the Co-ZrO_2/SiO_2 catalyst examined the effect of H_2-pulse duration on activity and product distribution, by varying the pulse duration (1, 2, 4-min of H_2) at a fixed pulse frequency (0.5 h^{-1}). The results of this study (not included here) are qualitatively similar to those of the variable-pulse-frequency study presented here: higher H_2-pulse duration causes an increase in both C_{10}-C_{20} and CH_4 yield, and the greater difference between these yields is obtained at the *intermediate* pulse duration of 2 min. Consequently, optimization of the pulse duration is also important in maximizing the formation of diesel-range FT products.

4. CONCLUSIONS

In contrast to "blank" or inert (N_2) pulsing, pulsing with H_2 has a significant impact on the activity and selectivity of the examined Co-ZrO$_2$/SiO$_2$ catalyst. H_2 pulsing causes significant increase in CO conversion, along with an observed enhanced reaction exotherm. Then, the CO conversion decreases gradually until the next H_2 pulse, indicating that the catalyst activity tends to return slowly to its steady state, as measured in base (no-pulse) runs. On the other hand, the selectivity to CH_4 increases instantaneously after each H_2 pulse, and gets quickly restored to its steady-state value.

Increasing H_2-pulse frequency has a positive effect on the yield of both CH_4 and C_{10}-C_{20}. The selectivity to C_{10}-C_{20} and C_{21+} compounds increases with H_2 pulsing compared to the base runs, but the chain-growth probability α is essentially unaffected. An optimum set of H_2-pulse parameters (frequency and duration) appears to be needed to maximize the C_{10}-C_{20} yield without substantially increasing the CH_4 yield.

5. ACKNOWLEDGEMENTS

REFERENCES

20. R.B. Anderson, The Fischer-Tropsch Synthesis, Acad. Press, New York, 1984.
21. M.E. Dry, Appl. Catal. A, 138 (1996) 319.
22. A.A. Adesina, Appl. Catal. A, 138 (1996) 345.
23. M.E. Dry, The Fischer-Tropsch Synthesis, in Catalysis - Science and Technology 1 (J.R. Ander and M. Boudart, eds.), Springer-Verlag, New York, 1981.
24. G. Parkinson, Chem. Eng., 4 (1997) 39.
25. C.D. Chang, W.H. Lang, and A.J. Silvestri, J. Catal., 56 (1979) 268.
26. R.J. Gormley, V.U.S. Rao, R.R. Anderson, R.R. Schehl, and R.D.H. Chi, J. Catal., 113 (1988) 195.
27. S. Bessell, Appl. Catal. A, 126 (1995) 235.
28. K. Jothimurugesan and S.K. Gangwal, Ind. Eng. Chem. Res., 37(4) (1998) 1181.
29. D.L. King, J.A. Cusamano, and R.L. Garten, Catal. Rev. Sci. Eng., 23(1-2) (1981) 233.
30. A.A. Adesina, R.R. Hudgins, and P.L. Silveston, Can. J. Chem. Eng., 25 (1995) 127.
31. J.W. Dun, and E. Gulari, Can. J. Chem. Eng., 64(2) (1986) 260.
32. G. Beer, Gas Conversion Process Using a Chain-Limiting Reactor, WO Patent No. 98/19979 (1997).
33. E. Peacock-Lopez and K. Lindenberg, J. Phys. Chem., 88 (1984) 2270.
34. E. Peacock-Lopez and K. Lindenberg, J. Phys. Chem., 90 (1986) 1725.
35. A.A. Khodadadi, R.R. Hudgins, and P.L. Silverston, Canadian J. Chem. Eng., 74 (1996) 695.
36. F.M. Dautzenberg, J.M. Heller, R.A. van Santen, and H. Berbeek, J. Catal., 50 (1977) 8.
37. A. Hoek, M.F.M. Post, J.K. Minderhoud, and P.W. Lednor, Process for the Preparation of a Fischer-Tropsch Catalyst and Preparation of Hydrocarbons from Syngas, US Patent No. 4,499,209 (1985).